



Durham E-Theses

Sedimentological analysis and hydrocarbon potential of the upper devonian-lower carboniferous Tahara sandstones, ghadames basin, western Libya

Burki, Milad Mohamed Milad

How to cite:

Burki, Milad Mohamed Milad (1998) *Sedimentological analysis and hydrocarbon potential of the upper devonian-lower carboniferous Tahara sandstones, ghadames basin, western Libya*, Durham theses, Durham University. Available at Durham E-Theses Online: <http://etheses.dur.ac.uk/5018/>

Use policy

The full-text may be used and/or reproduced, and given to third parties in any format or medium, without prior permission or charge, for personal research or study, educational, or not-for-profit purposes provided that:

- a full bibliographic reference is made to the original source
- a [link](#) is made to the metadata record in Durham E-Theses
- the full-text is not changed in any way

The full-text must not be sold in any format or medium without the formal permission of the copyright holders.

Please consult the [full Durham E-Theses policy](#) for further details.

**SEDIMENTOLOGICAL ANALYSIS AND
HYDROCARBON POTENTIAL OF THE
UPPER DEVONIAN-LOWER CARBONIFEROUS
TAHARA SANDSTONES, GHADAMES BASIN,
WESTERN LIBYA**

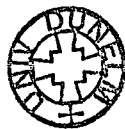
By

Milad Mohamed Milad Burki

A thesis submitted to the University of Durham in
fulfilment of the requirement of Master of Science

The copyright of this thesis rests
with the author. No quotation from
it should be published without the
written consent of the author an
information derived from it should
be acknowledged.

Department of Geological Sciences,
University of Durham
November 1998



11 MAY 1999

Thesis

1998/

BUR

Declaration

This is to certify that this work, submitted for the degree of Master of Science under the title of " Sedimentological Analysis and Hydrocarbon Potential of the Upper Devonian-Lower Carboniferous Tahara Sandstones, Ghadames Basin, Western Libya " is the original work of the author. I declare that the work contained in this thesis has not been submitted elsewhere for any other degree or qualification and is my own work, unless otherwise referenced.

Candidate:.....

Milad M. Burki

Director of research:.....

Dr. Brian R. Turner

Dedication

This thesis is dedicated to my mother, my wife, my daughters; Huda and Hager, and my son Mohamed.

ACKNOWLEDGEMENTS

First I would like to thank Allah, the Wise, for his guidance. My deepest gratitude goes to my supervisor Dr. Brian R. Turner for his open mind and never-ending patience throughout the period of this research, and for his guidance, comments and helpful suggestions.

There are many people who have helped me through my research. I would like to thank Prof. M. Tucker, Head of Department, for his helpful assistance. I would also like to take this opportunity to thank all the staff, postgraduate students and secretaries in the Geology Department for their assistance and support.

I thank exploration staff of Sirte Oil for their support and assistance in this research. My special thanks go to A. AL-Soghair for his assistance and support. My thanks also to R. Rahmani and Ed Tawadros for their guidance, and S. Rasul and R. EL-Zaroug for information on biostratigraphy.

Finally I would like to thank my mother for her prayers to God and good wishes. My grateful appreciation also goes to my wife and my children for their patience and support during my stay in the UK.

CONTENTS

	Page
List of figures	i
List of tables	v
Abstract	vi
Chapter 1	
Introduction and Geological History of Western Libya	1
1.1-Previous work	1
1.2-Location and aim of the study	3
1.3-Methodology and data source	4
1.4-Regional geology of the area	8
1.4.1-Tectonic framework	8
1.4.2-Ghadames basin	8
1.4.3-Murzuq basin	9
1.4.4-Geological setting	10
Chapter 2	
Sedimentary Facies	19
2.1-Introduction	19
2.2-Description and Interpretation of Facies	22
2.2.1-Laminated shale	22
2.2.2-Interlaminated and bioturbated shale and sandstone	25
2.2.3-Parallel laminated and ripple cross-laminated sandstone	26
2.2.4-Bioturbated sandstone and shale	31
2.2.5-Heterolithic facies	34
2.2.6-Planar cross-bedded and horizontally laminated sandstone and shale	48
2.2.7-Shale	64

Chapter 3

Sequence Stratigraphy	66
3.1-Introduction	66
3.1.1-Continental encroachment cycles	68
3.1.2-Major transgressive-regressive facies cycles	68
3.1.3-Sequence cycles	68
3.1.4-Parasequence cycles	68
3.2-Factors Effecting Sequence Stratigraphy	69
3.2.1-Eustatic effect	69
3.2.2-Tectonic	69
3.2.3-Sediment supply	70
3.3-Depositional Sequence Stratigraphy	70
3.3.1-Parasequences	70
3.3.2-Sequence boundary	71
3.3.2.a-Type 1 sequence boundaries	71
3.3.2.b-Type 2 sequence boundaries	72
3.3.3-Depositional System Tracts	72
3.3.3.1-Lowstand systems tracts (LST)	73
3.3.3.2-Transgressive systems tracts (TST)	76
3.3.3.3-Highstand systems tracts (HST)	76
3.3.3.4-Shelf-Margin systems tracts (SMST)	78
3.4-Sequence Stratigraphic Setting of the Tahara Formation	78
3.4.1-Introduction	78
3.4.2-Recognition of the sequences and sequence boundary	79
3.4.2.1-Sequence 1 (upper part)	82
3.4.2.2-Sequence 2	84

Chapter 4

Sequence Stratigraphy from Wireline Logs	89
4.1-Introduction	89
4.2-Geological Interpretation from Gamma Ray Log	89
4.2.1-Gamma-ray log (GR) trends	91

4.3-Sequence Stratigraphic Interpretation from Wireline Log Trends	95
4.4-Depositional System Tracts of the Tahara Succession from Wireline Logs	98
4.4.1-Transgressive systems tract	99
4.4.2-Highstand systems tract	100
4.5-Tahara Formation in Response to Sea-Level Changes	100

Chapter 5

Sandstone Petrology	102
5.1-Introduction and Sampling Methodology	102
5.2-Composition of Sandstones	102
5.2.1-Quartz	102
5.2.2-Feldspar	104
5.2.3-Rock fragments	104
5.2.4-Mica and clay minerals	106
5.2.5-Heavy minerals	106
5.2.6-Other minerals	107
5.3-Diagenesis	107
5.3.1-Silica cementation	108
5.3.2-Carbonate cement	109
5.3.3-Feldspars dissolution	110
5.3.4-Authigenic clay minerals	111
5.4-Texture	111
5.5-Porosity	115
5.6-Classification	116
5.6.1-Quartz arenite	116
5.6.2-Arkose	119
5.7-Comparison Between Upper and Lower Tahara Sandstones	119
5.8-Provenance	120

Chapter 6

Conclusions

123

References

136

LIST OF FIGURES

	Page
Chapter 1	
Fig. 1.1 Location map of Libya showing the study area	2
Fig. 1.2 Core coverage and sample locations in the six wells used in the study	7
Fig. 1.3 Location map of the sedimentary basins of Libya	10
Fig. 1.4 Stratigraphic column of the Palaeozoic and Mesozoic Ghadames basin, W. Libya	12
 Chapter 2	
Fig. 2.1 Lithology and sedimentary structures from type well C1-49	21
Fig. 2.2 Detailed core section for the cored interval of Facies 1 and 2	24
Fig. 2.3 Detailed core section of Facies 3 and 4	27
Fig. 2.4 Slabbed core sample from well C1-49 showing parallel lamination	28
Fig. 2.5 Block diagram of hummocky cross-stratification	30
Fig. 2.6 Trace fossil associations in marine ichnofacies sets	30
Fig. 2.7 Slabbed core sample from well C1-49 showing bioturbated sandstone and shale	32
Fig. 2.8 Detailed core section of the heterolithic type 1 facies	35
Fig. 2.9 Slabbed core sample from heterolithic type 1 facies	37
Fig. 2.10 Slabbed core sample from heterolithic type 1 facies	37
Fig. 2.11 Photomicrograph from heterolithic facies	38
Fig. 2.12 X-ray diffraction of the ironstone from heterolithic type 1 facies	38
Fig. 2.13 X-ray diffraction of the ironstone from heterolithic type 1 facies	40
Fig. 2.14 X-ray diffraction of the ironstone from heterolithic type 1 facies	40
Fig. 2.15 Slabbed core sample from heterolithic type 1 facies, well K1-1	41
Fig. 2.16 Detailed core section of the heterolithic and Facies 6 of well ATS2	44
Fig. 2.17 Slabbed core sample from heterolithic type 2 facies, well ATS2	45
Fig. 2.18 Slabbed core sample from heterolithic type 2 facies, well ATS2	47
Fig. 2.19 Close up of part of Fig. 2.17	47

Fig. 2.20	Detailed core section of Facies 6, well C1-49	49
Fig. 2.21	Slabbed core sample of part of lower Tahara sandstone, well C1-49	50
Fig. 2.22	Slabbed core sample from lower Tahara sandstone, well C1-49	50
Fig. 2.23	Slabbed core sample from lower Tahara sandstone, well C1-49	51
Fig. 2.24	Detailed core section of lower part of the lower Tahara sandstone, well A1-NC 151	53
Fig. 2.25	Slabbed core sample from well A1-NC 151	54
Fig. 2.26	Slabbed core sample from well A1-NC 151	54
Fig. 2.27	Slabbed core sample from well AST2	55
Fig. 2.28	Slabbed core sample from well C1-49	55
Fig. 2.29	Slabbed core sample from upper sandstone, well C1-49	57
Fig. 2.30	Detailed core section of Facies 6 from well K1-1	58
Fig. 2.31	Lithological profile from upper sandstone in well AST1	59
Fig. 2.32	Southwestern-northeastern cross-section showing lateral extent of the Tahara Formation	63
Fig. 2.33	Detailed core section of Facies 7	65

Chapter 3

Fig. 3.1	Hierarchy of stratigraphic cycles	67
Fig. 3.2	Schematic diagram showing distribution of systems tracts and parasequences	75
Fig. 3.3	Idealized block diagrams showing systems tracts	77
Fig. 3.4	Detailed vertical succession illustrating two sequences, sequence boundary and systems tracts of the Tahara Formation	80
Fig. 3.5	Sea level cycles of third and fourth order	82
Fig. 3.6	Stratigraphic cross-section along southwest-northeast trend	88

Chapter 4

Fig. 4.1	Wireline logs from type well C1-49	90
Fig. 4.2	Wireline log trends	92
Fig. 4.3	Three principle gamma ray shapes and their corresponding sedimentary interpretation	94
Fig. 4.4	Idealized log curve shapes from the gamma ray	94

Fig. 4.5	Schematic wireline log patterns for sequence stratigraphy interpretation	97
Fig. 4.6	Well log cross-section from SW to NE showing the gamma ray trends	101

Chapter 5

Fig. 5.1	Petrographic characteristics of the Tahara sandstones from well C1-49	103
Fig. 5.2	Paragenetic sequence of diagenetic events in the Tahara Sandstones	108
Fig. 5.3	Photomicrograph from the upper part of the lower Tahara Sandstone	109
Fig. 5.4	Photomicrograph from the upper Tahara sandstone showing calcite cement	110
Fig. 5.5	Idealized cumulative frequency curve	112
Fig. 5.6	Typical cumulative frequency grain size curves for the upper Tahara sandstone	113
Fig. 5.7	Typical cumulative frequency grain size curves for the lower Tahara sandstone	114
Fig. 5.8	Photomicrograph from the upper part of lower Tahara sandstone showing the quartz grains, feldspar dissolution and kaolinite	117
Fig. 5.9	Photomicrograph from the upper part of lower Tahara sandstone showing secondary porosity and microporosity	117
Fig. 5.10	Ternary QFRF plot showing the classification of the Tahara sandstones	118
Fig. 5.11	Photomicrograph from the upper Tahara sandstone showing quartz arenite composition	118
Fig. 5.12	Photomicrograph from the upper part of lower Tahara sandstone showing arkose composition	119
Fig. 5.13	Relation between framework composition of the Tahara sandstones	122
Fig. 5.14	Ternary QFRF plot showing the composition of the Tahara sandstone and its inferred source rocks	122

Chapter 6

Fig. 6.1	Late Pre-Cambrian cratons of Gondwana	124
----------	---------------------------------------	-----

Fig. 6.2	Early Palaeozoic palaeotectonic map of Gondwana	124
Fig. 6.3	Late Palaeozoic to Early Mesozoic palaeotectonic map of Gondwana	125
Fig. 6.4	Late Palaeozoic to Early Mesozoic regional tectonic regimes of Gondwana	126
Fig. 6.5	Generalised model for the Tahara depositional system	127
Fig. 6.6	Palaeogeographic interpretation of the Tahara Formation	128
Fig. 6.7	Schematic cross-section along the line A-B in Fig. 6.6	130
Fig. 6.8	Block diagrams illustrating the geological evolution of the Tahara Formation	133
Fig. 6.9	Location of possible updip areas proximal to the Gargaf arch	135

LIST OF TABLES

	Page
Table 1.1 Available core from upper Devonian-lower Carboniferous strata	6
Table 1.2 Intervals and age of palynological samples	6
Table 2.1 Description and interpretation of the facies	20
Table 5.1 Modal composition of samples from the upper Tahara sandstone	105
Table 5.2 Modal composition of samples from the lower Tahara sandstone	105

ABSTRACT

The Palaeozoic (Upper Devonian-Lower Carboniferous) Tahara Formation, western Libya, was deposited in shallow-water, marginal and nearshore marine environments influenced by waves and storms. These are interpreted to represent interactive shelf to nearshore, shoreface and fluvio-deltaic environments. The analysis and interpretation of the subsurface data of this formation allow for the recognition of seven facies on the basis of core and electric log data obtained from each of the study wells. Each facies is identified on the basis of lithology, sedimentary structures and biogenic features, and four of these facies have been grouped into a shelf-nearshore facies association. Vertical and lateral facies relations enable the Tahara Formation to be divided into upper and lower sandstones. The upper sandstone shows an increase in shale content accompanied by increased bioturbation, towards the southwest.

Sequence stratigraphic analysis indicates that the Tahara Formation is characterised by transgressive and regressive phases of deposition in response to changes in relative sea level. The overall succession stacks into two partial sequences separated by a Type 1 sequence boundary. The lower sequence below the sequence boundary represents a coarsening-upward prograding shoreline comprising sediments deposited as part of a highstand systems tract. Above the sequence boundary, the incomplete sequence 2, includes the Tahara sandstones. These are believed to have been deposited as part of a transgressive systems tract bounded at the top by a maximum marine flooding surface. The succession includes marine flooding surfaces of different hierarchical level which record a deepening of the depositional environment in response to sea-level rise. Both preserved sequences form part of a third-order cycle which in the upper part includes fourth-order higher frequency cycles. The deposition and distribution of facies within the sequences are controlled by different factors including rate of relative sea-level change, rate of subsidence and sediment supply. Gamma ray log shapes in the Tahara sandstones are variable from funnel to roughly cylindrical shape. The lower Tahara sandstone shows a serrate cylindrical gamma ray log shape in well C1-49 and AST2, and a funnel gamma ray log shape in well K1-1, A1-NC151 and AST1. The upper Tahara sandstone shows a funnel gamma ray log shape in well C1-49, a complex gamma ray log shape in well K1-1 trend, and a serrate cylindrical gamma ray log shape in wells A1-NC151 and AST2.

The Tahara sandstones can be classified as quartz arenites and arkoses in terms of their modal composition. The detrital quartz grain size of the Tahara sandstones is generally fine to very fine-grained, and well sorted with rounded to subrounded grains. The overall grain-size trends are slightly variable in both the upper and the lower sandstone with the coarser grains concentrated in the upper part of the lower sandstone. Three types of porosity are recognized in the Tahara sandstones: (1) primary intergranular porosity which occurs as isolated pores; (2) secondary porosity, which is the most common porosity, originates from dissolution of unstable minerals or authigenic grains during fluid movement; and (3) microporosity which occurs within kaolinite clay minerals. The upper part of the lower sandstone has a porosity of up to 27.6%. This reflects the secondary dissolution of feldspar and the development of secondary porosity and pore-filling kaolinite clays.

Palaeocurrent evidence from previous workers suggested that the sediments were derived from the uplifted Al Gargaf area to the southeast of the basin. Four sequential depositional models are proposed for the evolution of the Tahara Formation in response to relative sea-level changes:

1. Marine shelf sediment was deposited during a relative sea-level rise. This is interpreted to form part of an early transgressive systems tract before deposition of the lower Tahara sandstone.
2. The lower Tahara sandstone was deposited in a shoreface environment, and was gradually overlain by fluvio-deltaic deposits as the depositional system gradually prograded basinwards across the shelf. This sandbody overlies marine shelf deposits and records shoreline progradation and increased fluvial sediment supply from a nearby uplifted source area.
3. The unit represents a short-lived marine transgressive event which terminated lower Tahara sandstone progradation as the depositional system temporarily retreated landwards.
4. The final stage in the evolution of the depositional system was shoreline progradation during which the well-sorted, fine to very fine-grained upper Tahara sandstone was deposited in a shoreface environment. This sandbody once again overlies marine shelf deposits and records another phase of shoreline progradation, and the development of another a coarsening-upward package.

Chapter 1

Introduction and Geological History of Western Libya

1.1-Previous work

The geology of western Libya was first studied by Italian geologists from 1930 to 1940, and then by a French geologists between 1944 and 1950. In the late 1950's and early 1960's petroleum exploration programmes in the sedimentary basins of western Libyan, were undertaken by a number of companies after the discovery of oil. From that time research on the Palaeozoic outcrops of the area continued and a great number of boreholes, mostly in the Ghadames basin and then in the Murzuq basin, were drilled.

Bellini and Massa (1980) reviewed the previous publications and unpublished academic and oil company data on the Palaeozoic of the western sedimentary basins of Libya. Other work that has been done on the Ghadames and Murzuq basins include Hammuda (1980), Vos (1981 a, b), Van Houten and Karasek (1981), Whitbread and Kelling (1982), Clark-Lowes (1985), Pierobon (1991), Castro *et al.* (1991), Bracaccia *et al.* (1991), and Adamson *et al.* (1997) amongst others.

Previous work has been done on some 6 meters of core cut through part of the Tahara Formation in well A6-NC169 in the Al Wafa gas field northwest of well C1-49 in the present study area (Fig. 1.1). The Tahara Formation was interpreted to have been deposited under shallow-marine conditions, in a shoreface setting dominated by wave and storm conditions (Rahmani 1994).



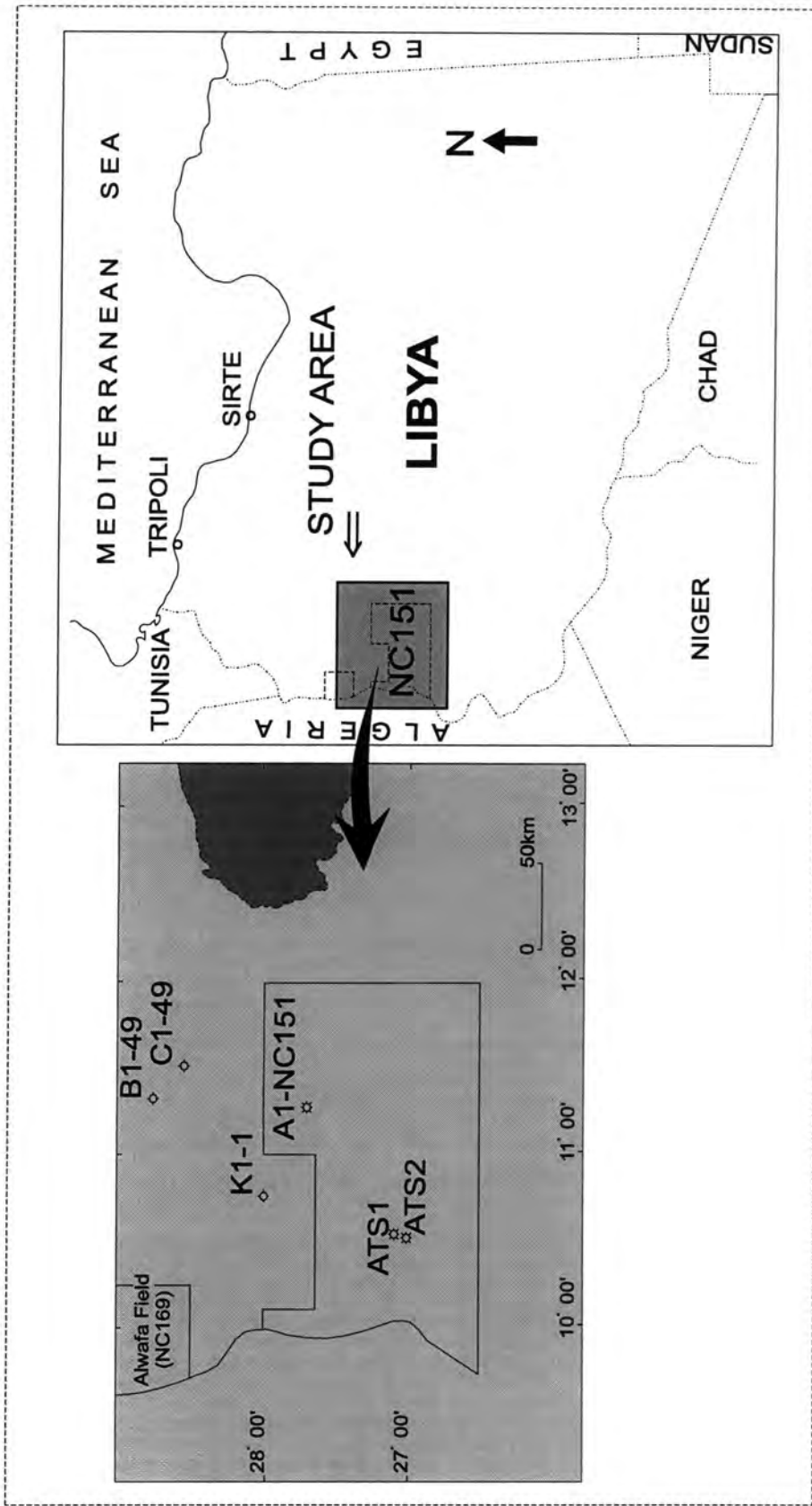


Fig. 1.1 Location map of Libya showing the study area in western Libya and the wells included in this study.

Petrographic analysis of the same core showed the Tahara sandstone to consist of fine- to very fine-grained, well-sorted sandstone with low porosity and permeability due to the presence of abundant silica and calcite cement (Tawadros 1994). This core occurs in the same stratigraphic position as the upper Tahara sandstone of the present study.

Despite the many published and unpublished works previously cited detailed core-based analysis of the Tahara Formation is rare. The main aim of this study is to provide a more detailed analysis of the Tahara sandstones in part of western Libya and to try and extend the results of the study into adjacent areas where no core data exist.

1.2-Location and aim of the study

The area of this study is located in western Libya between latitudes 26° 00' and 29° 00', and longitudes 10° 00' and 13° 00' (Fig. 1.1). The area is situated between the Ghadames basin to the north and Murzuq basin to south. The Ghadames basin is well known from numerous surface and subsurface studies in western Libya, but the Murzuq basin is less well known.

This is a subsurface based study of the late Palaeozoic (upper Devonian-lower Carboniferous) Tahara sandstones between the Murzuq and Ghadames basins in western Libya.

The main objectives of this study are as follows:

- 1) To describe and interpret individual facies, facies sequences and their depositional environments in order to develop facies-based sedimentological models of the Tahara Formation, based on core and electric log data;
- 2) To apply sequence stratigraphic methods to the Tahara Formation, using variations in facies tracts and stacking patterns in relation to changes in base level;

3) To review the use of wireline logs in sequence stratigraphy and to define various characteristic log patterns, especially gamma ray patterns, and integrate them with the core data; and

4) To examine the petrographic characteristics of the sandstones in the Tahara Formation, in order to identify textures, determine mineral composition, diagenetic features and porosity with a view to assessing the reservoir potential of the sandstones.

1.3-Methodology and data source

The data for this study is based on slabbed core and electric logs from six wells. Cored intervals in wells are illustrated in Fig. 1.2 and Table 1.1. Well C1-49 is considered the type well based on the core coverage of over 67 m, entire Tahara Formation. Well ATS2 is the second most important well because it encountered the lower Tahara sandstone and therefore provides useful information on the lateral facies variations between these wells.

The sedimentary structures and facies in the core have been photographed and petrographic, palynologic (from shale samples) and XRD analyses carried out. The location of all thin sections is shown in Fig. 1.2. The thin sections were impregnated with blue resin to determine the porosity and permeability, textural characteristics, mineral composition and diagenesis.

Wireline logs used in this study include gamma-ray (GR), Spontaneous potential (SP), neutron (N) and resistivity log (Res). These were used for facies correlation, determining the position of marker beds and the thickness of facies units. However, the gamma ray log was the most useful for delineating facies geometries and depositional relationships. Depth of core and wireline logs are given in feet, and thickness of internal structures is given in both imperial and metric scales.

Biostratigraphic analysis has been carried out on 19 samples from well C1-49 and B1-49 (Fig. 1.2) to determine the ages and palaeoenvironments. The

biostratigraphic study is based on shale sections, prepared according to standard techniques by company geological laboratory staff. These were prepared and studied in the geological laboratory of the Sirte Oil Company. Most of the slides contain abundant spores and woody debris, which represent both terrestrial and marine material. Biostratigraphic analysis suggests that the Tahara Formation was deposited in the latest Famennian (Struncian) (Table 1.2) based on the presence of spores such as *Retispora lepidophyta*. Other important spores are *Spelaeotrilets granulatus*, *Rugospora flexouosa*, *Hamenozonorilets explanatus* and *Tumulispora rartuberculata*.

The samples collected from the shale interval (1039 m-987 m) (M'rar Formation) in Facies 7 above the upper Tahara sandstone contain *Vallatisporites vallatus*. This spore may represent a lower Carboniferous (Early Tournaisian) age (Table 1.2) (Geological laboratory staff).

Biostratigraphic examination has also been carried out by the Compagnie des Petroles Total (Libya) (CPT (L) 1966, unpublished report) on micaceous black shale from 1428 m in well B1-49 (Fig. 1.2). This suggested that the upper Devonian (Lower Famennian) was deposited in a nearshore environment as evidence by disseminated marine fossils and spores and pollen.

Age dating of the Tahara Formation was attempted by Bellini and Massa (1980) and Weyant and Massa (1991), as part of a broader study of the biostratigraphy of the Devonian system in western Libya. These studies enabled the Devonian system to be subdivided into consistent chronostratigraphic units (see below in geological setting section).

Well Name	Core No.	Core Interval	Core Thickness
1-C1-49	7-15	974 m-1041 m	67 m
2-K1-1	9	1276 m-1281 m	7 m
	10	1126 m-1313 m	6 m
3-A1-NC151	1	545.5 m-855 m	4 m
4-ATS1	6	697 m-704 m	7 m'
5-ATS2	7-8	707 m-723 m	15 m

Table 1.1 Available core from upper Devonian-lower Carboniferous strata of five wells used in the study (after calibration with electric logs).

Well Name	Core Interval	Age
1-C1-49	977 m-987 m	L. Carboniferous (E. Tournasian)
	987 m-1039 m	L. Famennian (Strunian)
2-B1-49	1425 m-1435 m	L. Famennian (Strunian)
	1435 m-1442.5 m	L. Famennian

Table 1.2 Showing intervals and age of palynological samples from well C1-49 and B1-49. See Fig. 1.2 for location of samples.

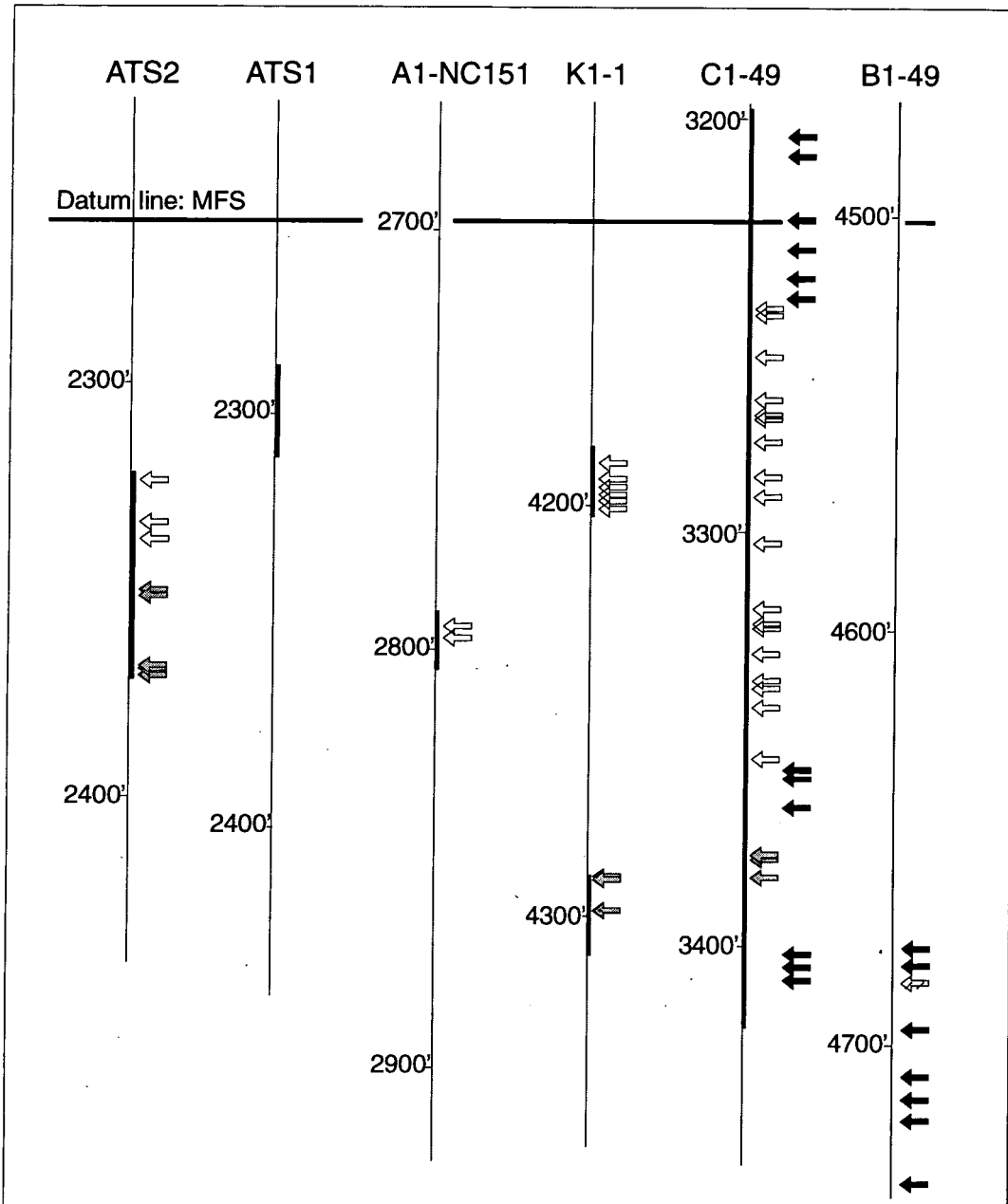


Fig. 1.2 Core coverage and sample locations in the six wells used in the study.

- ⇐ Petrographic samples (from the upper and lower Tahara sandstone)
 - Palynological samples (from shale sections)
 - ⇐ Samples from heterolithic facies for petrography and XRD analysis of ironstone composition
 - ⇐ Palynological samples examined by CPT (L)
- No horizontal scale

1.4-Regional geology of the area

1.4.1-Tectonic framework

Libya is located on the Mediterranean foreland of the African shield, a foreland that has been the site of deposition of vast blankets of continental debris interrupted by several marine incursions (Conant and Goudarzi 1967). Tectonically Libya is affected by two sets of faults, which are thought to parallel the rift system in the Gulf of Suez and east Africa (Conant and Goudarzi 1967). The geology of Libya can be divided into four depositional basins separated by major anticlinal swells (Fig. 1.3). These basins, of intracratonic type, have been effected by the Palaeozoic Caledonian and Hercynian orogenies (Bellini and Massa 1980). The Caledonian orogeny occurred from the middle Silurian to the lower part of the lower Devonian, and its influence can be traced into northern Chad and Niger. The Hercynian orogeny occurred in the middle to upper Carboniferous and possibly into the Permian (Bellini and Massa 1980). Reactivation of these earlier Palaeozoic structures during Cretaceous, middle Tertiary (Oligocene through Miocene) and Holocene times led to faulting, folding, subsidence and uplift (Goudarzi 1980). The Gargaf arch, Tibisti-Al Haruj uplift and Nafusa uplift represent the events that formed the structural and tectonic features in the south and northwest of Libya (Fig. 1.3). A palaeocurrent study of the Palaeozoic basins of Libya shows that the Palaeozoic structural arches controlled the sedimentary fill (Clark-Lowes 1985). A brief review of the Ghadames and Murzuq basins to the north and south of the study area is presented.

1.4.2-Ghadames basin

The Ghadames is bounded on the south by the Gargaf arch and on the east by the Hun graben and the Sirte embayment (Sirte basin). On the west the basin extends into Algeria and forms one of the largest basement depressions in Africa. The basin was affected by the Caledonian orogeny and in the south the Al

Gargaf arch separates it from the Gadames and Murzuq basin (Fig. 1.3). The northern part of the basin was uplifted during Hercynian folding followed by subsidence during the early Mesozoic.

The basin is filled by mainly Palaeozoic sediment overlain by a relatively thin Mesozoic–Tertiary sequence. Most of the Palaeozoic sediments consist of sandstones deposited in continental, transitional and marine environments. Palaeozoic sediments are thickest in the centre of the basin but thin gradually towards the southern margin of the basin which flanks the Al Gargaf arch (Hammuda 1980).

1.4.3-Murzuq basin

The Murzuq basin lies between the Sahara shield in the south and was separated from the Tethys Ocean by the Gargaf arch (Selley 1976a; Bellini and Massa 1980). It is located between three prominent tectonic elements: Al Gargaf uplift in the north, Tibesti-Haruj uplift in the east and the Precambrian Hoggar on the south which extends into Algeria and Niger (Fig. 1.3). The Murzuq basin is a good example of a cratonic basin (Selley 1976a). It was affected by late Hercynian movements towards the end of Viséan times and was totally emergent by the end of Baskirian times. Subsidence took place in late Silurian and early Devonian times.

The basin fill extends from the Cambrian to the Carboniferous with some Mesozoic and Cenozoic sediments also present. Palaeocurrent analysis of fluvial Cambro-Ordovician and Mesozoic sediments delineates a northerly palaeoslope over the Gargaf arch (Selley 1976a). The Cambrian to upper Devonian succession is characterised by fluvial, estuarine-deltaic and shallow-marine deposits, whereas the lower to middle Carboniferous is dominated by open-marine shales with sandstones and limestones. Ordovician sandstones of the Memouniat Formation constitute the known reservoirs in this basin.

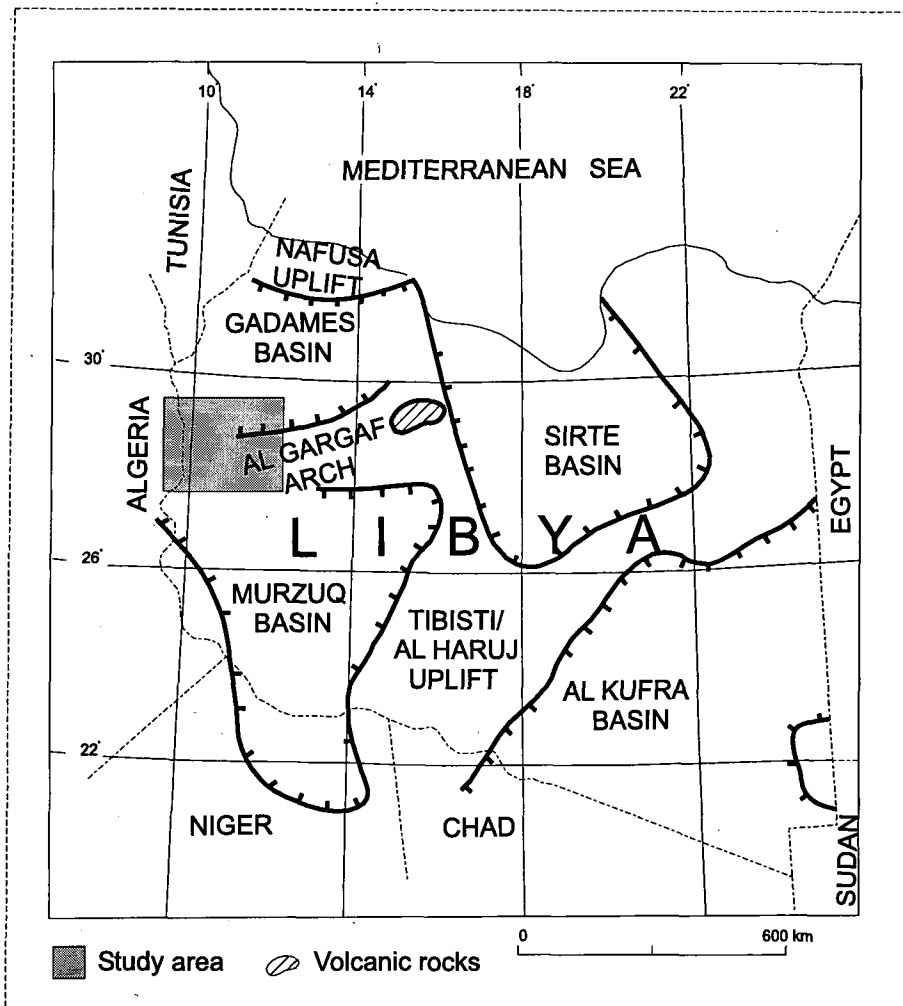


Fig. 1.3 Location map of the sedimentary basins of Libya.

1.4.4-Geological setting

The Palaeozoic in western Libya extends from the Cambrian to the Carboniferous. Undifferentiated basal Cambrian to lower Ordovician rocks are exposed in many places in southern Libya and consists of conglomeratic and coarse continental sandstones which pass upward into Ordovician sandstone, shale and diamictites with thicknesses of about 610-914 m known from the Murzuq and Al Kufra basins. Continental sediments, interrupted by minor marine transgressions in western Libya, extend across the southern border into Chad

and Niger where fine clastics with marine fossils were deposited. These are overlain by Silurian rocks indicative of a major marine transgression which extends into Chad and Niger. Silurian strata in the Murzuq basin are characterised by graptolitic shales (305 m thick) which grade upwards into thick regressive sandstones. Devonian strata in southern Libya comprise mainly continental sandstones about 305 m thick with marine beds known on the east and on the western flanks of the Murzuq basin. In the Ghadames basin the Devonian consists of two facies: the Fazzan facies, which corresponds to littoral clastic deposits; and an open-marine facies of shale with rare carbonate intercalations (Bellini and Massa 1980). The Carboniferous rocks are represented by the late Palaeozoic marine cycles. These consist of thick sequences, up to 914 m, of marine and non-marine fine clastics and subordinate limestone. Transgressive Carboniferous sediments show a mixed marine and lagoonal facies dated as upper Tournasian in age. Red continental sediments were deposited during the upper Carboniferous. Further details of the Palaeozoic succession are discussed below based on Bellini and Massa (1980), and the stratigraphic nomenclature and names of formations used by the Sirte Oil Company (SOC; Fig. 1.4). The same nomenclature is used in both basins because of their close genetic association (Bellini and Massa 1980).

Mourizidie Formation: Cambrian

Mourizidie Formation is well developed in the southeast of the Murzuq basin and may be sporadically present in the northern Ghadames basin (Bellini and Massa 1980). The sediments of this formation are overlain by the basal conglomerate of the horizontal strata of the Hassaona Formation.

Hassaona Formation: Cambrian

Hassaona Formation was introduced by Massa and Collomb (1960) after Jabal Hassaona. It is about 340 m thick and consists of medium to coarse-grained cross-bedded sandstone, containing *Tigillite*, *Cruziana* and *Harlania*. The

formation is unconformably overlain by fine-grained Ordovician clastics, but in the subsurface they are difficult to distinguish from one other (Pierobon 1991).

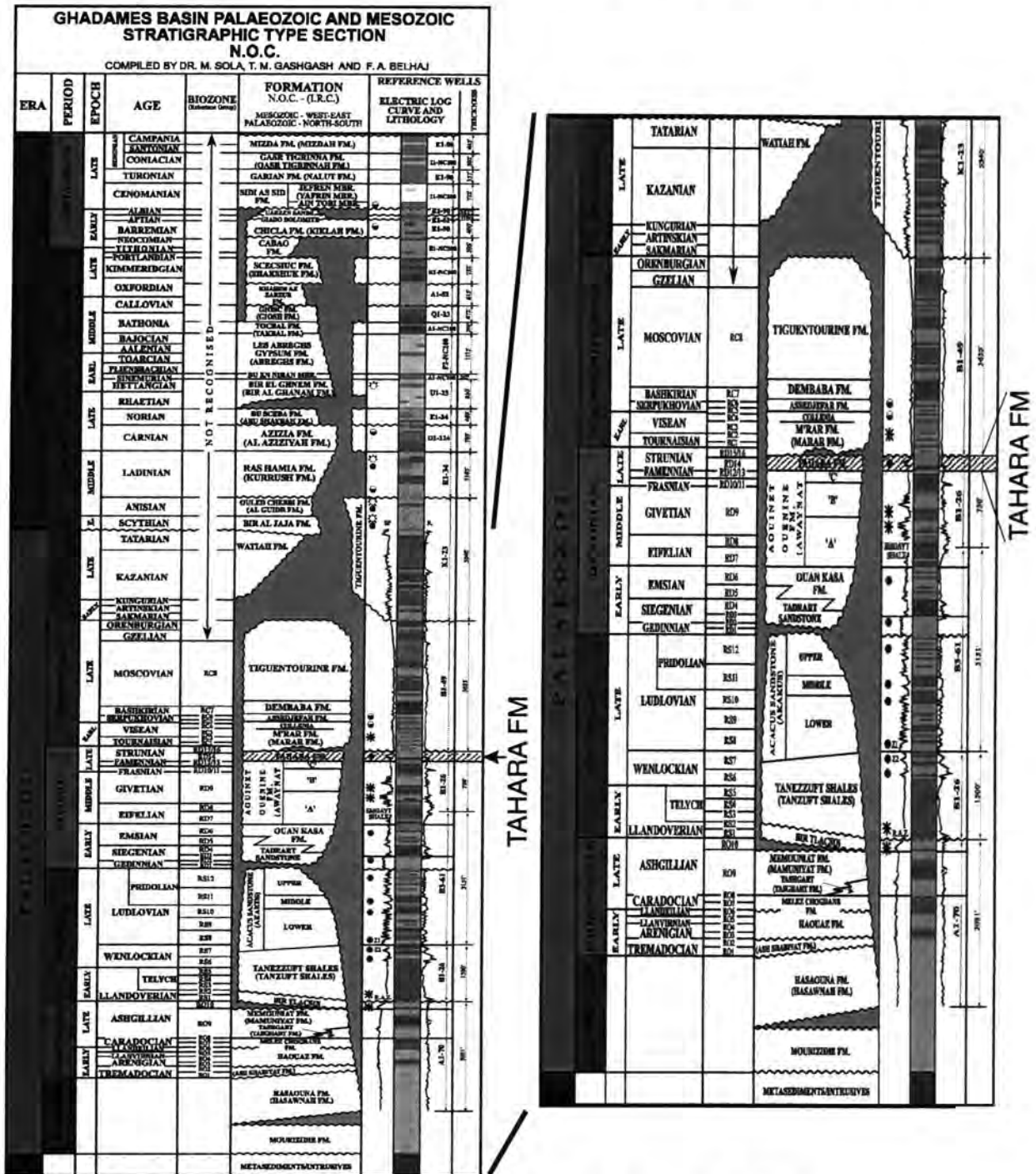


Fig. 1.4 Stratigraphic column of the Palaeozoic (See blow up on right for details) and Mesozoic, Ghadames basin, Western Libya.

Ashebyat Formation: Ordovician (Tremadocian)

Ashebyat Formation is represented by some 65 m of medium- to coarse-grained sandstone with abundant *Tigillites*, *Cruziana* and *Harlania*, and is transitional between the Cambrian and basal middle Ordovician (Bellini and Massa 1980). The Achybyat and Hassaona Formations are very similar in their lithology (Pierobon 1991).

Haouaz Formation: Middle Ordovician (Lianvirn-Liandeilo)

Haouaz Formation was defined by Massa and Collomb (1960) for the southern part of the Ghadames basin. It consists of fine-grained, cross-bedded quartzitic sandstone with thin shale intercalations and abundant *Tigillites* and stromatolites, with possible ferruginous ooids at its base (Bellini and Massa 1980). It is conformably overlain by the Melez Chograne Formation. A similar type section is described by Clark-Lowes (1985) in the Ghat region. The Haouaz Formation, on the other hand, described from a 120 m thick section in the central western Gargaf Arch, has been interpreted as a fan-delta system (Vos 1981a). The Formation ranges in thickness from 50 m (Dor al Qussah) to 280 m (Al Qargaf) and from 30-170 m in the subsurface (Pierobon 1991). Haouaz Formation is probably of middle Ordovician age (Lianvirn-Liandeilo) (Klitzsch (1981).

Melez Chograne Formation (Caradocian)

Melez Chograne Formation was introduced by Massa and Collomb (1960) from a 60 m thick type section in the southern part of the Ghadames basin. It characterised by an abundant fauna of trilobites, cystoides, bryozoans and brachiopods (Bellini and Massa 1980). This formation represents marine transgressive environments, and is Caradocian in age based on the first glacial-marine cycle (Bellini and Massa 1980).

Memouniat Formation (Ashgillian)

Memouniat Formation was introduced by Massa and Colomb (1960) based on a type section (up to 150 m thick) in the southern part of the Ghadames basin. It consists mainly of fine-grained sandstone and coarse-grained conglomeratic sandstone, with rare fauna, containing Ashgillian brachiopods (*Hirnantia* and *Plectothyrella*). It represents the second glacial-marine cycle, and is conformably overlain by Tanezzuft Shale of Silurian age (Klitzsch 1981).

Tanezzuft Formation: Silurian (Llandoveryian)

Tanezzuft Formation was described from outcrops 200-300 m thick in the Ghat area from Wadi Tanezzuft, Jabal Akakus. It consists mainly of shale with thin beds of siltstone and fine-grained sandstone organized into discrete depositional packages, containing marine fossils. The Tanezzuft shales are conformably overlain by the Acacus Formation. This formation represents the principle Palaeozoic source rock.

Acacus Formation: Silurian (Llandoveryian-Ludlovian)

Acacus Formation is about 150 m thick. It consists predominantly of sandstone with subordinate alternations of shale and siltstone. Bellini and Massa (1980) pointed out that the distinction between this formation and the underlying Tanezzuft Formation is not clear due to the gradational contact between them. Furthermore, from south to north a facies change occurs as the sandy fluvial-transitional Acacus Formation of the Ghat area is replaced by a sandy-shale marine unit in the northern Ghadames area (Castro *et al.*, 1991). The Acacus Formation has been dated middle Llandoveryian on the basis of graptolites found at its base (Bellini and Massa 1980), whereas the palynological data from wells A1-NC115 and E1-NC115 (south of study area) indicate a Ludlovian to Wenlockian age (Pierobon 1991). This formation represents the transgressive phase of the early Silurian (Pierobon 1991). In Dur al Qussah the Acacus Formation is a rhythmic alternation of shale, shaley siltstone and sandstone

which coarsens upward into massive, cross-bedded fluviatile sandstone (Pierobon 1991).

Tadrart Formation: Devonian (Siegenian)

Tadrart Formation is defined by the (International Stratigraphic Lexicon in Bellini and Massa 1980) from a type section in western Jabal Fezzan in the Awinat Wanin area where it is 317 m thick (Klitzsch in Clark-Lowes 1985). The formation comprises fine- to very fine-grained sandstone and subordinate siltstone. The lower part is thick-bedded and cross-bedded, and contains rare plant remains deposited in a predominantly continental environment. The upper part is thin-bedded and shows evidence of biogenic activity consistent with a marine environment. This formation is conformably overlain by the Ouan Kasa Formation. The basal part is marked by a ferruginous sandstone resting unconformably on Silurian rocks. Tadrart sandstones are usually poorly cemented and a good reservoir.

Ouan Kasa Formation: Devonian (Emsian)

Ouan Kasa Formation at Wadi Wan Kasa, in the Murzuq basin, is 43 m thick. It consists of a succession of shale interbedded with siltstone and fine-grained sandstone. It was first measured by Borghi *et al.* (in Clark-Lowes 1985) and later described by Klitzsch (in Clark-Lowes 1985). Subsurface data in the Ghadames basin reveal a rich assemblage of palynomorphs indicative of an Emsian age (Massa and Moreau-Beroit 1976). The Ouan Kasa is overlain conformably by the Aouinate Ouenine Formation.

Aouinate Ouenine Formation: Devonian (Couvianian-Famennian)

Aouinate Ouenine Formation was defined from western Jabal Al Qargaf. The Aouinate Ouenine Formation is raised to the rank of group where it is divided into four formations (I to IV) ranging in age from Couvianian to Famennian on the basis of the micro- macro fauna as well as microflora (Bellini and Massa 1980). Clark-

Lowes (1985) reported a thickness of 107 m in the Murzuq basin. This formation is composed of very fine- to medium-grained sandstone and thin argillaceous siltstone beds containing an abundant fauna of brachiopods and bivalves.

A 150 m thick section of this formation exposed along the northern flank of the Gargaf Arch in Ghadames basin has been studied by Vos (1981b). He recognized three cycles, and interpreted them as a deltaic complex containing both progradational and transgressive facies. More recently Castro *et al.* (1991) reported tempestite deposits from the third cycle of Vos's study. The Formation is conformably overlain by the Tahara Formation.

Tahara Formation: Devonian-Carboniferous (Strunian)

Tahara Formation has been defined in Compagnie des Petroles Total (Libya) (CPT (L)) from well B1-49 (within study area) which is located in Wadi Tahara. This formation consists of sandstone and shale in which the sandstones are generally fine- to very fine-grained, feldspathic and commonly ferruginous and hematitic (Bellini and Massa 1980). It was interpreted as a deltaic deposit with continental influences and plant debris (Lycophytes). Palynological studies assign the formation to the Strunian (Devonian-Carboniferous transition; Bellini and Massa 1980) due to the presence of *Spelaeotriletes lepidophytus* (Kedo) and *Hymenozonotriletes lepidophytus*. The Tahara Formation may mark the end of the Devonian (Bracaccia *et al.*, 1991).

Castro *et al.* (1991) described tempestites from the lower part of the Tahara Formation in the Murzuq basin. The Tahara Formation has similarities with the Aouinate Ouenine Formation (IV). Bracaccia *et al.* (1991) suggested that this formation together with the Aouinate Ouenine Formation (IV) was deposited as a single sedimentary cycle. Furthermore, Weyant and Massa (1991) argued that the Tahara Formation and underlying Aouinat Ouenine Formation (IV) represent the final cycle of Devonian age. These two formations make up the Strunian and the Famennian, and it is difficult to distinguish between them despite the abundant spores (Weyant and Massa 1991). In the Ghadames basin, it is a

subsidence (Massa and Moren- Beroit 1976). The M'rar Formation conformably overlies the Tahara Formation.

M'rar Formation: Carboniferous (Tournasian-Viséan)

M'rar Formation, described from Awaynat Wanin-Dembaba (type section) and core in well B1-49 and A1-49 (Billini and Massa 1980) is over 800 m thick at the type section locality. The M'rar Formation consists of silty shale intercalated with sandstone and siltstone. Sandstone within this formation (M2 member, informal nomenclature of Sirte Oil Company), described from wells in western Libya, is well sorted, fine- to very fine-grained, with subangular to subrounded grains and slightly calcareous. It contains traces of mica and has excellent porosity (Machinsky *et al.*, 1987). The M'rar Formation is known to contain significant gas shows and has oil potential. It comprises deltaic deposits developed on relatively stable cratonic areas which contain 15, dominantly coarsening-upward, depositional cycles (Whitbread and Kelling 1982). In the present study the base of this formation is recognized in well C1-49 where shale was deposited above the upper Tahara sandstone (based on the core data and palynological samples). Thus, the basal part of the M'rar Formation forms the cap rock and possible hydrocarbon source for many of the producing reservoirs in the underlying Tahara sandstones.

Assedjefar Formation: Carboniferous (Serpukhovian-Lower Moscovian)

Assedjefar Formation is also described from the Awaynat Wanin-Dembaba type section and core in well B1-49 and A1-49 (Bellini and Massa 1980). The lower part consists of thick sandstone with abundant Lycophytes, whereas the upper part consists of shale and limestone (Bellini and Massa 1980). The upper contact of the Assedjefar Formation is conformable with the overlying Dembaba Formation.

Dembaba Formation: Carboniferous (Bashkirian-Lower Moscovian)

The Dembaba Formation is a marine to transitional sequence of carbonates (limestone and dolomitic marls), locally intercalated with thin, very fine to fine-grained sandstone. Based on the brachiopods and foraminifera, Bellini and Massa (1980) suggested that the lower Dembaba was Bashkirian whereas the upper was lower Moscovian.

Burollet (1960) divided this formation into three members: an upper limestone member with a rich fauna of productids and gastropods; a middle shale member with local sandy dolomitic beds and rare gypsum; and a lower limestone and marl member intercalated with dolomite and green shale. The Dembaba Formation passes gradationally upwards into the overlying Tiguentourine Formation.

Tiguentourine Formation: Upper Carboniferous

The Tiguentourine Formation is recognized from outcrops south of Al Hamada al Hamra (Ghadames basin) and from subsurface data (well A1-49 and B1-49) in the southern part of the Ghadames basin. This formation is described from Algeria (near Algeria-Libya boundary) where thicknesses reach 300 m. It consists of homogeneous red-brown dolomitic shale and layers of shaly dolomite and anhydrite.

Chapter 2

Sedimentary Facies

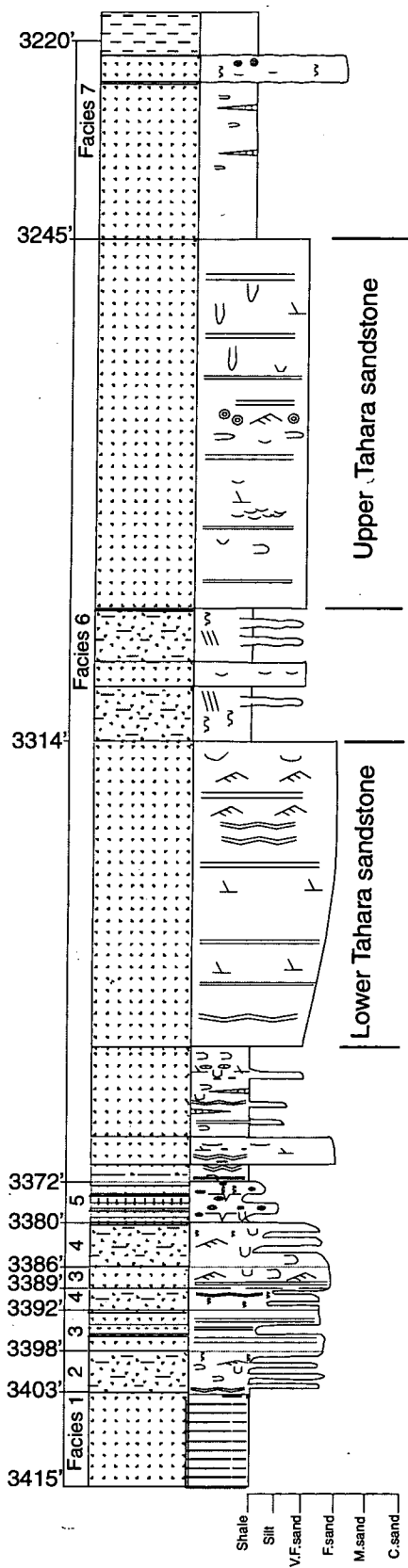
2.1-Introduction

Facies is defined as a body of rock with specific features (Reading 1986; Walker 1992). It can be classified on the basis of bedding, composition, texture, biogenic features and sedimentary structures. Facies analysis from borehole cores provides a reliable method for subsurface study, particularly where cores are continuous and include the boundary between facies. Facies can then be subdivided into subfacies or grouped into facies associations or assemblages, which provide the basis for interpretation of the depositional environment.

This study has been carried out on slabbed cores and has focused mainly on lithofacies analysis, vertical facies sequences in each of the wells, and lateral facies relationships between wells. The vertical relationships and characteristic sedimentary structures of each facies identified in the wells are presented in Fig. 2.1. Facies analysis and analogue modelling of modern depositional environments suggest that most of the sediments were deposited in shallow-water marginal and nearshore-marine environments characterised by waves and storms. The analysis and interpretation of the core succession allow seven facies to be recognised based on core and electric log data from type well C1-49, supplemented by core data and wireline log data from the other 5 wells (K1-1, A1-NC151, ATS1, ATS2 and B1-49) (Fig. 1.1). Each facies is identified on the basis of lithology, sedimentary structures and biogenic features. The first four facies have been grouped into a facies association (Table 2.1).

Facies	Description	Interpretation
1-Laminated shale 2-Interlaminated to bioturbated shale (60%) and sandstone (40%) 3-Parallel laminated and ripple cross-laminated sandstone 4-Bioturbated sandstone and shale	<p>Black to dark-grey, micaceous, silty, horizontally laminated with sand and silt lenses, slightly bioturbated.</p> <p>Shale, dark-grey to yellowish-grey, horizontal to subhorizontal, wavy laminae. Sandstone is light grey, very fine-grained, well sorted, laminated with symmetrical to asymmetrical ripples and hummocky cross-stratification. Locally highly bioturbated (<i>Skolithos</i>, <i>Chondrites</i>).</p> <p>Sandstone, fine to very fine-grained, carbonaceous, parallel laminae, locally massive. Small-scale, low angle cross lamination interpreted as hummocky cross-stratification, parallel to subparallel lamination, wavy, interlaminated sandstone and mudstone, slightly bioturbated (<i>Skolithos</i>, <i>Chondrites</i>).</p> <p>Sandstone (75-60%), fine-grained, well sorted, mottled, laminated, flaser bedding, ripple profiles. Shale (25-40%), light brownish-grey, wavy, highly bioturbated, (<i>Skolithos</i> or? <i>Arenicolites</i>, <i>Diplocraterion</i>, <i>Chondrites</i>).</p>	Shelf- Nearshore
5-Heterolithic	Ironstone, silty shale, mudstone, sandstone, varicoloured, bioturbated, oolitic, sideritic nodules, desiccation cracks.	Lagoonal, periodic exposure
6-Planar cross-bedded and horizontally laminated sandstone and shale	<p>Sandstone (80%), fine to very fine-grained, white, light grey, micaceous, carbonaceous, well-sorted. Subordinate shale, dark grey to brownish-grey, highly micaceous and carbonaceous detritus.</p> <p>Subfacies (a) (lower part) consists of shale with silt and sand laminae; some beds, contain vertical and horizontal burrows (<i>Skolithos</i> and <i>Chondrites</i>). This package is overlain by horizontally laminated and structureless sandstone grading up into planar cross-bedded sandstone with small-scale ripple cross-lamination and flaser type laminae.</p> <p>Subfacies (b) (upper part) consists of interlaminated to bioturbated shale and sand followed by horizontally laminated, structureless and subordinate cross-bedded sandstone. Abundant shell fragments and <i>Skolithos</i>, <i>Planolites</i>, <i>Chondrites</i>. A subordinate, 80 cm thick muddy sandstone, contains carbonaceous material and ooids (mm's in diameter).</p>	Shelf-Shoreface/ Fluvio-deltaic (The latter reported only from well C1-49) Shelf-Shoreface
7-Shale	Dark to medium dark grey, micaceous, pyritic, slightly bioturbated. A subordinate bioturbated sandstone bed containing shell fragments, rip-up clasts and oolites occurs.	Shelf

Table 2.1 Description and interpretation of the facies recognized from the succession in the study area. For more details see text.



Key

- | | | | |
|--|-------------------------------|--|----------------------------|
| | Ripple Cross-Lamination | | Abrupt Contact |
| | Wavy and Irregular Lamination | | Gradational Contact |
| | Bioturbation/Mottled | | Vertical/Oblique Burrow |
| | Planar Cross-Lamination | | Horizontal Burrow |
| | Parallel Lamination | | Shell Fragments |
| | Planar Cross-Bedding | | Oolites |
| | Rip-up Clasts/Coalified wood | | |
| | Flaser/Lenticular Bedding | | |
| | Structureless/Massive | | |
| | Desiccation Cracks | | |
| | Sandstone | | Sandstone/Shale |
| | Shale | | Shale/Siltstone/Sandstone |
| | Ironstone | | Sandstone/Siltstone Lenses |

Fig. 2.1 Lithology and sedimentary structures for the cored interval between 1041 m (3415') and 981 m (3220') in type well C1-49.

2.2-Description and Interpretation of Facies

The maximum vertical succession is approximately 67 m (220') in type well C1-49 (Fig. 2.1). The sedimentary facies and their lithological, sedimentological and biogenic characteristics are described below:

2.2.1-Laminated shale

Description

This facies is restricted to the lowermost part of the succession and is represented by the cored interval from 1041 to 1037 m in well C1-49 (Fig 2.2). It consists of horizontally-laminated shale with between 10-20% of very fine-grained sandstone and siltstone.

The shale is black to dark-grey, locally brownish black, highly micaceous, and silty in character with fine sub-mm thick, horizontal laminae. The subordinate sandstone and siltstone occur as parallel to very gently inclined, mm to sub-mm thick laminae and lenses within the shale. These commonly have sharp bases and locally diffuse tops, gradational into siltstone and/or shale. Very rare small-scale ripple cross-lamination < 1 cm thick is present in the sandstone and siltstone.

About 10% of the total facies is bioturbated. Burrows, which occur within the shale laminae, are < 5 mm long and mostly vertical to oblique but with some horizontal burrows up to 2 mm in diameter. The burrows are filled with very fine sandstone and/or siltstone. A dark reddish brown ironstone bed 2 cm to 4.5 cm thick is prominent at the top, and along the base of the facies (Fig. 2.2). The top ironstone bed is nodular with individual nodules < 2 cm long, containing small-scale vertical to horizontal cracks, possibly filled with white kaolinite clay.

Interpretation

Since the dominant lithology of this facies is fissile dark-grey to black shale with minor siltstone and/or sandstone laminae, the most likely depositional setting is a quiet-water marine environment (De Raaf, *et al.*, 1965; Hein *et al.*, 1991). The weak bioturbation and lack of body fossils imply an oxygen-deficient environment, unsuitable for supporting an extensive benthic fauna. Black shale facies are characterised by variations in the oxygen conditions under which they accumulated (Johnson and Baldwin 1996). The dark-grey to black colour of the shale probably represents the high content of very fine carbonaceous detritus, whereas the presence of horizontal laminae indicates deposition mainly from suspension under low-energy conditions such as an offshore shelf (Johnson and Friedman 1969). Mud and silt were probably washed onto the shelf by rivers, especially during flood events, and by shelf storm events as documented below.

The facies shows subtle changes in colour from darker shale to lighter siltstone/sandstone indicating periodic changes in sedimentation rates from relatively slow to fast. Weak grading is developed in the paler sandy and silty laminae and lenses. The sand laminae and lenses probably record storm events on the shelf throwing sediment into suspension, followed by traction currents and the development of small ripple bedforms, subsequently preserved by fine suspension deposits (Reineck and Singh 1972). The laminae commonly have sharp bases and locally diffuse tops, features characteristic of shelf storm deposits (tempestites). Graded layers have been attributed to diverse causes in different environments (Clifton 1969; Figueiredo *et al.*, 1982). On marine shelves thin graded layers may reflect deposition from distal storm-generated flows which alternated with mud deposited from suspension during fair-weather (Johnson and Baldwin 1996). Swift (1969) argued strongly that storms on shelves generate graded deposits. Reineck and Singh (1972; 1973) interpreted a couplet of coarse and fine sediments in the North Sea as a storm deposit, and Kumar and Sanders (1976) described storm deposits in cores from the nearshore environment in New York and Virginia. They argued that the sand was dispersed in turbulent

suspension or transported into the offshore. Thin laminated sand with possible ripple profiles was rapidly deposited out of suspension as the storm waned.

The facies is locally reddish brown in colour due to the presence of iron minerals within the sediment. Locally developed ironstone, however, typically accumulates in a marine or near marginal setting. The ironstone nodules suggest an early diagenetic origin as explained in detail below.

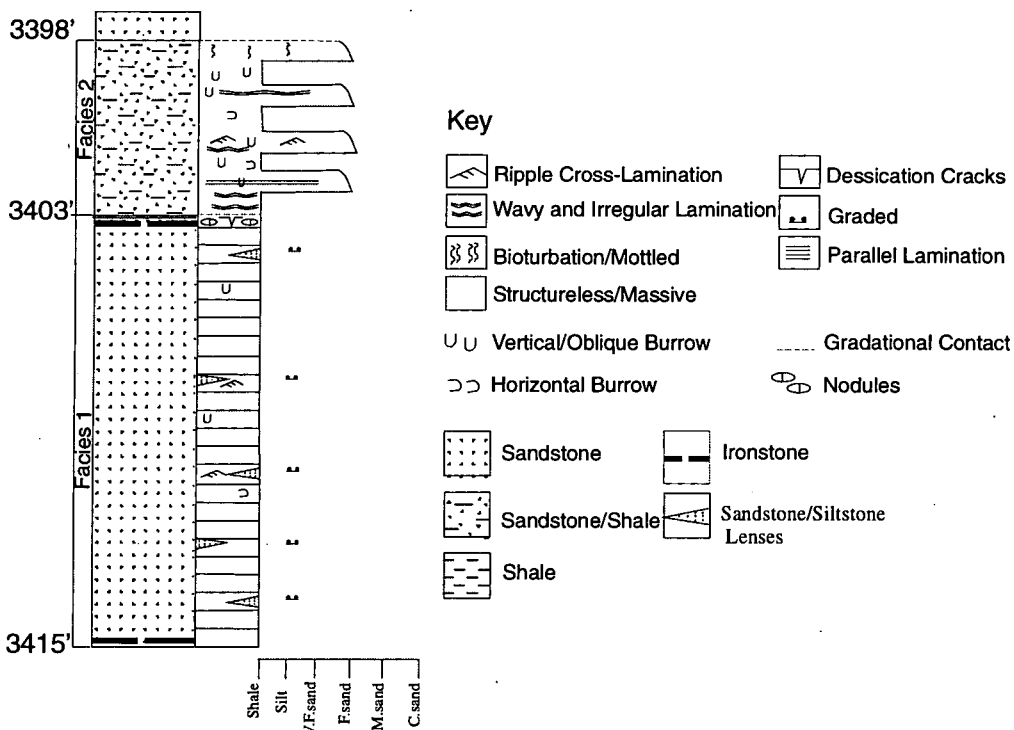


Fig. 2.2 Detailed section for the cored interval between 1041 m (3415') and 1036 m (3398') in well C1-49, showing Facies 1 and 2 (Table 2.1).

2.2.2-Interlaminated and bioturbated shale and sandstone

Description

This facies, represented by the cored interval 1037 m to 1036 m in well C1-49 (Fig. 2.2), and the cored interval 1310 m to 1309 m from well K1-1 gradationally overlies the laminated shale facies. It consists of irregularly interlaminated shale (60%) and sandstone (40%), and is commonly moderately bioturbated.

The shale is dark-grey to black with horizontal to subhorizontal and irregular wavy laminae < 1 cm thick. The laminae generally have sharp bases and tops, some grade into siltstone. Millimetre to sub-mm thick streaks and lenses of fine sandstone and siltstone up to 1 cm long appear to "float" within the shale. Burrows occur in the shale and are prominent on bedding surfaces. These are < 1 cm long, vertical to oblique and locally curved. Horizontal burrows less than 1 cm in diameter, filled by siltstone, also occur. The sandstone is light grey, very fine-grained, well-sorted and mature with individual grains predominantly rounded to subrounded. It occurs as irregular laminae and beds a few mm's to 1.5 cm thick, with sharply defined horizontal to subhorizontal inclined laminae. A subordinate sandstone bed from well C1-49 shows rare prominent hummocky cross-stratification up to 2.5 cm thick, interrupted by bioturbated shale. Vertical to subvertical burrows < 5 cm long, and < 5 mm wide occur throughout the sandstone. Burrows which occur within the facies include *Skolithos* and *Chondrites*.

Interpretation

The facies contains a trace-fossil assemblage which is considered to be the product of variable energy conditions in an open-marine environment (Frey and Pemberton 1984). The increase in sand content from the underlying laminated shale facies, and gradational contact between them, indicates that generally they form part of the same progradational succession. The irregular alternation between sand and shale reflects alternating periods of high and low-energy, and

fluctuations in sediment supply and current velocity, typical of shelf storm events, as described by De Raaf *et al.* (1965). The dominance of shale and thinner siltstone and sandstone indicate a shelf receiving mainly fine-grained detritus (Turner 1980). The sharp bases and tops to sandstone laminae are considered to have been emplaced by storm conditions. Furthermore, sharp laminae are indicative of rapid emplacement of sediment concomitant with high flow velocities. The parallel and subparallel lamination was possibly created by wave generated currents above wave base (Rine and Ginsburg 1985; Hamblin and Walker 1979).

The sandstone locally shows hummocky cross-stratification. The latter was originally defined by Harms *et al.* (1975) who suggested that the long, low undulating bedforms were produced by storm wave energy below fair-weather wave-base. Hummocky cross-stratification interrupted by bioturbation suggests that the latter were developed during fair-weather conditions. Sandstone layers may form from settling of suspension clouds during floods when abundant fine sand is flushed on to marine shelves, especially during river floods. The presence of escape burrows within the sandstone suggests storm sand layers. This facies is interpreted to represent deposition in a marine-shelf setting.

2.2.3-Parallel laminated and ripple cross-laminated sandstone

Description

This facies represents the interval from 1036 m to 1034 m and 1033 m to 1032 m in well C1-49 (Fig. 2.3a). The sandstone contains parallel lamination and small-scale, low-angle ripple cross-lamination interpreted as hummocky cross-stratification (Figs 2.4 and 2.5). The sandstone consists predominantly of clean, micaceous, fine to very fine-grained sandstone containing disseminated fine-grained carbonaceous detritus. The laminae, which range from 5 mm to < 1 cm thick, are defined by very thin mm to sub-mm thick, carbonaceous drapes. Some sandstones are massive or indistinctly laminated.

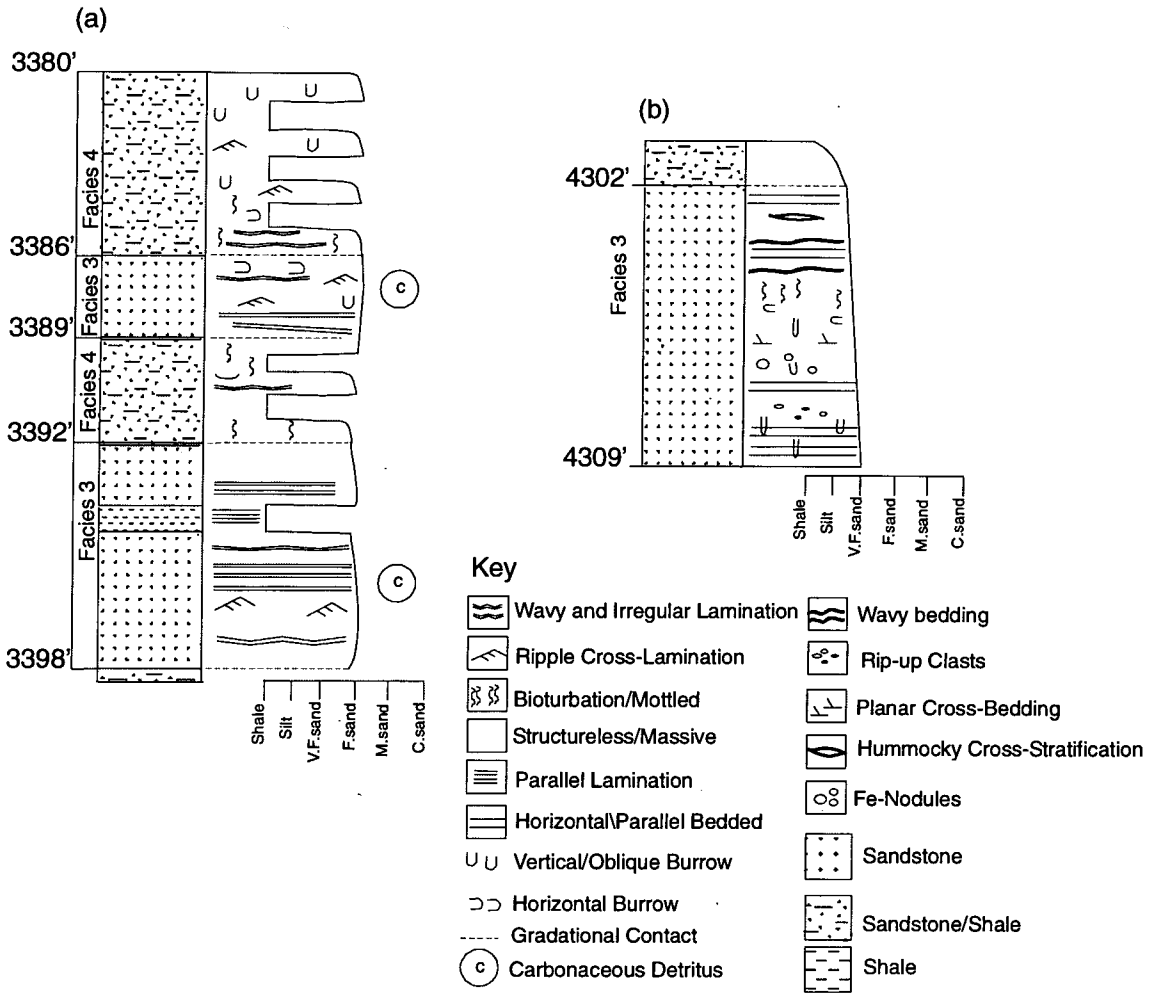


Fig. 2.3 Detailed section for the cored interval (a) 1036 m (3398') and 1030 m (3380') in well C-1-49 and (b) 1313 m (4309') to 1311 m (4302') in well K-1-1, illustrating facies 3 and 4 (Table 2.1).

The facies locally consists of thin, irregularly interlaminated sandstone and greyish-brown shale. A subordinate 50 cm thick shale bed, containing mm to sub-mm thick streaks and lenses of fine sandstone and/or siltstone occurs in the middle of the facies (Fig. 2.3a). Burrows occur, mainly associated with the shale, but some also occur in sandstone. They are predominately horizontal, < 1 cm in diameter, and filled with light grey siltstone or very fine sandstone. A few small, narrow vertical burrows < 1 cm long also occur in the sandstone. The burrows include *Skolithos* and *Chondrites* (Fig. 2.6)

WELL NO: C1-49. CORE No. 15
BOX No. 1
DEPTH 3386 ft.-3390 ft.



Fig. 2.4 Slabbed core sample from well C1-49 showing parallel lamination in the lower part overlain by hummocky cross-stratification, emphasised by very thin mm thick carbonaceous drapes. Arrows show curvature of lamination within the hummocky cross-stratification.

This facies is similar to the facies in the cored interval 1313 m to 1311 m in well K1-1 (Fig. 2.3b). This interval consists predominantly of sandstone and subordinate shale (10%), and is mainly structured by horizontal bedding and low-angle cross-stratification. The lower part of the facies, with an overall thickness of 90 cm, is characterised by horizontally-bedded sandstone containing vertical burrows up to 5 cm long, and rip-up mud clasts < 3 cm in diameter. The latter rarely occur in the upper part of this facies and show a distinct fabric parallel to bedding. Individual beds are > 1.5 cm thick, with local thicker sandstone beds ranging from 3 cm to 12 cm but with poorly developed sedimentary structures. This lower part is followed by a 15 cm thick bioturbated sandstone with ferruginous nodules 2 cm in diameter, which is directly overlain by low-angle

cross-bedded sandstone that passes upwards into bioturbated and mottled sandstone with minor shale. This in turn grades upwards into horizontal and wavy-bedded sandstone locally interbedded with shale.

The sandstone locally shows prominent hummocky cross-stratification in 2 cm thick sets, defined by mud drapes, near the top of the facies. Shale occurs throughout the facies as 1.5 cm to 3 cm thick beds with mm to sub-mm thick streaks of siltstone with sharp bases and tops. The shale is usually dark-grey in colour. Most of the facies is slightly bioturbated, but in some cases bioturbation is locally intense and some sandstone beds are thoroughly burrowed and homogenised. The burrows occur mostly as narrow tubes up to 5 cm long and up to 5 mm wide. Small horizontal burrows a few mm's in diameter, associated with the shale, also occur. The dominant burrows encountered within the facies are *Skolithos*, *Arenicolites* and *Planolites* (Fig. 2.6).

Interpretation

Parallel-laminated sandstone, defined by thin carbonaceous drapes, may be the product of either lower or upper flow regime, plane-bed conditions. The most common type of parallel lamination is that produced by microturbulent bed-load segregation during upper plane bed conditions. Lamination produced in this way is laterally more persistent and characterised uniquely by parting lineations preserved on bedding surfaces, none of which was directly observed in the core. Parallel-laminated sand is the dominant physical sedimentary structure formed in the nearshore facies according to Howard and Reineck (1981). Parallel lamination and low-angle cross-stratification, interpreted to represent hummocky cross-stratification (Fig. 2.5), suggest deposition by storm events below fair-weather wave-base (Harms *et al.*, 1975; Hamblin and Walker 1979; Dott and Bourgeois 1982). The recognition of hummocky cross-stratification is useful for environmental interpretation, because it develops in the coarser siltstone or fine to very fine-grained sandstone deposited in wave-dominated shallow-marine environments (Duke 1985). Some sandstones lack structure either due to small contrasts in mean grain size of the adjacent laminae, or an influx of rapidly

deposited storm sand. The lower part of the facies in well K1-1 probably formed during storms when wave surge moved sand in suspension, much of it being transported seaward. The velocities of wave surges are able to move not only sands, but also rip-up clasts.

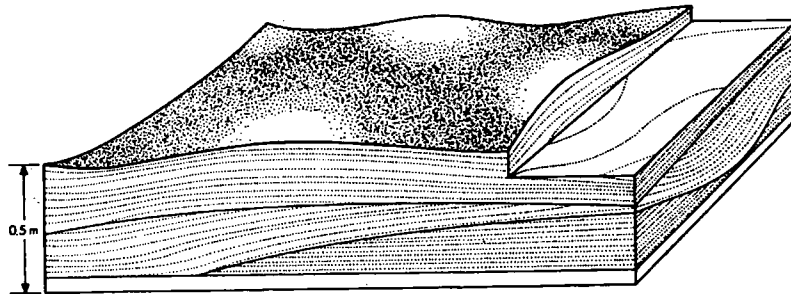


Fig. 2.5 Block diagram of hummocky cross-stratification. It is common in very fine shoreface-offshore sandstone (After Harms *et al.*, 1975).

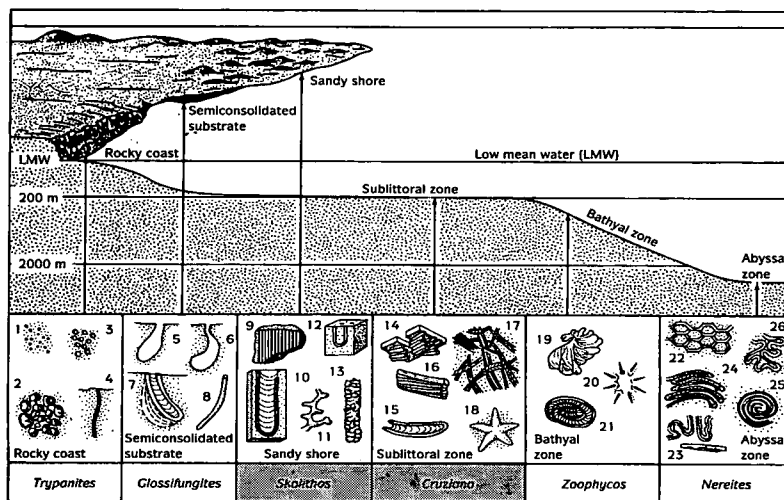


Fig. 2.6 Trace fossil associations in marine ichnofacies sets. The shaded area represents the facies constitute a mixed *Skolithos-Cruziana* ichnofacies found in the Tahara Formation of the study area (from Frey and Pemberton 1984).

The interlaminated sandstone and shale unit in this facies suggests variable depositional conditions and periodic higher energy currents affecting a normally quiet-water environment (Hein *et al.*, 1991). The thick shale bed within the facies from well C1-49 may have formed during a minor transgression and increased water depths. The bioturbation is minor, but in some cases bioturbation is locally intense (well K1-1) and the burrows belong to the *Cruziana* and *Skolithos* ichnofacies (Fig. 2.6). Nevertheless, the presence of these burrows represents variable energy conditions and suggests that they were deposited below fair-weather wave-base. The sharp bases of sandstone laminae and presence of predominantly horizontal burrows on the surface of the sediments probably indicates that the sediments were deposited by unusually high-energy short-term events (Rice 1984).

The facies is interpreted to represent a nearshore, storm deposit (Kumar and Sanders 1974; Vos 1977, 1981b). Such an environment has been described by Johnson and Friedman (1969) from a nearshore sand-bar environment in the Catskill deltaic complex (upper Devonian) in New York State.

2.2.4-Bioturbated sandstone and shale

Description

This facies, which consists of two subfacies (a) and (b), is represented by the cored intervals 1034 m to 1033 m and 1032 m to 1030 m from well C1-49 (Fig. 2.3a). The facies typically consists of intensely bioturbated sandstone (60%) and shale (40%). Subfacies (a) consists of mottled sandstone and shale, with irregularly laminated sandstone beds up to 2 cm thick whereas subfacies (b) consists of intensely bioturbated sandstone and shale, and locally massive to indistinctly laminated sandstone. Both subfacies comprise well-sorted, very fine sandstone to siltstone. Some sandstone beds and laminae show small-scale ripple profiles and burrows, but the latter are less common than in the shale. Very thin flaser-type laminae are present within the sandstone beds, which have sharp, irregular scoured bases and tops.

The shale is brownish to light brownish-grey and locally greyish-red. It forms irregular wavy to lenticular laminae < 1 cm thick containing mm thick streaks and lenses of sandstone and siltstone. Burrows occur throughout the facies, but are more concentrated in the shale than sandstone. The burrows are vertical, oblique and curved, from 1 mm to 1.5 cm wide, and up to 10 cm long. There are also horizontal burrows with diameters from 2 mm to 7 mm. The infill of large burrows are themselves burrows (Fig. 2.8). The burrows, which occur throughout the facies, are feeding-dwelling structures and include *Skolithos*, *Diplocraterion* and *Chondrites* (Fig. 2.6).

WELL No: C1-49. CORE No. 14
BOX No. 6
DEPTH 3376 ft.-3380 ft.



Fig. 2.7 Slabbed core sample from well C1-49 showing bioturbated sandstone and shale, with vertical and horizontal burrows. Note in-fill of large burrow (arrow) and obliteration of sedimentary structures by burrows, except for some remnant streaky wavy lamination.

The facies also occurs in the cored interval from 1311 m to 1310 m in K1-1. It is characterised by extensively bioturbated sandstone with an increase in the proportion of shale towards the top. The burrows within the facies have obliterated most of the original sedimentary structures, but where the sandstone is not so intensely bioturbated it shows streaky wavy to parallel lamination, and minor occurrences of small-scale low-angle cross-stratification in sets up to 2 cm thick. Burrows are dispersed throughout the facies from bottom to top. Most of these burrows are not identifiable, but they include vertical, curved and horizontal types, some of which show characteristics of the *Skolithos* and *Cruziana* ichnofacies (Fig. 2.6). Vertical burrows 2 cm to 3.5 cm long and up to 6 mm wide may include *Skolithos* or? *Arenicolites*.

Interpretation

The facies lacks hard body fossils but contains a well-preserved suite of trace fossils characteristic of shallow-marine environments. The trace-fossil assemblage is considered to be indicative of variable energy conditions in an open-marine setting between wave-base and storm wave-base (Ekdale *et al.*, 1984; Frey and Pemberton 1984). The abundance of vertical burrows may indicate higher energy, possibly shoaling conditions, enhanced by the preservation of the sedimentary structures and deep penetrating burrows (i.e. escape during high energy regime) (Frey and Pemberton 1984; Pemberton *et al.*, 1992; Fig. 2.7).

Coarser-grained material introduced by storm events was of a magnitude and frequency to permit bioturbation. The finer sediments deposited during calm water imply deposition in an offshore quieter water shelf setting. These coarser and finer deposits were subsequently totally bioturbated with the result that the sediments show little evidence of primary physical structures except for local traces of remnant stratification. This intense bioturbation is presumably due to low rates of sedimentation (Reineck and Singh 1973). Furthermore, bioturbation increases away from the shore as water depths increase and sediment becomes

finer-grained. Similar patterns of bioturbation are characteristic of typical nearshore shelf sequences.

The sedimentary structures observed, such as ripples and irregular laminae, suggest sedimentation under oscillatory waves or possibly wave reworking (Howard and Nelson 1982). The sharp-based sandstone beds are indicative of rapid emplacement of sediment consistent with strong flow velocities. Lenses and flaser bedding (Reineck and Wunderlich 1968) suggest intervals of bedload transport interspersed with quiet, slack-water conditions.

2.2.5-Heterolithic facies

The heterolithic facies is present in type well C1-49 and K1-1. In the lower sequence, in well ATS2, deposits with similar features occur but they also show some differences in biogenic structures, shale:sandstone ratio, and amount of ironstone compared to the facies in well C1-49 and K1-1. In view of this, these sediments of the heterolithic facies are described separately below and classified as type 1 and type 2 respectively.

1-Heterolithic type 1

Description

This facies represents the interval from 1030 m to 1028 m in well C1-49 (Fig. 2.8). It erosionally overlies the bioturbated sandstone and shale facies, and is composed of ironstone, silty shale and mudstone with subordinate siltstone and very fine sandstone. It is characterised by the presence of variable light grey to greenish-grey and moderate to light-brown colours.

The ironstone makes up about 60% of the total facies. It alternates irregularly with silty shale and mudstone; the contacts between them being sharp. The ironstone is bioturbated to massive, from 5 cm to 25 cm thick with disseminated ooids (Fig. 2.9). Closely spaced, poorly oriented desiccation cracks 5 mm to 1.5

cm deep, occur within the ironstone unit, filled with kaolinite and ooids (Fig. 2.10). The ooids are up to 2 mm in diameter, ovoid to flattened in shape and well-sorted. The ironstone under the microscope has a micritic carbonate matrix and contains ooids rimmed by calcitic microspar. Ooids are replaced by kaolinite, which contains some unaltered detrital feldspar (Fig. 2.11). These may have acted as a nucleus for the formation of the ooids and a precursor to the formation of kaolinite. Other ooids preserve concentric laminae. The micrite contains angular to subangular fine-grained quartz crystals, feldspar and remnant detrital fine muscovite.

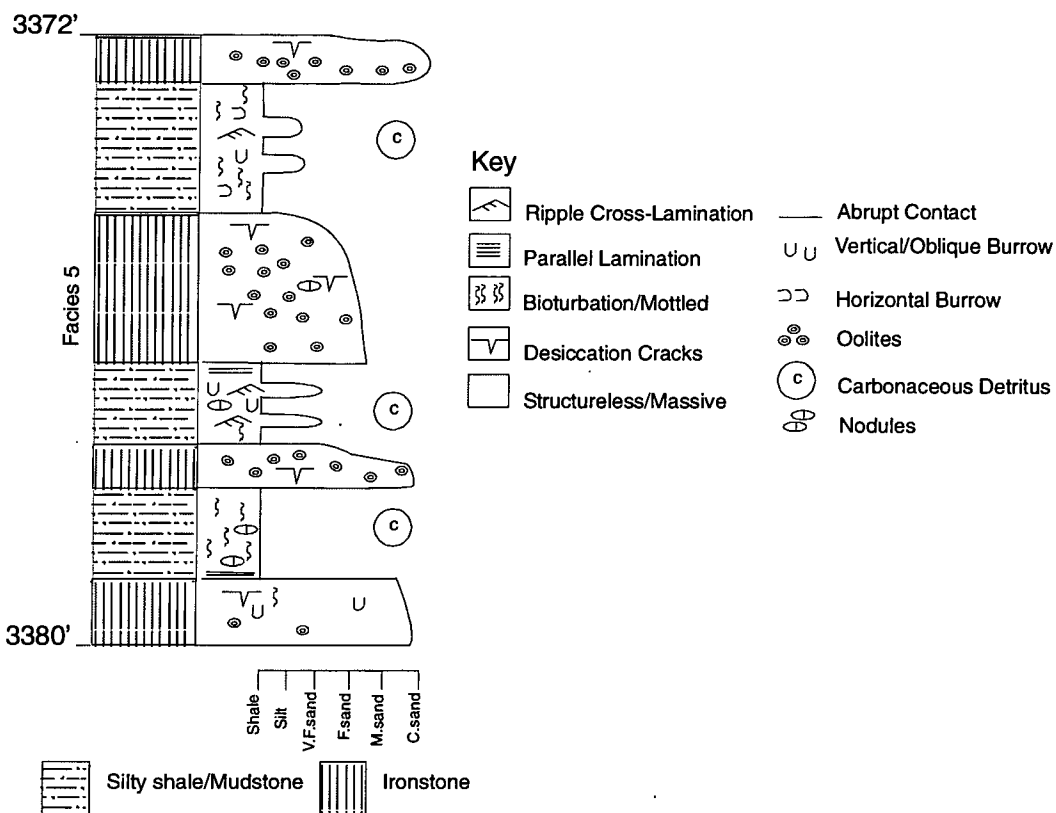


Fig. 2.8 Detailed section for the cored interval between 1030 m (3380') and 1028 m (3372') in well C1-49 showing the heterolithic type 1 facies (Facies 5; Table 2.1).

The ironstone is made up mainly of siderite with quartz grains and kaolinite, as shown by XRD analysis (Fig. 2.12). The base of this facies contains a 20 cm thick bed of ironstone riddled by vertical burrows up to 12 cm long and up to 2 cm wide, passing up into laminated and bioturbated mudstone. This is followed by bioturbated and laminated mudstone and silty shale, which contains disseminated fine-grained carbonaceous detritus and abundant mica.

Most of the vertical and horizontal burrows occur within the silty shale unit (Fig. 2.10). Nodules of ironstone 5 mm to 1 cm long are dispersed in the mudstone. Irregular sandstone laminae with sharp, scoured bases, occur within the silty shale and locally within the ironstone. Some laminae show well-preserved small-scale ripple profiles 1-2 cm thick.

A similar heterolithic facies occurs in the cored interval 1308 to 1307.5 m from well K1-1. It is composed of silty shale, muddy sandstone and ironstone (mainly siderite with low chamosite content according to the XRD analysis shown in Figs 2.13 and 2.14). The two prominent characteristics of this interval are the vertical burrows in the lower part and abundance of plant roots associated with ferruginous nodules (1-2 cm in diameter) in the upper part (Fig. 2.15). The sediments are riddled by conspicuous vertical tubes, up to 5 cm deep, of *Skolithos* burrows which are prominent on bedding surfaces and commonly filled with very fine quartz grains, non-calcareous ooids and calcite cement. Closely spaced vertical and horizontal desiccation cracks, possibly filled with calcite, also occur.

WELL No: C1-49. CORE No. 14
BOX No. 6
DEPTH 3376 ft.-3380 ft.

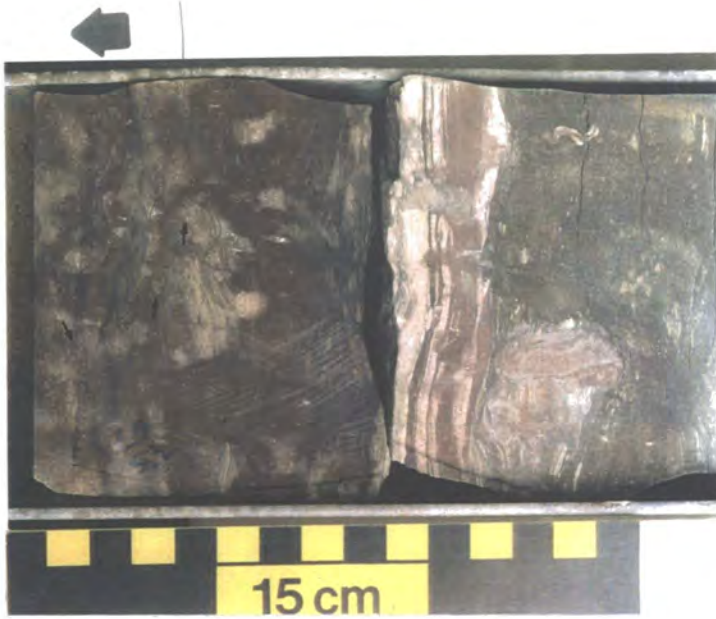


Fig. 2.9 Slabbbed core sample from heterolithic type 1 facies, well C1-49, showing silty shale at the bottom overlain by sideritic bed with very fine sandstone laminae and disseminated oolites (arrows) and small desiccation cracks possibly filled with calcite. Note the vertical burrows within the silty shale and sandstone laminae.

WELL No: C1-49. CORE No. 14
BOX No. 5
DEPTH 3372 ft.-3376 ft.



Fig. 2.10 Slabbbed core sample from heterolithic type 1 facies, well C1-49, showing bioturbated mudstone, silty shale and sandstone. Note vertical burrows (arrow) and dispersed horizontal burrows. At the top is an ironstone bed with sharp contact, containing streaky sandstone laminae and closely spaced desiccation cracks (filled with calcite, small arrow).

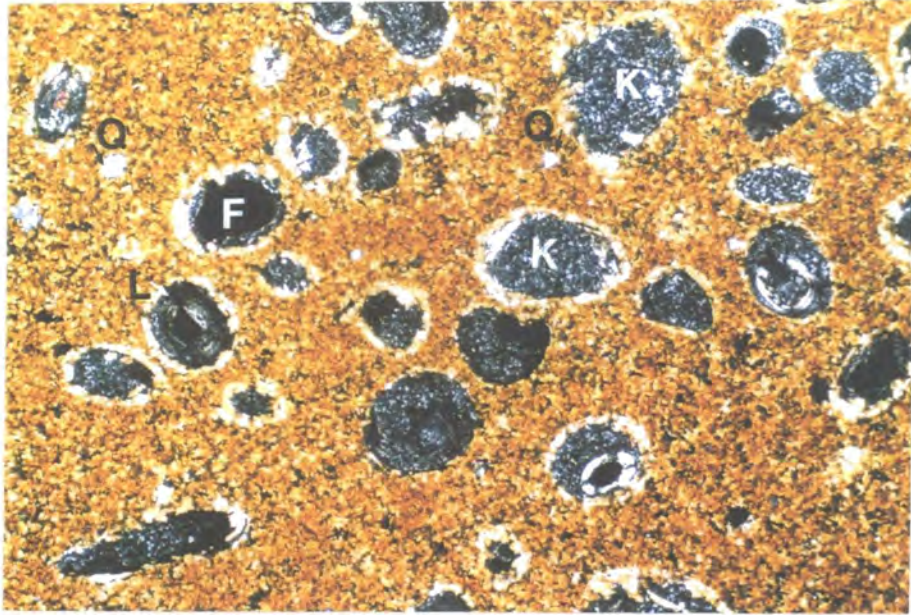


Fig. 2.11 Thin section photomicrograph from heterolithic facies showing ooids replaced by kaolinite (K). The ooids contain detrital feldspar (F) within a micritic carbonate matrix. Some ooids have preserved concentric lamination (L). The micrite contains angular to subangular fine-grained quartz (Q). PPL (X4).

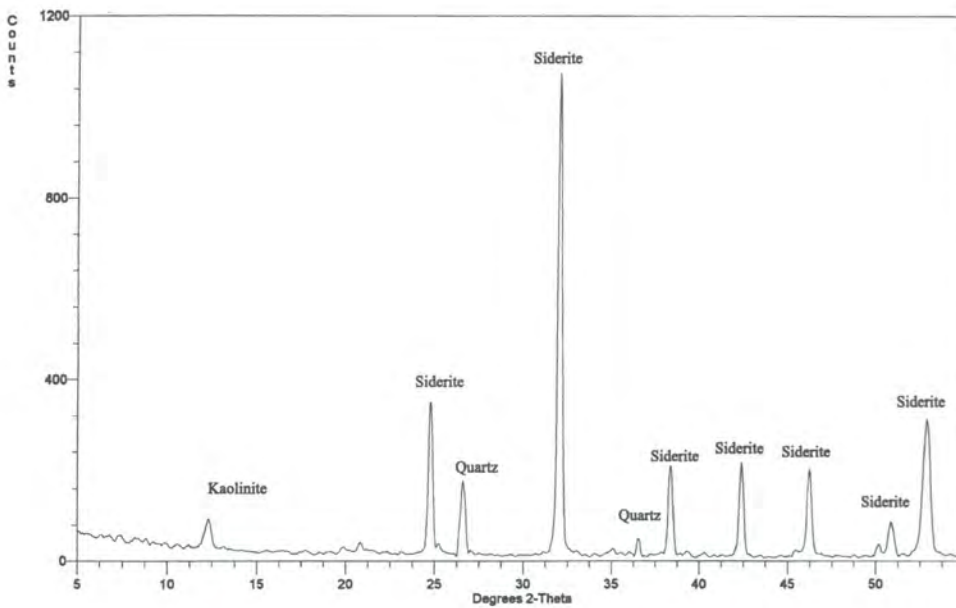


Fig. 2.12 X-ray diffraction analysis showing the composition of the ironstone from heterolithic type 1 facies, well C1-49.

Interpretation

The facies consists of varicoloured heterolithic sediments. It contains trace fossils characteristic of an open-marine environment and alternating energy conditions (Howard and Reineck 1981; Frey and Pemberton 1984). The sediment texture, however, is largely a result of burrowing activity and some of the ironstone (sideritic) beds contain irregular ooid-filled tubes. The presence of red to brown colours indicates deposition in an oxidising environment, whereas grey colours suggest deposition under more reducing conditions (Reineck and Singh 1973). The red colour is due to the presence of iron minerals, which are typical of humid tropical climates (Reineck *et al.*, 1973; Collinson and Thompson 1989) where the source material was sufficiently deeply weathered to supply free ferric oxide.

The iron mineral may also be introduced to the sea from the land in colloidal suspension. Talbot (1974) suggested that muddy sediment with burrows was deposited in a calm, protected environment, whereas the abundance of iron suggests proximity to a river. Ooids, concentrated in burrows, suggest moderate agitation along a sediment surface penetrated by burrows (Van Houten and Karasek 1981). The ooids are typical of those developed in other ironstone formations in many parts of the world.

The silty shale and mudstone imply an offshore shelf environment where ironstones typically accumulate under shallow, high-energy conditions (Taylor and Curtis 1995). Sandstone and ironstone in shale were deposited during high-energy storms. The sharp bases between ironstone, silty shale and mudstone represent rapid deposition by storm events. Oolitic ironstones have been described from the Devonian Shatti Formation in west central Libya (Van Houten and Karasek 1981) which is equivalent to the Tahara Formation. Oolitic iron deposits occur within marine beds, but they may form pedogenically in certain types of soil such as laterites.

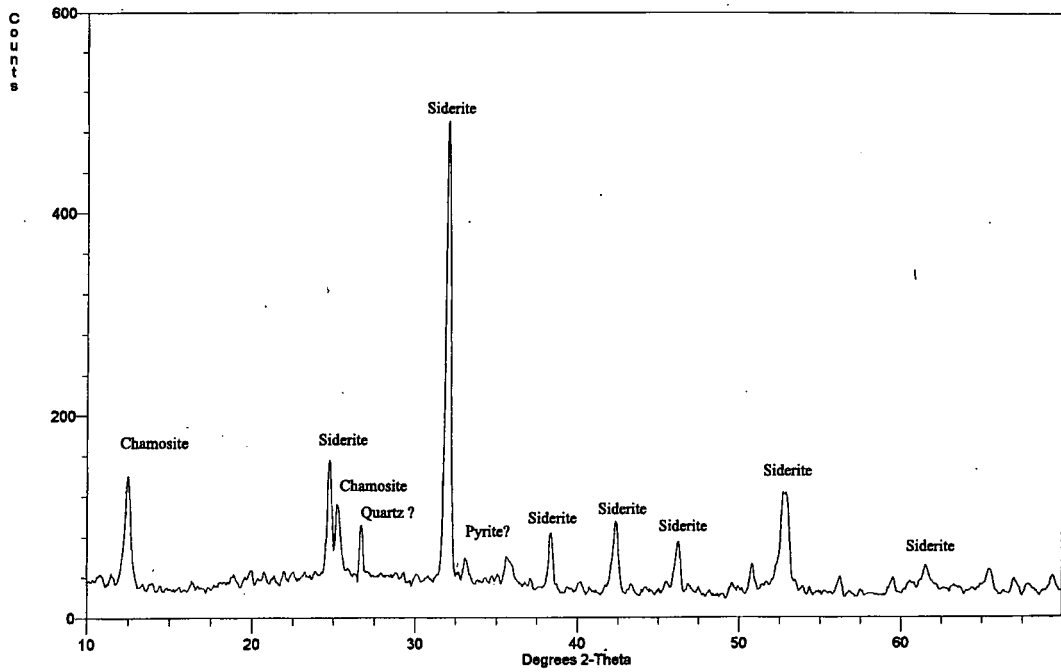


Fig. 2.13 X-ray diffraction analyses showing the composition of the ironstone. Sample from the top of heterolithic type 1 facies from well K1-1.

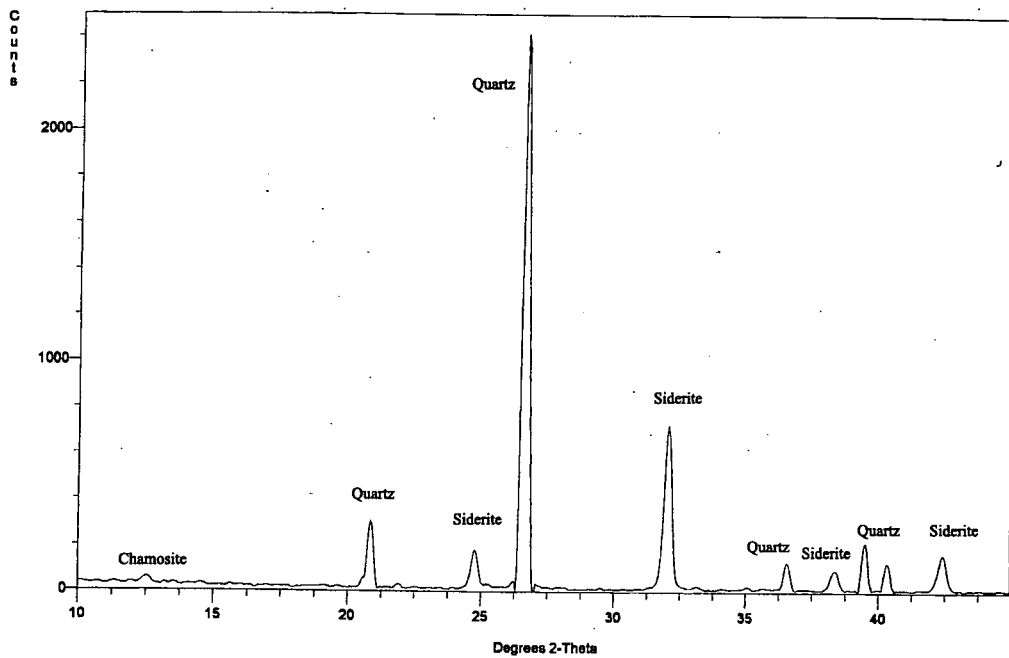


Fig. 2.14 X-ray diffraction analysis showing the composition of the ironstone. Sample from bottom of the heterolithic type 1 facies from well K1-1.

WELL No: K1-1 CORE No. 10
BOX No. 1
DEPTH 4290 ft.-4294 ft.



Fig. 2.15 Slabbed core sample from heterolithic type 1 facies, well K1-1, showing the ironstone beds with disseminated ooids (small arrow). Note possible plant root fragments with ferruginous nodules (large arrow).

The siderite nodules are found in both marine and non-marine shales (Blatt 1982). The nodules in the muddy unit formed by diagenesis of iron under reducing conditions in organic-rich mud (Ho and Coleman 1969). Gautier (1982) argued that the siderite concretions formed during the early compactional history at shallow depth in fine-grained sediments containing large volume percent ages of carbonate. Scattered ferruginous nodules in these sediments possibly grew during change in position of the ground-water table, producing drying and wetting of the soil. Most of the root traces are carbonised plant fragments and relatively small.

Kaolinite is the constituent of the ooids. It is a common primary and secondary mineral formed by weathering or hydrothermal alteration of aluminium silicates,

particularly feldspar. It is found in soil and can be transported by water and mixed with quartz and other minerals (Klein and Harbut 1993). The author has found vertical tubes without an ooid-fill interpreted as roots. Apart from roots the facies contains desiccation cracks and disseminated carbonaceous detritus indicative of periods of subaerial emergence of the shelf (Reineck *et al.*, 1973; Hobday and Horne 1977; Elliott 1983; Collinson 1986).

2-Heterolitic type 2

Description

This facies is represented by the cored interval from 723 m to 715 m in well ATS2. It occurs in the lower part of the cored succession (Fig. 2.16). The facies extends over some 8 m of the cored thickness and is composed of silty shale, mudstone and fine-grained sandstone. The facies is light grey to brownish-grey and locally red-brown in colour. It is mainly intensely bioturbated to mottled (Fig. 2.17). The effect of biogenic reworking can be seen in the light grey coloured mottling of shale and sand, and the presence of coarser quartz grains. Local abundant ooids < 2 mm in diameter occur, especially near the bottom of the facies (base of the core). It is well to moderately sorted and locally pyritic. Bioturbation has destroyed the primary structures and homogenised the sediment (Fig. 2.18).

The burrows are dispersed, but decrease in abundance upward through the facies. Trace fossils are common especially long vertical-type burrows. These burrows have a complex to simple structure and are filled with sand, silt and some ooids grains (Fig. 2.19). Long vertical burrows more than 20 cm deep and 1.5 cm wide are confined to the lower and middle of the facies. Horizontal burrows, a few mms in diameter, are also common throughout the facies as well as ferruginous concretions, which occur as either single or coalesced nodules ranging from 1.5 cm to 5 cm in diameter. Some broken shell fragments may be present in the upper third of the facies.

The middle part of this facies includes two thick sandstone beds (Fig. 2.16). The lower one is a 90 cm thick fine-grained sandstone, with scoured basal surface with local relief of up to 2.5 cm, containing rounded to subrounded poorly sorted fine rip-up mud clasts. The sandstones contain laminated shale flasers and minor soft-sediment deformation structures, and local vertical burrows < 2.5 cm long passing upward into highly bioturbated shale. The second sandstone bed is 60 cm thick and is also extensively bioturbated, with vertical and horizontal burrows. The upper part of the facies is sandier and locally contains less well burrowed laminated silty shale. In many cases the sandstone is lenticular.

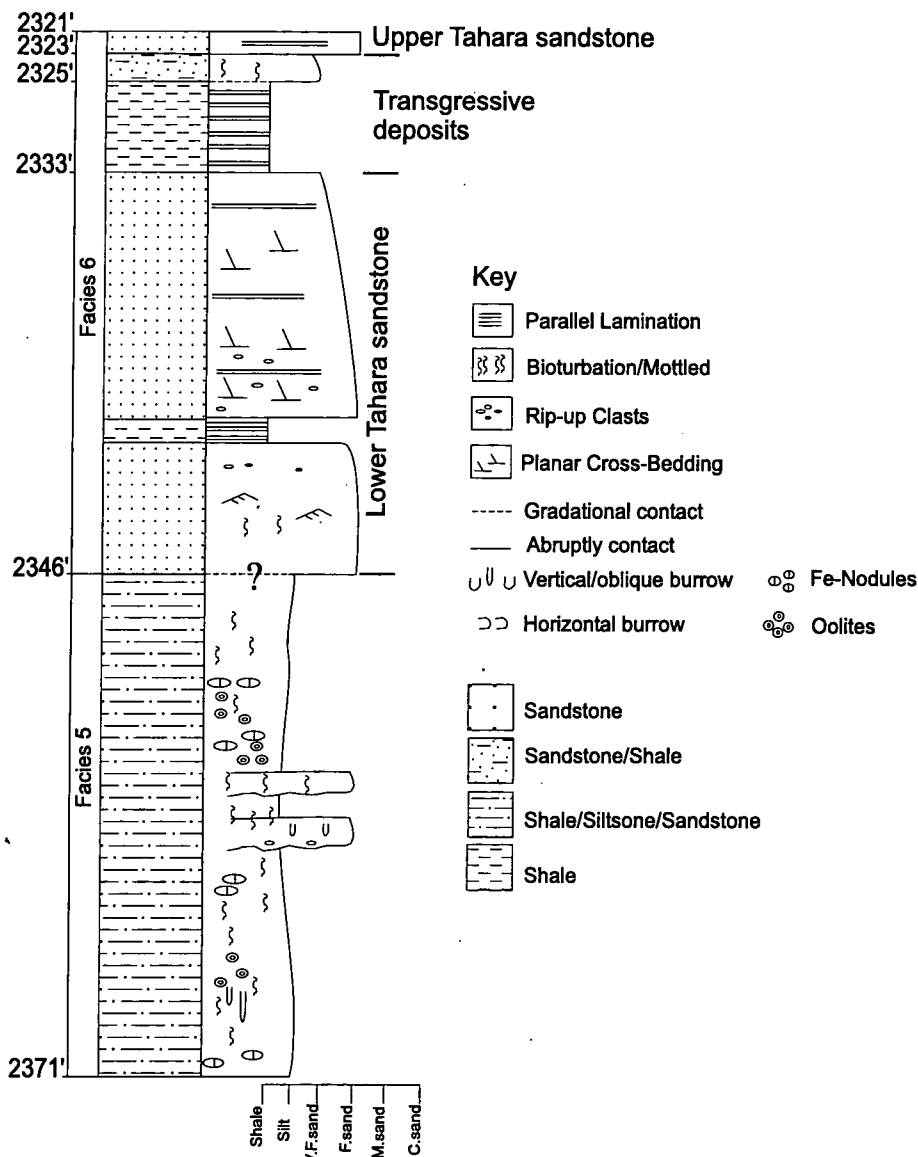


Fig. 2.16 Detailed section for the cored interval between 723 m (2371') and 707 m (2321') in well ATS2. The section illustrates the heterolithic type 2 facies overlain by the lower Tahara sandstone. See Fig. 2.1.

Interpretation

The trace fossil association contains a mixture of vertical and horizontal burrows of shallow-water marine affinity (Ekdale *et al.*, 1984; Frey Pemberton 1984). Intensity of bioturbation has caused mixing of the lithologies, especially in the shale-dominated beds. Burrowing organisms cause varying degrees of bioturbation, which in extreme instances, can thoroughly homogenise the

sediments. Vertical burrows in the lower part of the facies probably reflect attempts by the animal to escape as water depth increased. Some vertical burrows filled with ooids suggest agitation along a sediment surface penetrated by the burrows (Van Houten and Karasek 1981). Silty shale and mudstone deposited in quiet environments may be finely laminated, but are commonly homogenised due to bioturbation.

WELL No: ATSHAN 2. CORE No. 8
BOX No. 5
DEPTH 2369 ft.-2372 ft.



Fig. 2.17 Slabbed core sample from heterolithic type 2 facies, well ATS2, showing example of intensely bioturbated and light grey colour mottling of shale and sandstone. The bioturbation has destroyed the primary structures and homogenised the sediment.

The colour ranges from grey to brown or red similar to those in type 1. The latter suggest an oxidising early diagenetic regime whereas the grey colour records reducing pore water. Iron is believed to be derived from regolith (primary residual red beds) and transported in colloidal solution or adsorbed from part of the

suspended load of incoming rivers (Talbot and Allen 1996). The presence of concretions or impersistent beds of ironstone are common, having formed by early pre-compaction diagenesis (see interpretation of heterolithic type 1 for more details).

The sandstone beds are produced mainly from deposition of suspension clouds. The latter are thought to be produced by wave action where shoaling waves take much sand into suspension (Reineck and Singh 1973). Individual sandstone beds were probably deposited rapidly and represent a single waning flow event, which frequently possessed a strong oscillatory flow component. Minor development of the basal scoured surfaces of sand beds and rip-up clasts may indicate storm events and possibly channelised currents (Harms *et al.*, 1975). Locally abundant broken shell fragments are probably storm transported and reworked. The ichnofacies assemblage shows a low diversity and reduced trace size towards the top of the facies. However, the distribution of sediments and sedimentary structures which are extensively bioturbated, together with deep burrows suggests deposition in a protected area such as a back-barrier lagoon setting (Van Straaten 1959; Reineck and Singh 1973; Ekdalee *et al.*, 1984).

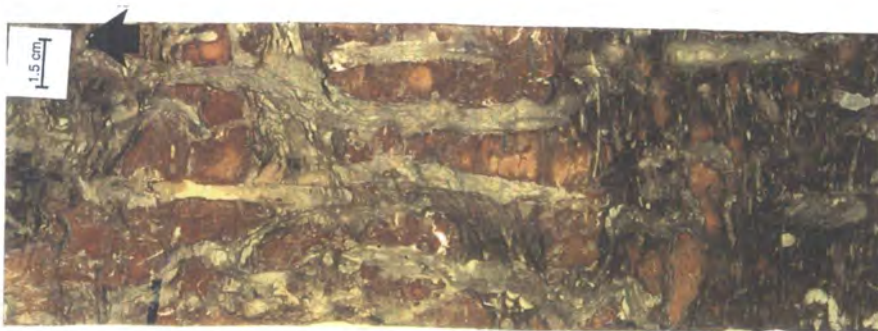


Fig. 2.18 Slabbed core sample from heterolithic type 2 facies, well ATS2, showing burrows with complex to simple structure filled with sand, silt and ooids grains. Note the bottom and top sample characterised by bioturbated silty shale with small horizontal burrows (mm's in diameter) and ferruginous nodules.

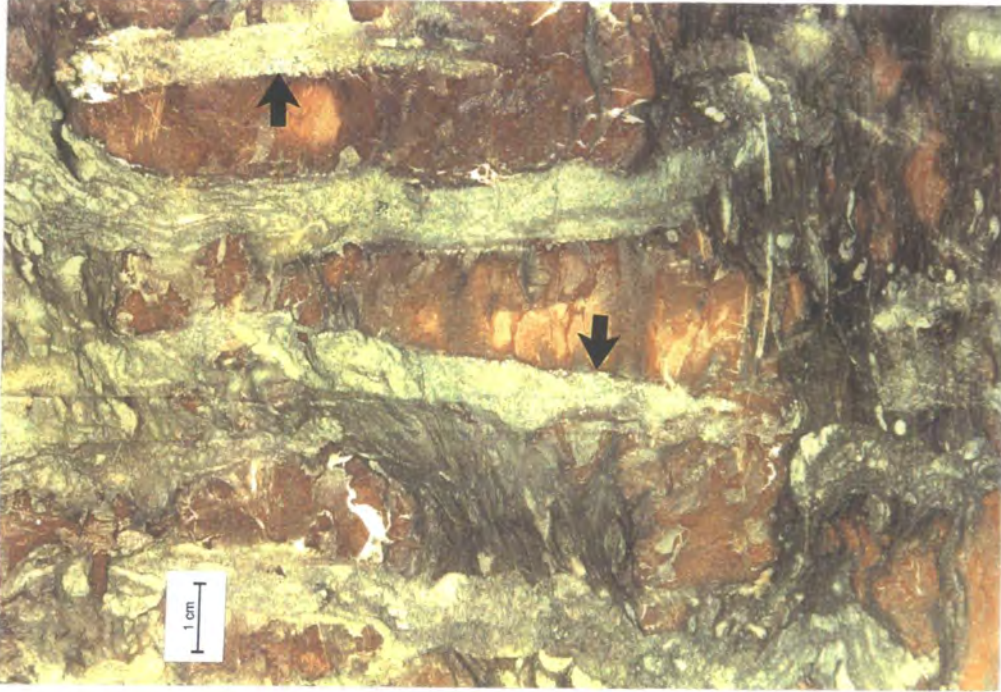


Fig. 2.19 Closely spaced large vertical burrows filled with ooids (arrows). Close up of part of Fig. 2.17.

2.2.6-Planar cross-bedded and horizontally-laminated sandstone and shale

Description

This facies, which comprises over 58% of the total cored thickness in type well C1-49, is represented by the interval 1028 m to 989 m. It attains a maximum thickness of approximately 39 m (Fig. 2.20). The facies extends to the southwestern part of the area away from type well C1-49 to well ATS2 (Fig. 1.1). It is composed predominantly of 85%, fine- to very fine-grained, white, light grey to very light grey, well-sorted sandstone containing fine-grained carbonaceous detritus (for more details of sandstone composition see chapter 5). The shale is dark grey to brownish grey, highly micaceous, with abundant fine-grained carbonaceous detritus. The sandstone consists of two distinct sandbodies, each of which is underlain by a bioturbated and laminated sand and shale unit. The contact between the sandbody and the bioturbated and laminated sand and shale unit is unclear due to broken core. These sandbodies together with the bioturbated and laminated sand and shale unit are arranged into two subfacies (a) and (b), on the basis of their lithology and sedimentary structures.

Subfacies (a) is represented by an 18 m thick coarsening-upward unit beginning with dark grey shale intercalated with siltstone and sandstone in the lower 5 m of the subfacies. The shales normally contain mm to sub-mm thick streaks and lenses of light grey silt and sand with sharp irregular bases and tops. Siltstone and sandstone occur as < 1 cm to 8 cm thick parallel to wavy laminae and beds. Some sandstone layers have sunk into the shale producing deformed structures; others show planar cross-lamination (7 cm thick) with thin ironstone laminae and rare 5 mm to 1.5 cm long rip-up mud or siderite clasts. Horizontal burrows, a few mm's in diameter, locally concentrate within the shale unit, whereas faint narrow tubes > 5 cm long, are present in the sandstones. The burrows include *Skolithos* and *Chondrites*. This part of the subfacies is overlain by fine to very fine-grained sandstone, most of which contains planar cross-bedding and less common horizontally to wavy laminated sandstone with remnant patches of thin, muddy or carbonaceous laminae. The lower part of this sandstone is structureless with

local irregular, wavy laminae from 5 mm to < 1 cm thick, that grades upward into horizontal laminae and minor low to high-angle planar cross-bedding (Figs 2.21, 2.22, 2.23).

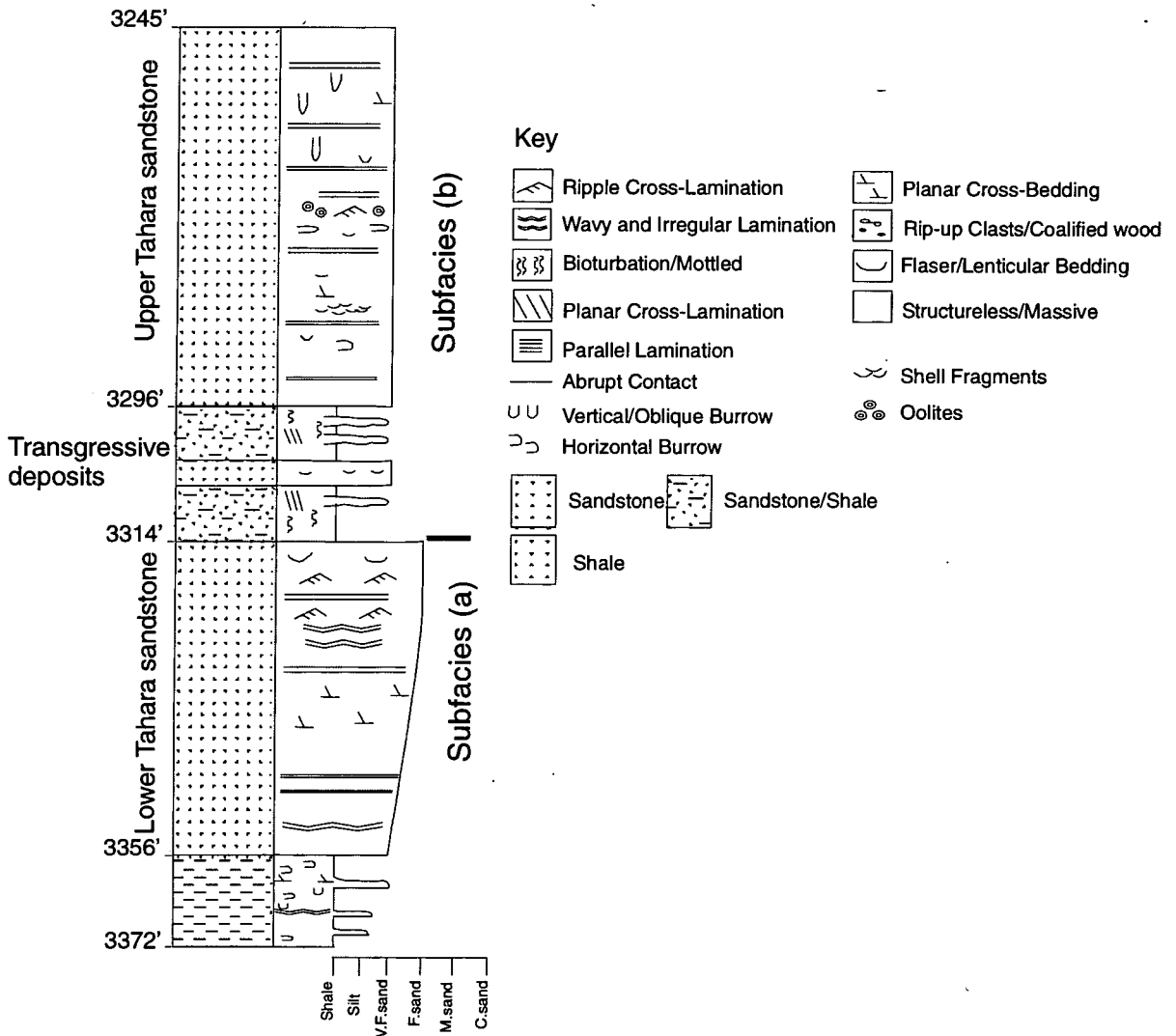


Fig. 2.20 Detailed section for the cored interval between 1028 m (3372') and 989 m (3245') in well C1-49 illustrating the lower and the upper Tahara sandstone. Note slight coarsening-upward trend in lower sandstone terminated by a marine transgressive shale.

WELL No: C1-49. CORE No. 13
BOX No. 8
DEPTH 3352 ft.-3356 ft.



Fig. 2.21 Slabbed core sample from well C1-49, of part of lower sandstone of the Tahara Formation showing the lack of structure and disseminated fine carbonaceous detritus.

WELL No: C1-49. CORE No. 13
BOX No. 4
DEPTH 3336.5 ft.-3340 ft.



Fig. 2.22 Slabbed core sample from lower Tahara sandstone, well C1-49, showing planar cross-bedded sandstone.

The middle part of the the sandbody of subfacies (a) is structured mainly by planar cross-bedding and horizontal laminae, overlying a chaotic association of fine carbonaceous detritus. The sandstone in the upper part is composed of small-scale ripple cross-lamination with thin mud partings and flasers, and rare soft-sediment deformation.

WELL No: C1-49. CORE No. 13
BOX No. 2
DEPTH 3328.5 ft.-3332.5 ft.



Fig. 2.23 Slabbed core sample from lower Tahara sandstone, well C1-49, showing the horizontally laminated sandstone enhanced by very thin carbonaceous laminae.

Other less common structures in the subfacies include: (1) a single subordinate < 1 m (E-Log) thick bed of brownish-grey to brownish-black mudstone where the colour seen in core, (2) three interlaminated sandstone and parallel to wavy laminated mudstone units from 5 cm to 7 cm thick; and (3) a deformed bed up to 6 cm thick of moderate brown mudstone. This subfacies, not cored in well K1-1, can be recognized from the wireline log.

In well A1-NC151, the interval from 855 m to 850 m includes part of the subfacies (a) (Fig. 2.24). The lower part of the succession consists of interlaminated sandstone and shale with individual shale and sandstone laminae a fraction of a mm to < 1 cm thick; local layers > 1 cm thick of sandstone occur. Some sandstone laminae have sharp, scoured bases. The lower part of this subfacies is gradationally overlain by very fine sandstone. This sandstone, characterised by horizontal laminae and low-angle planar cross-bedding (in sets 2 cm to 5 cm thick), passes into structureless sandstone with no evidence of any visible sedimentary structures (Fig. 2.25). This is overlain by a 23 cm thick sandstone which shows conspicuous deformed structures enhanced by thin diffuse coaly laminae. Although the original bedding is not clearly visible, crude, diffuse, small-scale, low-angle cross-bedding is observed in the uppermost part of this package. The basal part of the deformed sandstone and its contact with underlying structureless sandstone is not well preserved, but it may be an erosive surface defined by abundant mm to cm-diameter rip-up clasts and coaly fragments incorporated within the sediment (Fig. 2.26). The deformed sandstone gradationally overlain by wavy-bedded sandstone and shale forming a fining-upward trend (Fig. 2.24).

The cored interval from 715 m to 711 m in well ATS2 (Fig. 2.16) represents the total thickness of the sandbody. It commonly has similar textural characteristics and sedimentary structures (Fig. 2.27) to the sandbody of subfacies (a) except for the less well developed biogenic features. This sandstone contains scattered poorly sorted mud clasts (up to 7 cm long and up to 2.5 cm in diameter) and directly overlies the heterolithic type 2 facies but with no clearly visible contact.

Subfacies (b) consists of 5.5 m of laminated, bioturbated shale and sandstone identical to those present below the lower sandstone of subfacies (a). Sandstone laminae here are generally < 1 cm thick, very fine-grained, and contain horizontal lamination and low-angle planar cross-lamination. Some of the sedimentary structures have been obliterated by biogenic reworking as a result of mixing of interlaminated sand and shale. Burrows are common along the base and the top of the sandstone and shale interface. Some of the burrow tubes are just a few

mm's in length. They are oblique, vertical and horizontal, the latter being a few mm's in diameter. A subordinate 2 m thick bed of structureless sandstone, with abundant shell fragments and rare local bioturbation occurs in the sandstone. This lower part of subfacies (b) is overlain by 15.5 m thick very fine sandstone.

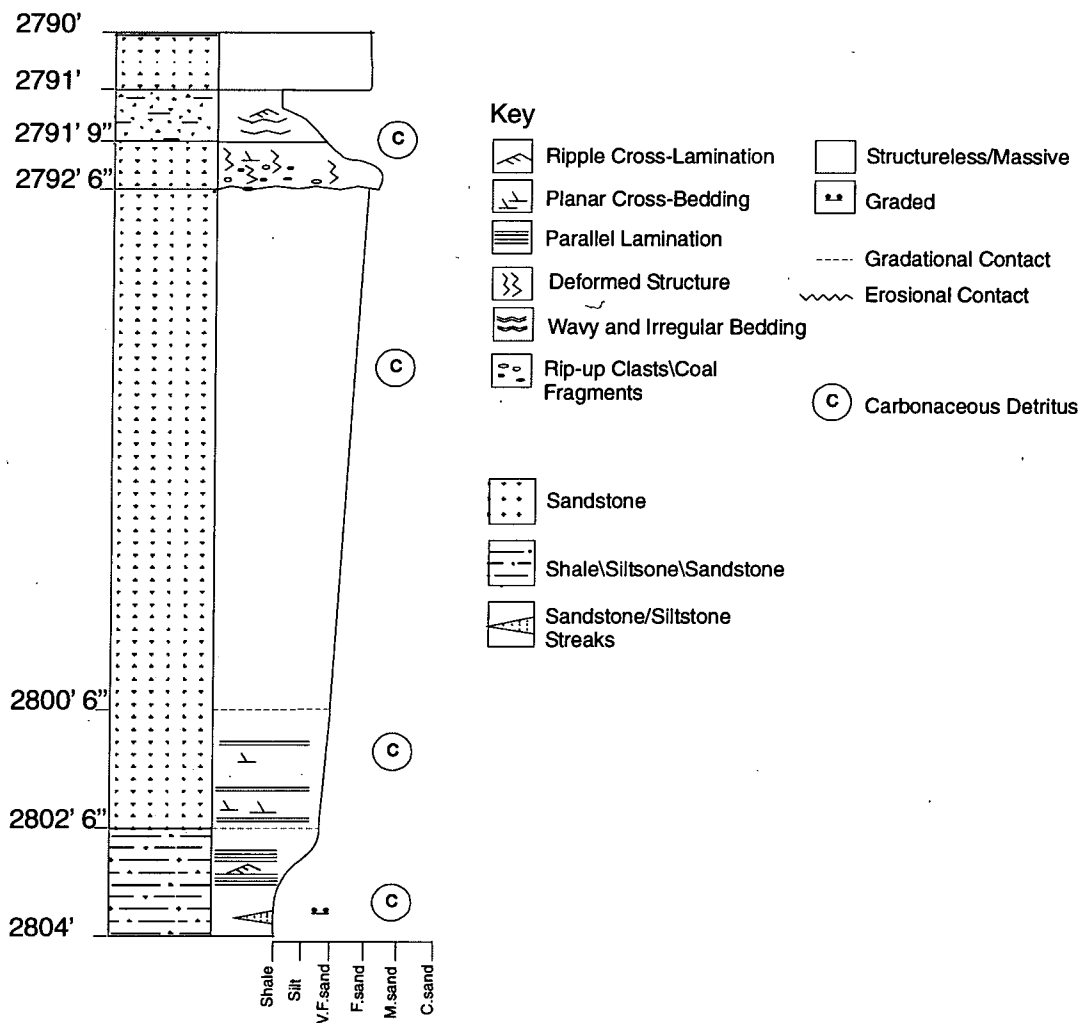


Fig. 2.24 Detail section for the cored interval between 855 m (2804') and 850 m (2790') in well A1-NC 151 showing coarsening-upward trend of the lower part of the lower Tahara sandstone (subfacies a).

WELL No: A1-NC151 CORE No. 1
BOX No. 2
DEPTH 2793.5 ft.-2797.5 ft.

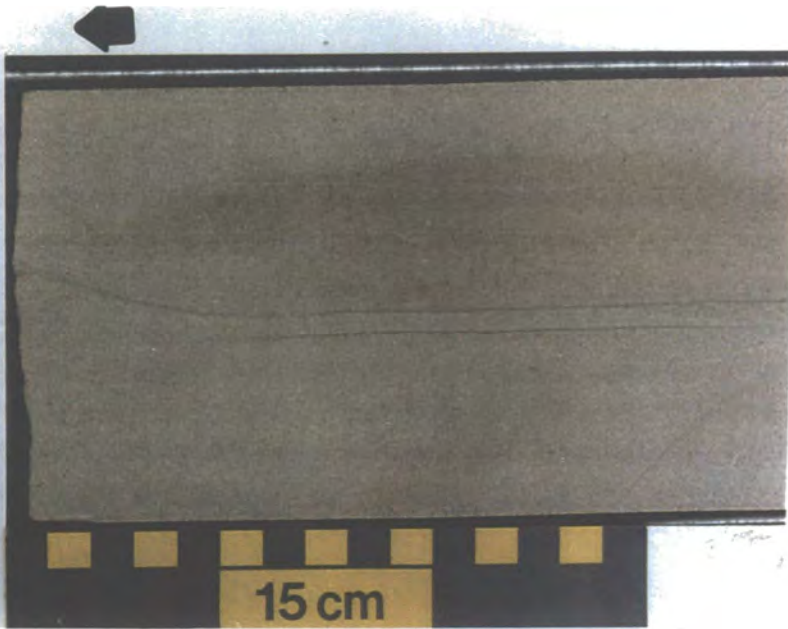


Fig. 2.25 Slabbed core sample from well A1-NC151, showing structureless sandstone from the lower part of lower Tahara sandstone (subfacies a).

WELL No: A1-NC151 CORE No. 1
BOX No. 1
DEPTH 2790 ft.-2793.5 ft.



Fig. 2.26 Slabbed core sample from well A1-NC151, showing deformed structures enhanced by thin diffuse coaly laminae (large arrows). Note disseminated coaly fragments (small arrows). This sample is present above structureless sandstone within the lower Tahara Sandstone interval (subfacies a).

WELL No: ATSHAN 2. CORE No. 7
BOX No. 4
DEPTH 2333.9 ft.-2337.7 ft.

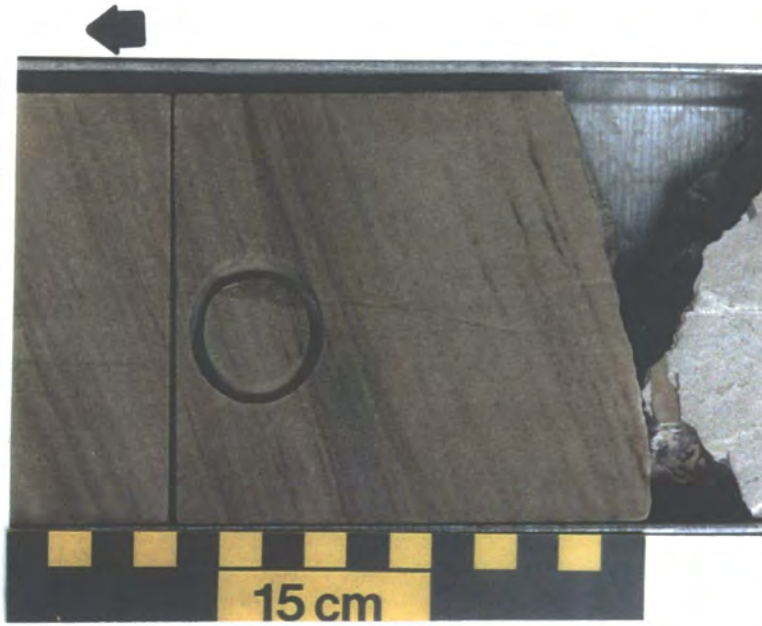


Fig. 2.27 Slabbed core sample from well ATS2, showing example of planar cross-bedded sandstone similar to that in the lower sandstone (subfacies a) in well C1-49.

WELL No: C1-49. CORE No. 11
BOX No. 7
DEPTH 3292.5 ft.-3296.5 ft.

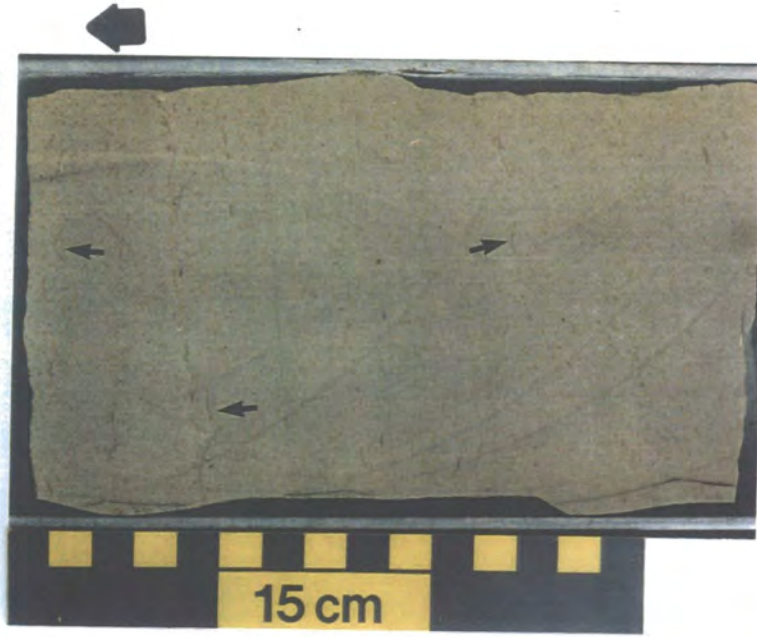


Fig. 2.28 Slabbed core sample from well C1-49, showing abundant shell fragments (possibly brachiopods) with different orientations (arrows) in the upper sandstone (subfacies b).

The sandstone contains mainly horizontal laminae with subordinate cross-bedding (similar characteristic features are noted in the lower part of the lower sandbody) and structureless sandstone, and beds of silty shale from 5 cm to 1 m thick. The middle part of this subfacies contains a prominent 80 cm (E-Log) thick bed of grey to dusty-brown, fine-grained muddy sandstone containing a dark layer of carbonaceous material and disseminated ooids a few mm's in diameter. It contains rounded to subrounded quartz grains. Abundant shell fragments, some locally concentrated into shell nests, occur in the subfacies (Fig. 2.28). Vertical to oblique burrows of low diversity, 9 mm to 7 cm long, and up to 5 mm wide (Fig. 2.29), and horizontal burrows, a few mm's in diameter also occur within the shale. The burrows within the subfacies (b) include *Skolithos*, *Planolites* and *Chondrites* (see Fig. 2.6).

A similar sandstone to subfacies (b) has been recognised in the cored interval, 1281 m to 1276 m in well K1-1 (Fig. 2.30). This part of the sandbody is characterised mainly by structureless sandstone and is overlain by the wavy bedded sandstone and shale, with individual beds up to 3.5 cm thick. The sandstone beds contain small-scale ripple cross-lamination up to 2 cm thick and 7 cm long. Burrows occur mainly with the shale as mostly horizontal burrows, 2 mm to 4 mm in diameter, which include *Planolites*.

Subfacies (b) was also observed in the cored interval 2310'6" to 2288' in well ATS1 (Fig. 2.31). It consists of structureless sandstone and irregular to wavy bedded sandstone intercalated with shale. Sandstone beds are 2 cm to 10 cm thick, and generally contain small-scale ripple cross-lamination. Shale here is usually dark-grey to black in colour, micaceous and silty in character with disseminated fine-grained carbonaceous detritus. This is mainly moderately to strongly bioturbated, which has destroyed the bedding and homogenised the sediments. Burrows occur throughout the subfacies and are prominent on bedding surfaces. These burrows are filled with very fine-grained sandstone and/or siltstone.

Burrows are vertical to oblique (< 2 cm long and up to 5 mm wide) and horizontal (5 mm to 1 cm in diameter), the latter characteristic of the *Cruziana* ichnofacies (Fig. 2.6).



Fig. 2.29 Slabbed core sample from upper sandstone, well C1-49, showing vertical burrows (*Skolithos*, large arrow) and shell fragments (small arrows).

The same subfacies (b) is also present in the cored section 711 m to 707 m in well ATS2 (Fig. 2.16). This section starts with interlaminated shale and sandstone with minor bioturbation that passes upwards into intensely bioturbated sandstone and shale with an increase in the proportion of sand towards the top of the succession. This package is overlain by 60 cm of sandstone which commonly represents the lower part of the upper sandbody. This sandstone is very fine-grained, well sorted with disseminated fine-grained pyrite and carbonaceous detritus. It is mainly structureless with small subvertical fractures.

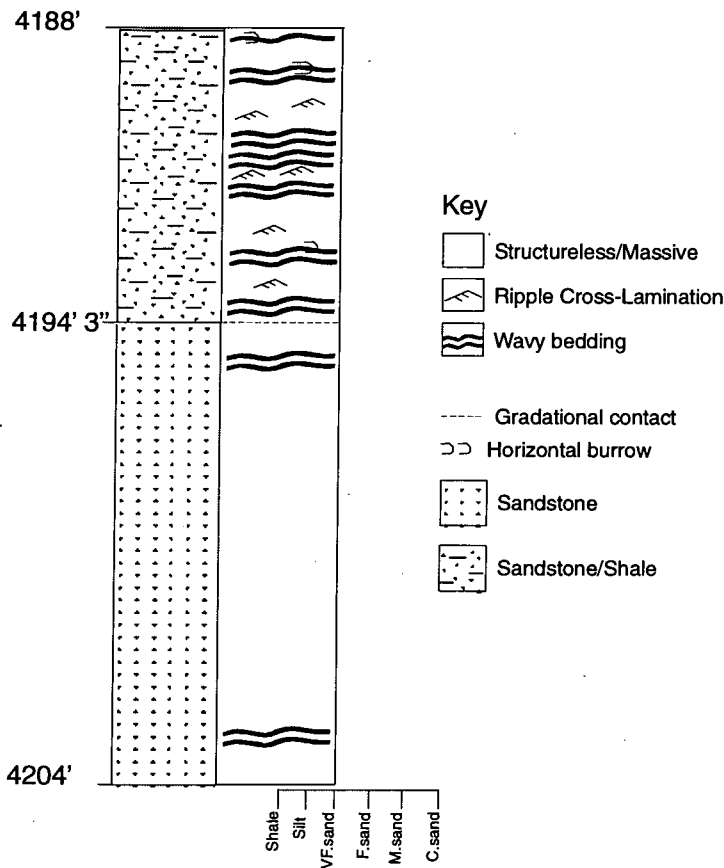


Fig. 2.30 Detailed section for the cored interval between 1281 m (4204') and 1276 m (4188') in well K1-1 showing lower part of the upper Tahara sandstone (subfacies b) and its increased mud content compared with well C1-49.

Interpretation

The variation in texture, sedimentary structures and biogenic features in the lower parts of both subfacies indicates deposition in a marine-shelf environment (Reineck and Singh 1973; Elliott 1986b). The occurrence of interlaminated sand and shale disturbed by burrow activity implies discontinuous energy conditions (storm events), and is a characteristic feature of marine-shelf environments (Frey and Pemberton 1984). On the other hand, the intensity of bioturbation reflects the fact that the subfacies lies below wave base or that it was receiving very little new sediment (low rate of sedimentation).

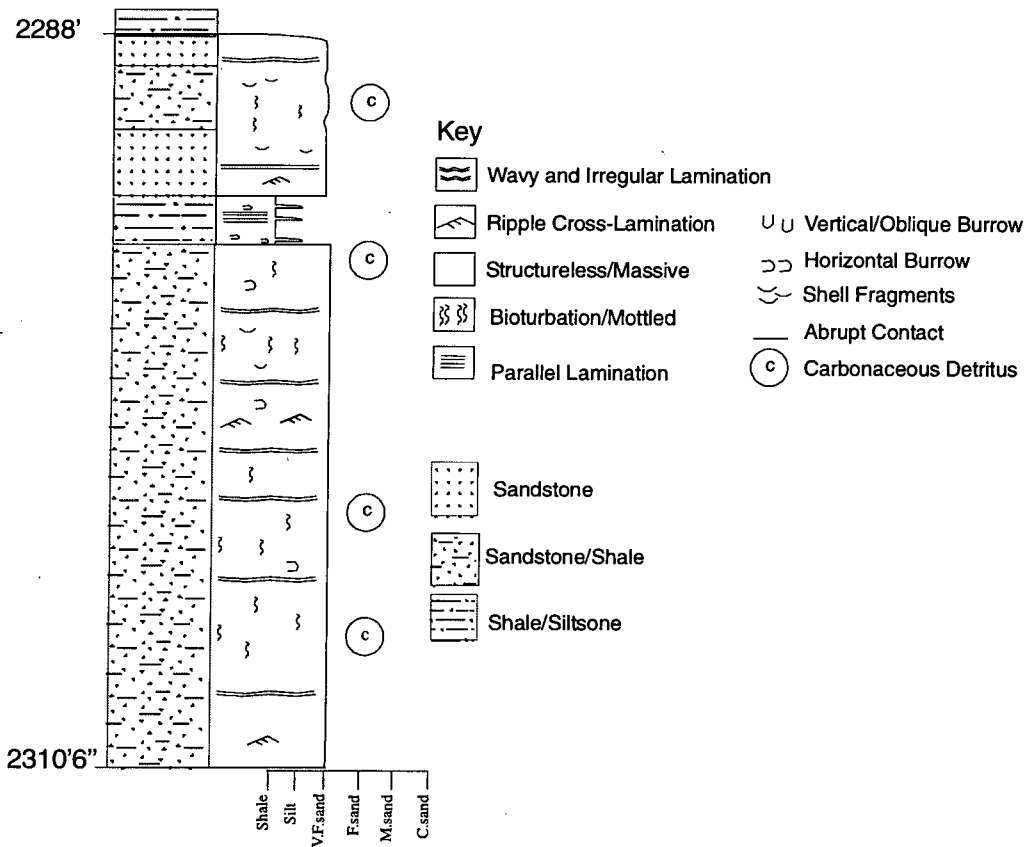


Fig. 2.31 Lithological profile through the interval between 704 m (2310' 6") and 697 m (2288') in well ATS1 showing the upper sandstone (subfacies b) of the Tahara Formation. Note increase in the mud and amount of bioturbation in the sandstone compared to subfacies (b) in well C1-49.

The change from shale to silt and sand in the lower parts of subfacies (a) and (b), and the upward transition from wavy to horizontal laminae, and cross-bedding was probably caused by variation in the rate of sediment supply to the shelf and storm conditions as interpreted elsewhere in the study area.

The sandstone of subfacies (a) in the type well displays a slight coarsening-upward trend and a change in sedimentary structures indicative of proximity to a detrital influx and gradual shallowing of the water (Turner 1991). The absence of bioturbation in this sandbody is probably due to high sedimentation rates (Bosence 1973). Deformed structures are present (Fig. 2.25), and are probably

produced from rapid periods of sand deposition (Fruit and Elmore 1988; Howell *et al.*, 1996). Abundant fine carbonaceous detritus in the upper part are probably related to irregularity in supply of carbonaceous material or proximity to a river mouth (Rahmani 1988).

The coarsening-upward trend in well A1-NC151 may record shoreline progradation and forms part of a shallowing-upward unit. The parallel lamination with low-angle cross-bedded sandstone is typical of many modern shoreline deposits (Allen 1965; Weimer *et al.*, 1982). The clasts are scattered throughout the deformed sandstone implying that the current was of high energy possibly erosive, but somewhat episodic suggesting channelised flow (Prave *et al.*, 1996). The presence of alternations of sandstone and shale in the upper part of the fining-upward unit in the fining-upward package in well A1-NC151, possibly represents a change from channel activity to channel abandonment conditions (Donaldson *et al.*, 1970).

In well ATS2, the lower sandbody of subfacies (a) which form a coarsening-upward package rests on the lagoonal back-barrier facies (heterolithic type 2), with a possible erosion surface between them. The occurrence of this succession represents the landward migration of a shoreline during transgression (Fischer 1961; Oomkens 1970; Franks 1980; Elliott 1986b).

Subfacies (b) contains predominantly well-sorted, very fine-grained sandstone, containing mainly horizontal lamination with local structureless sandstone. Horizontal laminae are thought to result from suspension clouds produced by shoaling waves (Reineck and Singh 1973; Kumar and Sanders 1976; Turner 1991). The plane-bedded sandstone is interpreted as upper flow regime swash generated deposits, which developed on channel margin bars (Brenchley *et al.*, 1979). The general scarcity of sedimentary structures and biogenic reworking in some sandstone beds are attributed to rapid sedimentation with little reworking within a shallow-marine environment, possibly influenced by high current activity. Furthermore, the scarcity of mud in some parts of the sandstone from well C1-49 and A1-NC151 may be due to low concentration of suspension sediments or

effectiveness of wave process carrying it offshore. Cheng (1982) suggested that the absence of mud layers within sandstone indicates deposition of sandstone in a very shallow basin but which maintained enough turbulence to prevent mud deposition. The alternations of sand and shale layers within sandstones of the subfacies (b) observed in well K1-1, are seen to increase in well ATS1 toward the southwest, and probably reflect fluctuating energy conditions (Reineck and Wunderlich 1968; Elliott 1983). On the other hand the increase in shale intercalated with sand indicates short-term decreases in current velocity. Harms *et al.* (1975) suggest that shaley layers represent deposition under quieter conditions. The burrowed sandstone in well ATS1 is more intensely burrowed compared with type well C1-49. It could represent periods of slow deposition, i.e. bioturbation slight in well C1-49 due to rapid deposition but increases in well ATS1 due to decrease in sedimentation rates. The alternation of sandstone and shale, containing abundant burrows within the sandstone, suggests deposition under low-energy conditions (Frey and Pemberton 1984) possibly reflecting a change in the rate of deposition from rapid to slow (Harms *et al.*, 1975).

The occurrence of shell fragments and trace fossils indicates a marine origin. Shell fragments, which occur throughout the subfacies, are broken and appear to be mainly storm transported and reworked. Shell fragments are concentrated in nests or hashes in well C1-49 and represent an environment lacking both deposition and erosion (Coleman and Gagliano 1965). The overall characteristics of this subfacies indicate a marine origin with deposition probably occurring in a shoreface dominated by wave and storm condition.

The thick muddy sandstone in the middle of the subfacies contains shell fragments, ooids (2 mm) and carbonaceous material. It produces a spiky pattern on the gamma ray log, which may result from a high concentration of heavy minerals or glauconite within muddy sandstone (Rider 1990). However, muddy sandstone within a shallow marine depositional environment containing glauconite suggests a slow rate of sedimentation (Tucker 1991). Local development of ooids indicate an agitated shoal water (Johnson and Freidman 1969). Furthermore, the sandstone package and underlying sand-shale

intercalations show an upward increase in energy as evidenced by changes in sedimentary structures, grain size, and upward increase in the sand:shale ratio. This may represent shoreline progradation within a shoreface/foreshore environment (Harms *et al.*, 1975; Vos 1981b; Reinson 1984).

The lower part of the lower subfacies (a) in the lower sandbody and subfacies (b) in upper sandbody were subjected to sediment reworking by wave and currents resulting in increased levels of sand maturity. The deposits suggest a shoreface setting overlying shelf sediments during progradation of the shoreline system (Harms *et al.*, 1975; Elliott 1986b; Reinson 1984; Turner 1991). The upper part of subfacies (a) in the lower sandbody contains small-scale planar cross-bedding, with small mud drapes and internal scoured surfaces. This part of the sandbody is coarser in grain size than the underlying sandstone, producing a coarsening-upward trend representing a gradual shallowing of the water. The upper part of the lower sandstone, which is reported only from type well C1-49 possibly represents fluvio-deltaic influenced depositional conditions. These fluvio-deltaic sediments were deposited on shoreface deposits with no evidence of an erosion surface between them (may be due to gradual, low-energy progradation of the depositional system) forming a coarsening-upward unit. This was followed by a return to transgressive shelf conditions as relative sea-level rose. These transgressive bioturbated sandstone and shale deposits separate the upper and lower Tahara sand-bodies.

Both subfacies (a) and (b) can be traced laterally for more than 200 km and in vertical section varies from 34 m (111')-18 m (60') thick when traced from northeast to southwest (Fig. 2.32). Similar patterns of deposition to this facies have been described from the Cretaceous Gallup Sandstone in New Mexico (Campbell 1971; McCubbin 1982), Middle and Upper Devonian deposits from Aouinate Ouenine Formation in Western Libya (Vos 1981b) and from the Palaeozoic (Silurian-Devonian) in Al Kufra basin (Turner 1991).

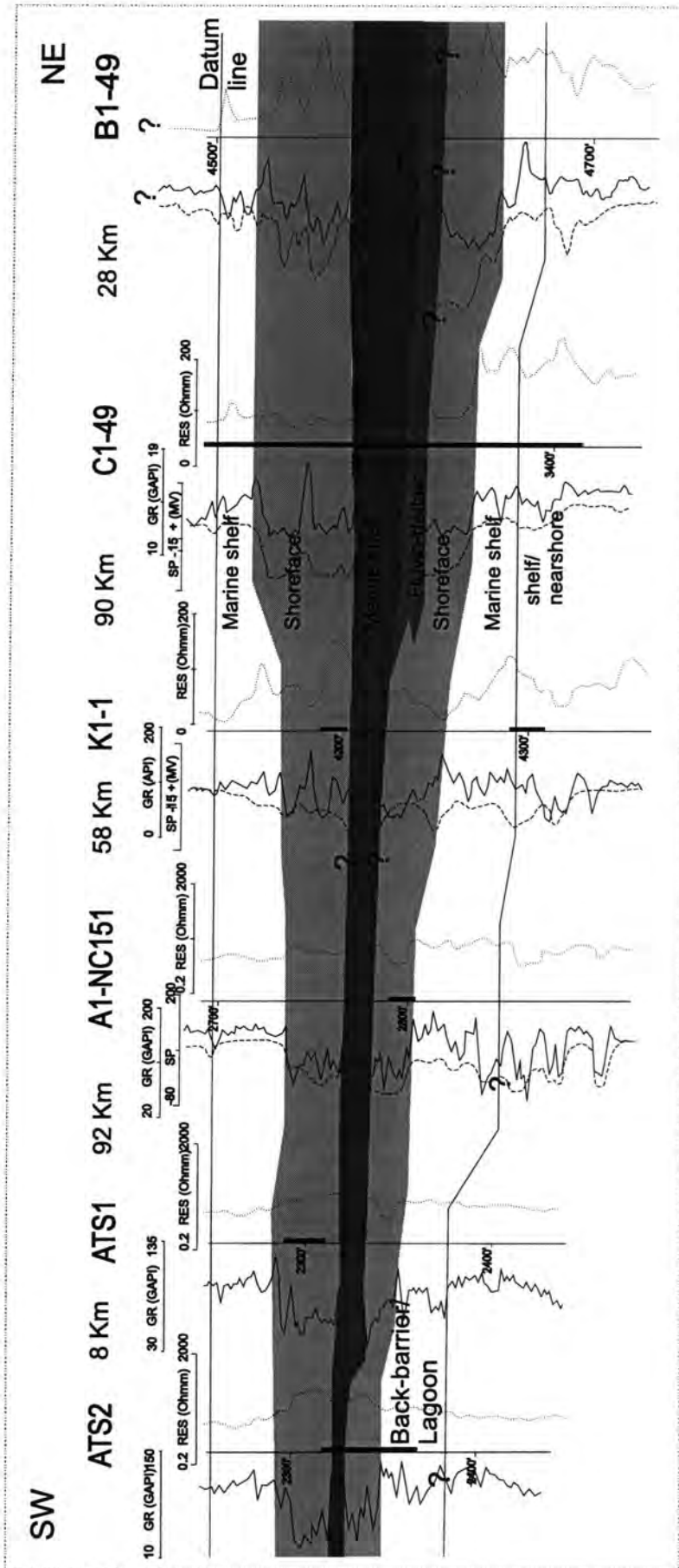


Fig. 2.32 Southwestern-northeastern cross-section showing lateral extent of the lower and the upper sandstones of the Tahara Formation and depositional environments. Note sandbodies thinning towards the southwest and possible extent of fluvio-deltaic influences. Datum line is bioturbated sandstone. See Fig. 1.1 for wells location.

2.2.7-Shale

Description

This facies is confined to the upper part of the succession above the upper sandstone. It represents the top of the succession and is recognised only from type well C1-49, in the interval from 989 m to 974 m (Fig. 2.33). The facies consists predominantly of shale, which has been broken, probably due to drilling.

The shale is dark to medium dark-grey, moderately fissile, highly micaceous, and locally silty with disseminated small pyrite grains. The facies is slightly bioturbated. Burrows, which occur within the shale, are a few mm's in diameter, mostly horizontal, and filled with light grey siltstone. Irregular, very fine-grained sandstone and siltstone lenses up to 1 cm thick occur within the shale. These normally have sharp bases and tops, and grade into siltstone and shale respectively. The middle of the facies contains a 2 m thick, grey to greenish-grey, locally light brown, medium-grained and moderately sorted, strongly bioturbated argillaceous sandstone with abundant shell fragments, some rip-up clasts and disseminated pyrite grains. Sedimentary structures have been destroyed by bioturbation. The uppermost part of this bed consists of ferruginous sediments with some oolitic ironstone. The bed has poorly defined contacts with the enclosing shale.

Interpretation

Minor bioturbation occurs throughout the facies in the form of discrete, small horizontal burrows indicative of a marine environment. Abundant dark shale and rare sand and silt within the facies indicates a low energy, low oxygen and organic-rich environment into which local influxes of sand and silt were injected probably by storms. Mud was deposited during periods of slack water and just before and after the slack water conditions. It is quite probable that the sand and silt laminae were deposited during current and wave activity. Sandstone and siltstone are rather thin, usually evenly laminated and/or lenticular and locally

graded. The latter result from deposition by waning current activity (Reineck and Singh 1973) possibly from distal storm-generated flows which alternated with mud deposited from suspension during fair-weather (Johnson and Baldwin 1996). Similar sediments from the North Sea and the Gulf of Gaeta were described by Reineck and Singh (1973). The facies contains bioturbated sandstone, 2 m thick, which indicates very slow deposition in marine conditions (Harms *et al.*, 1975; Johnson *et al.*, 1996).

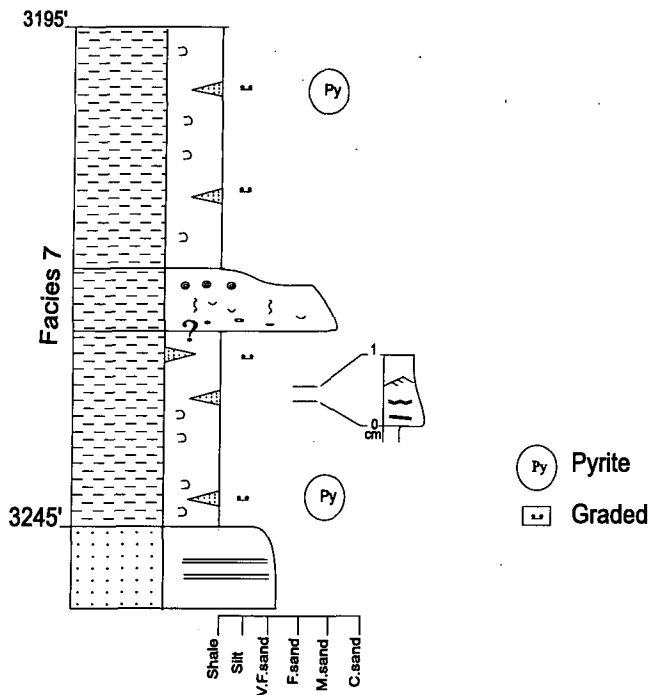


Fig. 2.33 Detailed section for the cored interval between 989 m (3245') and 974 m (3195') in well C1-49 illustrating transgressive marine shale Facies 7 (Table 2.1) above upper Tahara sandstone. See Fig. 2.19 for index.

Chapter 3

Sequence Stratigraphy

3.1-Introduction

Sequence stratigraphy is a relatively new branch of geology. It is defined as the study of rock relationships within a chronostratigraphic (time stratigraphic) framework of repetitive, genetically related strata bounded by surfaces of erosion or non-deposition or their correlative conformities (Van Wagoner *et al.*, 1988). It suggests that depositional facies are arranged in a predictable fashion within depositional sequences. High-resolution sequence stratigraphy and sequence stratigraphy of outcrop, core, and wireline log data are increasingly recognised as a technique for correlating and predicting stratigraphy in the subsurface. Sequence stratigraphy aims to use the vertical and lateral variations in sedimentary successions which are controlled by relative sea-level changes to provide a chronostratigraphic framework for sedimentary facies and stratigraphic prediction.

The main aim of this chapter is to apply sequence stratigraphic methodology to the interpretation of the shallow-marine clastic deposits of the Tahara Formation using variations in facies tracts and stacking patterns in relation to changes in base level. The essential ideas of sequence stratigraphy and terminology are summarised in AAPG Memoir 26 (Payton 1977), SEPM 42 (Wilgus *et al.*, 1988) and AAPG Methods in Exploration 7 (Van Wagoner *et al.*, 1990). Sequence stratigraphy is based on a cyclic stacking hierarchy (Fig. 3.1) of deposition, bounded above and below by unconformities (Emery and Myer 1996). The constituent sequences and their boundaries are interpreted to form cycles related to fluctuations in relative sea-level (Duval and Vail 1992). Four types of stratigraphic cycles are recognised by Duval *et al.* (1992).

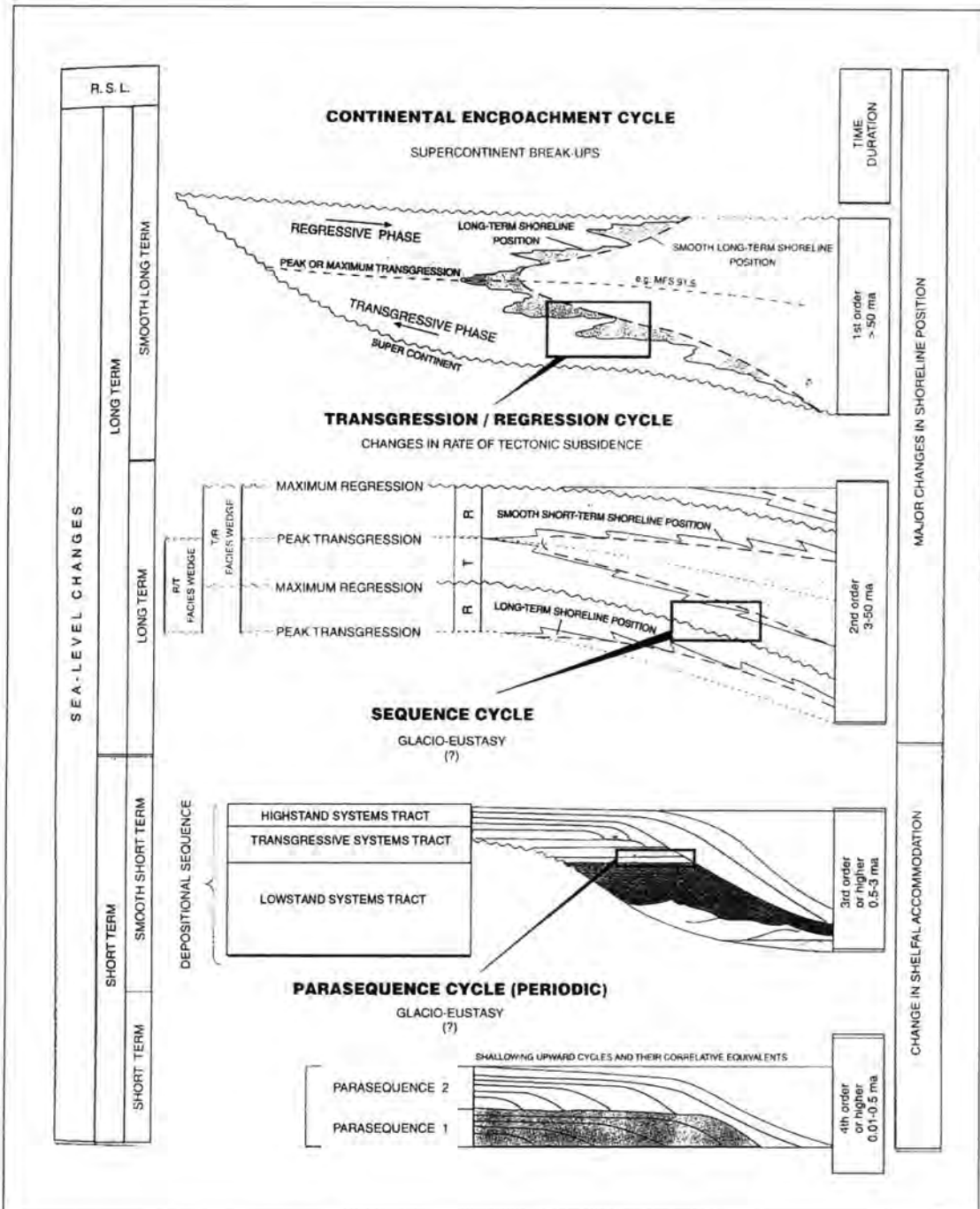


Fig. 3.1 Hierarchy of stratigraphic cycles (After Duval and Vail 1992).

3.1.1-Continental encroachment cycles

These are defined as first order cycles they have a duration of > 50 million years (Fig. 3.1). Continental encroachment cycles are defined on the basis of the relative extent to which the continents are covered by sedimentary rocks at the time of deposition (Duval and Vail 1992). First-order continental encroachment cycles have been attributed to tectono-eustasy (i.e., changes in ocean basin volume induced by continental break-up and aggradation).

3.1.2-Major transgressive-regressive facies cycles

These cycles are defined on the basis of changes in the shoreline position and have durations of 3-50 million years. They are defined as second-order cycles (Fig. 3.1). Second-order transgressive and regressive facies may be produced by regional tectonic changes such as changes in the rate of subsidence and uplift related to the rate of sea-floor spreading, and change in size of ocean basins (Duval and Vail 1992).

3.1.3-Sequence cycles

These are defined as third order cycles and have durations of 0.5-3 million years (Fig. 3.1). These cycles are related to changes in shelfal accommodation space and are probably caused by glacio-eustasy (Vail *et al.*, 1991). They are composed of lowstand, transgressive and highstand systems tracts and are bounded by sequence boundaries.

3.1.4-Parasequence cycles

These cycles represent shallowing-upward facies bounded by surfaces of abrupt deepening (Fig. 3.1). Duval and Vail (1992) suggested that the parasequence cycles range from fourth to the sixth order and have durations of 0.1-0.5 million years. Parasequence cycles are the building blocks of the systems tracts in third order sequences.

3.2-Factors Effecting Sequence Stratigraphy

Several workers have emphasized that depositional patterns are controlled by three main factors: eustasy, tectonics and sediment supply (Posamentier *et al.*, 1988; Van Wagoner *et al.*, 1988, 1990; Galloway 1989; Emery and Myer 1996; Miall 1996). Sequence stacking patterns result from interaction of these factors. Eustasy and tectonic processes result in relative changes of sea-level, which control the space available for sediments (accommodation space) and the distribution of facies within such a genetically related package (Posamentier *et al.*, 1988; Van Wagoner *et al.*, 1988).

3.2.1-Eustatic effect

Eustasy (global sea-level) is the position of sea surface relative to the centre of the Earth, which is controlled by changes in both the volume of the ocean basins and volume of water in the ocean (glacio-eustasy) (Plint *et al.*, 1992; Walker 1992; Emery and Myer 1996). Eustatic changes in sea-level effect the location and position of the shoreline where sediment flows into the basin (Galloway 1989).

Relative sea-level is defined as the position of the sea surface with reference to a datum or near the sea floor (Posamentier *et al.*, 1988). Relative sea-level changes reflect the combined effect of eustatic sea-level and basin subsidence. In coastal plains, however, base-level changes are also created during changes of tectonic movements of the basin or eustatic changes of sea-level (Miall 1996). Thus determining whether or not new space is being made available for sediment to fill (i. e. relative rise adds space whereas relative fall removes space).

3.2.2-Tectonics effect

The stratigraphic development of sedimentary basins is controlled by tectonic activity, which includes subsidence and uplift, and which may result from two principle mechanisms: (1) increasing or decreasing crustal/lithospheric thickness;

and (2) loading or unloading of the lithosphere (Williams 1993). Tectonism influences the amount and types of sediment deposited in the basin. It produces changes in elevation of sediment source areas and effects the rate of erosion, which increases with increase in land elevation.

3.2.3-Sediment supply

Sediment supply is essentially driven by tectonism and possibly climate. It is important in prograding basin margins where input must exceed the accommodation possibility of the receiving basin. The rate of sediment supply will reflect both how much and to what degree the accommodation is filled. Different thicknesses of sediment body may develop with different rates of sediment supply. Low rates of sediment supply promote retrogradation, while increases in sediment supply (high rate) promote aggradation and progradation.

3.3-Depositional Sequence Stratigraphy

The fundamental unit of sequence stratigraphy is the sequence. A sequence is used to identify stratigraphic units that are commonly bounded by unconformities. Sloss (1963) defined a sequence as an unconformity-bounded stratal unit. He recognised six sequences on the North American craton ranging in age from late Precambrian to Holocene. Sequences are interpreted to have been deposited during a complete cycle of relative sea-level change (Mitchum 1977). They are bounded by unconformities and their correlative conformities (Mitchum *et al.*, 1977; Van Wagoner *et al.*, 1988), and are composed of parasequences and parasequence sets that define systems tracts (Mitchum *et al.*, 1991) see Fig. 3.2.

3.3.1-Parasequences

The essential building blocks of sequences and systems tracts are parasequences and parasequence sets (Van Wagoner *et al.*, 1990). A parasequence is defined as a relatively conformable succession of genetically related beds or bed sets bounded by marine flooding surfaces and their

correlative surfaces. Parasequence and parasequence set boundaries form in response to an increase in water depth. The general depositional characteristics of a parasequence are interpreted to record a gradual decrease in water depth (coarsening-upward stacking). Their gradual shallowing is followed by an abrupt deepening, which produces the marine flooding surface forming the parasequence boundary. Parasequences are common in siliciclastic rocks, and most siliciclastic parasequences are progradational. This means that the parasequence is deposited in progressively shallower water. Some siliciclastic and most carbonate parasequences are considered aggradational and shoal upward (Van Wagoner *et al.*, 1990). Parasequences are successful in interpreting marine successions, but they have not been used extensively in non-marine or deep-marine successions. This is because non-marine depositional systems respond to a variety of allocyclic processes such as climatic, tectonic and eustatic changes. Parasequences are developed in sets, "as a succession of genetically-related parasequences that form a specific stacking pattern, bounded by major marine flooding surfaces and their correlative surfaces" (Van Wagoner *et al.*, 1990). Stacking patterns of parasequences within parasequence sets may be progradational, retrogradational or aggradational depending on the ratio of depositional rates to accommodation rates. Stacking patterns of parasequences in these sets define systems tracts (Fig. 3.2).

3.3.2-Sequence boundary

The rate of relative fall in sea-level determines the type of sequence boundary that bounds the sequence. Sequence boundaries, therefore, form in response to relative falls in sea-level and are of two types (Type 1 and Type 2 sequence boundaries) as illustrated in Fig. 3.2.

3.3.2.a-Type 1 sequence boundaries

This surface is the most common sequence boundary (Fig. 3.2A). It occurs when sea-level falls below the depositional shoreline break (Vail *et al.*, 1991). Type 1 sequence boundaries are identified by:

- 1) subaerial exposure and erosion of the exposed shelf;
- 2) onlap of overlying coastal strata; and
- 3) abrupt shallowing of the facies across the boundary (Van Wagoner *et al.*, 1990). Van Wagoner *et al.* (1988) suggest that a Type 1 sequence boundary forms when the rate of eustatic fall exceeds the rate of basin subsidence at the depositional shoreline break (off break), producing a fall in relative sea-level.

3.3.2.b-Type 2 sequence boundaries

Type 2 sequence boundaries (Fig. 3.2B) are less common in siliciclastic rocks than Type 1 sequence boundaries (Mitchum and Van Wagoner 1991). Type 2 surfaces form when the rate of eustatic fall is slightly less than or equal to the rate of basin subsidence at the existing depositional shoreline break at the time of the eustatic fall, thus no relative fall in sea-level occurs at this shoreline position (Posamenttier *et al.*, 1988; Van Wagoner *et al.* 1988). Recognition of Type 2 sequence boundaries is based on:

- 1) changes in parasequence stacking patterns below and above the sequence boundary (e. g. change from progradation to aggradation);
- 2) minor subaerial erosion and exposure at the shelf (no incised valleys); and
- 3) downward shift of coastal onlap to a location landward of the offlap break (on seismic data). These criteria should occur on the shelf above the depositional shoreline break.

3.3.3-Depositional System Tracts

Depositional systems are composed of successions of genetically-related strata deposited under specific environmental conditions (e.g., fluvial, deltaic and shelf) combined with eustatic fall and rise cycle. These associated depositional systems are called systems tracts. System tracts are characterised by their geometry and facies associations, and a linkage of contemporaneous

depositional systems (Brown and Fisher 1977). Depositional systems are composed of laminae, beds, and parasequences. These units involve the sedimentary structures that reflect the depositional environment and associated processes. Siliciclastic sedimentary deposition is affected by relative sea-level fluctuations (Posamentier *et al.*, 1988; Posamentier and Vail 1988; Van Wagoner *et al.*, 1990; Vail *et al.*, 1991; Haq 1991). The fundamental component of the systems tract within siliciclastic sequences is the recognition of coarsening and fining-upward parasequences, that depend on the position within the sequences. Coarsening-upward and thickening-upward trends of parasequences are identified by increase in grain-size and thick beds of sandstone (increase in sand/shale ratio). Upward-fining and thinning-upward trend parasequences are marked by decrease in grain-size of the sand (increase in shale/sand ratio). Parasequences and their boundaries, attributed to cycles of relative fall and rise of sea-level, stack to form aggradational, retrogradational and progradational sets. These cycles are represented by the systems tracts for siliciclastic rocks, which provide a high degree of facies prediction away from the surface or subsurface data. There are four systems tracts: lowstand, transgressive, highstand and shelf margin (Fig. 3.3). Each systems tract is interpreted to be deposited during a specific phase or portion of one complete cycle of eustatic fall and rise in sea-level.

3.3.3.1-Lowstand systems tracts (LST)

This is the first systems tract above the sequence boundary and it is deposited during sea-level fall. A fall in relative sea-level associated with a Type 1 sequence boundary results in an abrupt basinward shift in facies tracts (Figs 3.2A and 3.3a). The lowstand systems tract has a variety of parasequence stacking patterns. When lowstand systems tracts are deposited in a basin with a shelf break, it can be divided into a basin floor, a slope fan and a lowstand wedge (Van Wagoner *et al.*, 1988). The basin floor fan is dominated by deposition of a submarine fan on the lower slope or basin floor. The base of the basin floor fan (coincident with the base of lowstand systems tract) is the Type 1

sequence boundary. The slope fan consists of turbidite levee channel and over bank deposits (Van Wagoner *et al.*, 1990). The lowstand wedge is characterised on the shelf by an incised valley fill, which is dominated by fine grained and wedge shape deposits. It consists of progradational to aggradational parasequence sets. The top of the lowstand wedge (coincident with the top of lowstand systems tract) is a marine flooding surface (transgressive surface) across the shelf within the sequence. When a lowstand systems tract is deposited in a basin with a ramp margin (no shelf edge) it consists of two parts. The first part comprises stream incision and sediment by-pass of the coastal plain during relative sea-level fall. The second part of the wedge is characterised by a slow relative sea-level rise, resulting in the filling of the incised valleys (Posamentier *et al.*, 1988; Van Wagoner *et al.*, 1988). This part of the wedge consists of one or more progradational parasequence sets, the top is the transgressive surface and the base is the sequence boundary.

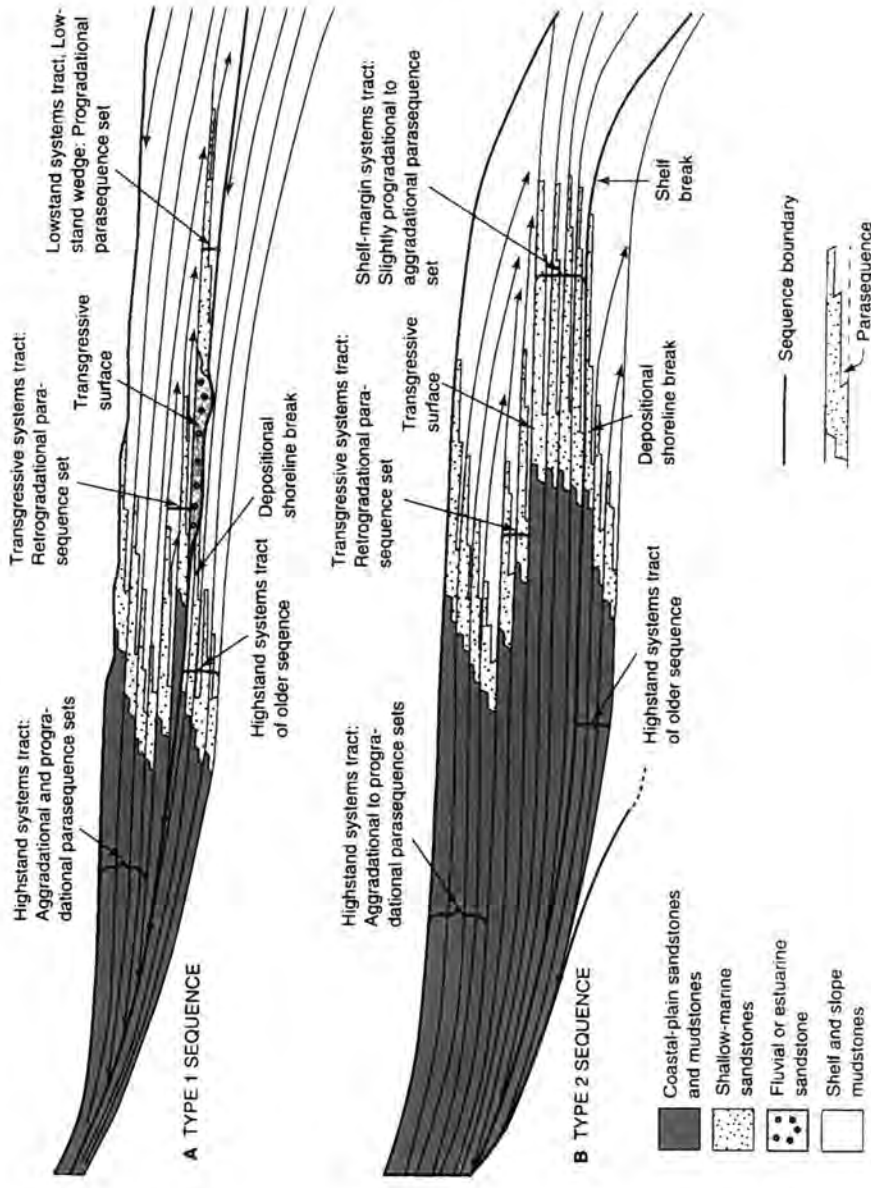


Fig. 3.2 Schematic showing distribution of systems tracts and parasequences in: (A) Type 1 sequence and (B) Type 2 sequence (After Boggs 1995, originally from Van Wagoner *et al.*, 1990).

3.3.3.2-Transgressive systems tracts (TST)

It is characterised by one or more retrogradational (backstepping) parasequence sets (Fig. 3.3b). Transgressive systems tracts are bounded below by a transgressive surface and above by maximum flooding surface (Van Wagoner *et al.*, 1990). Van Wagoner *et al.* (1988) suggested that the base of this systems tract is the transgressive surface at the top of a lowstand or shelf margin systems tract whereas the top is the downlap surface (marine flooding surface) as illustrate in Fig. 3.2. Parasequences within the transgressive systems tract onlap onto the sequence boundary in a landward direction and downlap onto the transgressive surface in a basinward direction.

Transgressive systems tracts are interpreted to form during relative sea-level rise. Thus, progressively younger parasequences become thinner and represent deeper water facies. Deposits of this systems tract blanket the shelf, infilling any residual topography associated with incised valleys. The typical feature of the transgressive systems tracts is the overall fining upward patterns (retrogradational type) which can be recognised on well logs (GR or SP logs).

3.3.3.3-Highstand systems tracts (HST)

The highstand systems tract is the upper systems tract in either a Type 1 or Type 2 sequence (Fig. 3.3c). This systems tract consists of the youngest strata within a depositional sequence and may be characterised by one or more progradational parasequence sets (Fig. 3.2). It is interpreted to be deposited during the eustatic highstand (Posmentier *et al.*, 1988; Van Wagoner *et al.*, 1988). It tends to progress from aggradational (early highstand) to progradational (late highstand) parasequences. Highstand systems tracts are common on the shelf and bounded at the base by the maximum flooding surface and at the top by a sequence boundary.

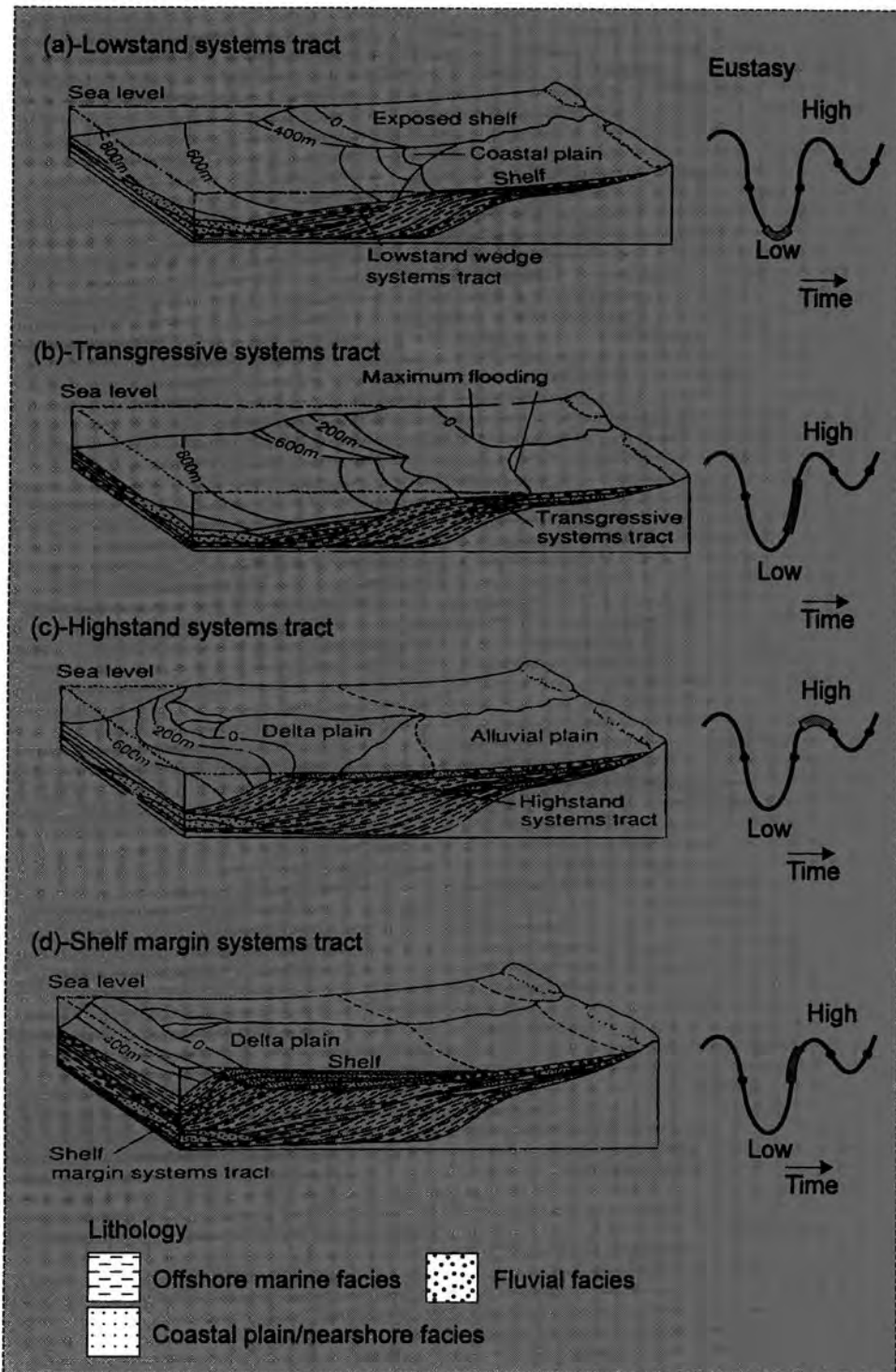


Fig. 3.3 Idealized block diagrams showing systems tracts and their relation to the eustatic sea level curve (After Posamentier *et al.*, 1988).

On the other hand, the highstand systems tract is bounded at the top by a Type 1 or Type 2 sequence boundary and at the bottom by the marine flooding surface (Van Wagoner *et al.*, 1988) as shown in Fig. 3.2.

Highstand systems tracts are deposited during the late stages of a relative rise sea-level and the early stages of a relative fall in sea-level. During early highstand, shelf deltas or the coastal margin must first advance across the drowned shelf of the underlying transgressive systems tract to the margin created by the previous lowstand wedge (Emery and Myer 1996).

3.3.3.4-Shelf-Margin systems tracts (SMST)

These systems occur above a Type 2 sequence unconformity (Fig. 3.3d). The top of the shelf margin systems tract is the transgressive surface (probably the base of transgressive systems tract), while the base of this system is a Type 2 sequence boundary (Fig. 3.2B). It is distinguished by one or more slightly progradational to aggradational parasequence sets (i.e., decrease progradation followed by aggradational parasequence stacking patterns). The shelf margin systems tract replaces lowstand systems tracts in the Type 2 sequence.

3.4-Sequence Stratigraphic Setting of the Tahara Formation

3.4.1-Introduction

Through the application of sequence stratigraphic concepts previously discussed, and sedimentological interpretations from cored wells (discussed in Chapter 2), sequences and key surfaces within the Tahara Formation in western Libya can be recognized. The subaerial exposure surface characterised by the presence of remnant plant roots, mud cracks and sideritic mudstone (heterolithic facies) (Fig. 3.4) is interpreted to be sequence boundary at depth 1028 m (3372') in the type well C1-49. This surface is also interpreted in well K1-1, but becomes more difficult to recognise in the southwestern part of the area, where core is lacking (Fig. 3.5).

The facies successions are frequently bounded by surfaces of different hierarchical level (Fig. 3.4), which record a deepening of the depositional environment. Parasequences are readily observed above and below the

sequence boundary and are bounded by marine flooding surfaces. A maximum flooding surface is recognised in well C1-49 (core and GR-log data), and is characterised by a bioturbated sand interval (transgressive surface) (Figs 3.3 and 3.4).

The overall succession was initiated in response to periodic sea-level fall and rise. It is dominated by shallow-marine deposits showing evidence of storm-wave conditions. The deposition and distribution of the facies within the parasequences are controlled by different factors including rate of relative sea-level change, rate of subsidence and sediment supply.

3.4.2-Recognition of the sequences and sequence boundary

The detailed core examination and electric well-log correlation allow the recognition of two partial sequences (1 and 2) separated by a Type 1 sequence boundary (SB) of a lowstand palaeosol (Fig. 3.4). These sequences defined by correlation of strata using electric well log and core data are illustrated in Figure 3.4. Identification of a sequence boundary within the succession is based on the facies lithology. The sequence boundary was initiated during a fall of sea-level below the depositional shoreline break (Posamentier *et al.*, 1988). This sequence boundary, however, is more difficult to pick away from type well C1-49 especially where core control is rare or absent. Below the sequence boundary is the preserved upper part of a highstand systems tract and above the sequence boundary is a transgressive systems tract with no preserved recognisable lowstand deposits (Fig. 3.4). The transgressive systems tract is bounded at the base by a laterally extensive Type 1 sequence boundary, and at its top by a maximum flooding surface.

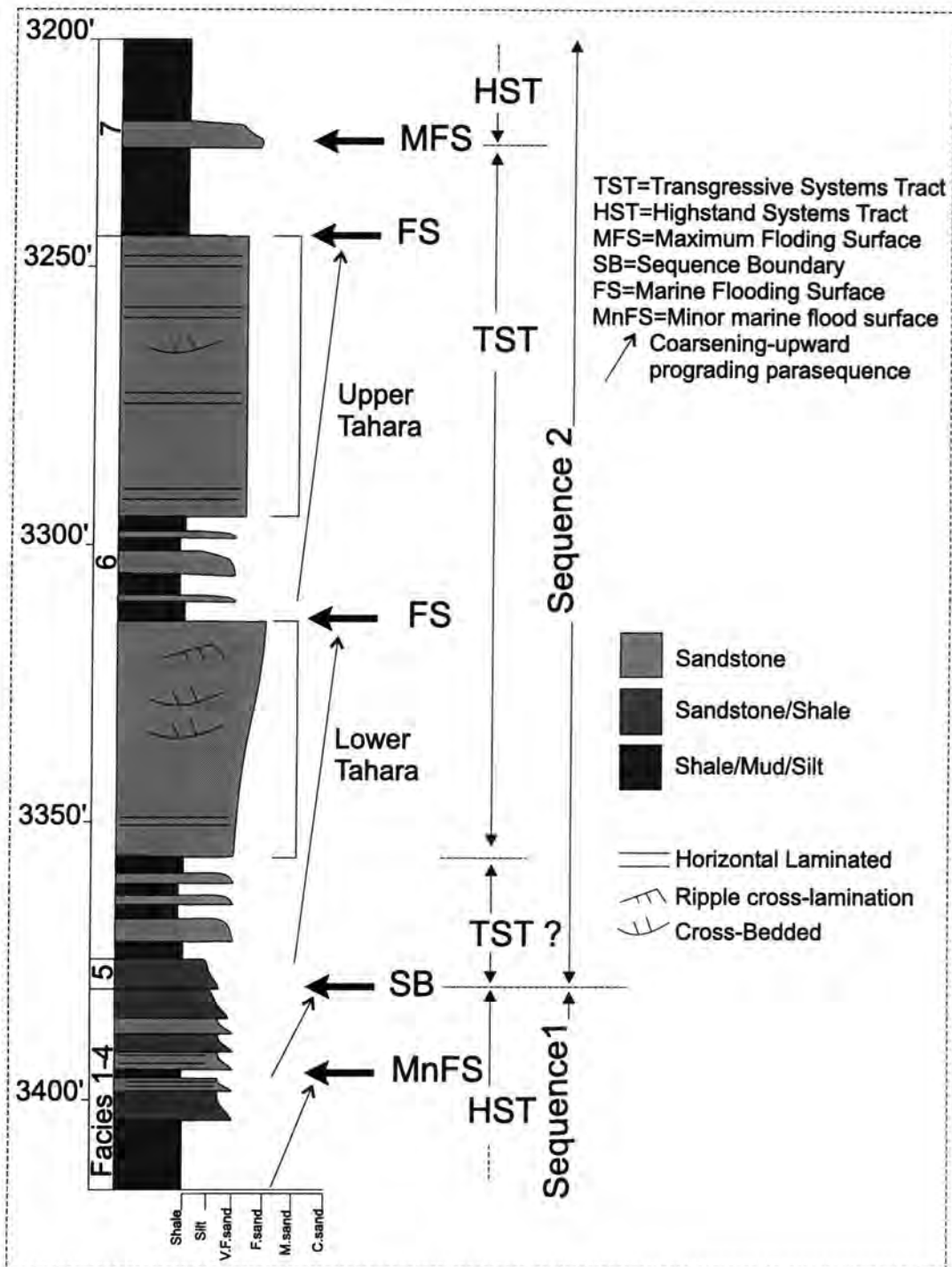


Fig. 3.4 Detailed vertical succession illustrating two incomplete sequences separated by a lowstand (palaeosol) sequence boundary and systems tracts (highstand and transgressive systems tract) of the Tahara Formation from type well C1-49. Below the sequence boundary is the upper part of a HST and above the sequence boundary is a TST with no recognised lowstand deposits. Classification based on stratal geometry and facies tracts.

The maximum flooding surface is overlain by the lower part of an incompletely exposed highstand systems tract. The maximum flooding surface consists of a 2 m thick bioturbated sandstone containing rip-up clasts and shell fragments. This material was deposited during a marine transgression and concentrated as a discrete bed on the top of the transgressive systems tract within sequence 2, in a marine-shelf environment (Fig. 3.4).

Vertical stacking of these sequences is indicative of a transgressive-regressive event. Transgressive and regressive describe the direction of movement of the shoreline landward and seaward respectively (Reinson 1984; Posamentier and James 1993). The movement of the shoreline is a function of the balance between sediment supply and the space available on the shelf (accommodation).

These two incomplete sequences, which are described in more detail below, are believed to have been deposited as part of third-order cycles with the upper one including fourth-order higher frequency cycles (Vail *et al.*, 1977; Van Wagoner *et al.*, 1990) that occurred in response to relative sea-level fluctuations and/or tectonic mechanisms (Miall 1996). The fourth-order of this model may have produced similar cycles to that observed in fourth-order cycle "B" (Van Wagoner *et al.*, 1990; Nummedal *et al.*, 1993) illustrated in Fig. 3.5. These two incomplete coarsening-upward and fining-upward cycles which are about 220' (67m) in thickness (Fig. 3.4) extend over hundreds of km's down depositional dip into the basin concomitant with a decrease in thickness (Fig. 3.6).

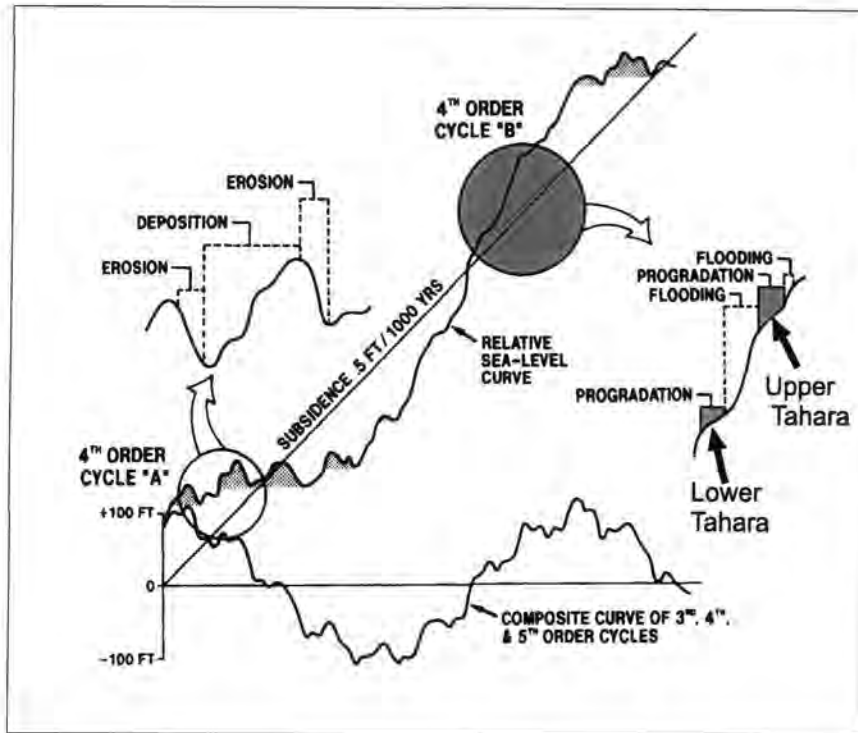


Fig. 3.5 Sea level cycles of third and fourth order resulting from rise and fall of sea level. Fourth order of cycle "B" represents the fluctuation rise of sea level superimposed on the third order similar to that observed in TST part of sequence 2 in Fig 4.1, which represents the upper and the lower Tahara sandstone (Progradation) terminated by marine flooding (Flooding) (From Nummedal *et al.*, 1993, originally from Van Wagoner *et al.*, 1990).

3.4.2.1-Sequence 1 (upper part)

The base of this sequence has not been cored, but is bounded at the top by a subaerial erosional surface, interpreted as a Type 1 sequence boundary (SB) (Van Wagoner *et al.*, 1990), which clearly suggests a period of relative sea-level fall. The sediments present below this sequence boundary, represent the upper part of sequence 1 (Fig. 3.4) and include Facies 1-4 (Table 2.1, Chapter 2). The core information shows it to be composed of a coarsening and upward thickening progradational succession. It consists of two parasequences. The first parasequence is overlain by a subordinate thin shale bed which may have formed during minor transgression (relative sea-level rise), interpreted as a minor

marine flooding event (Fig. 3.4). The second parasequence is truncated at the top by the sequence boundary defining the base of sequence 2.

The lower preserved part of sequence 1 includes a marine shale facies (Facies 1), which reflects low-energy conditions. This facies is interbedded with thin sandstone and siltstone laminae. These "tempestite" laminae reflect deposition by storm events. The sand proportion increases upward through the sequence (Facies 2-3) and is interpreted to represent deposition in response to progradation under increasing energy levels. The intensely bioturbated sandstone and shale (Facies 4) in the upper part of the sequence points to episodes of rates of low sediment rate (Reading and Levell 1996). The sequence is capped at the top by a thin oolitic ironstone and shale facies (heterolithic facies) (Fig. 3.5).

The vertical stacking pattern of this package suggests that the shoreline prograded probably during source area uplift and base-level fall concomitant with an increase in sediment supply to the shelf (Van Wagoner *et al.*, 1990; Swift *et al.*, 1991). Reading and Collinson (1996) pointed out that sequences like this occur when the rate of sediment supply exceeds the rate of creation of accommodation space or exceeds the rate of dispersal by marine processes.

The facies association (Facies 1-4; Fig. 3.4) within this sequence is characterised by:

- 1) an upward increase in grain-size;
- 2) an upward increase in sand content; and
- 3) the facies gradually shoals-upward throughout to the top of the sequence.

The overall succession has been interpreted to represent shelf to nearshore deposition under conditions of fluctuating energy (Chapter 2). The sequence is interpreted as part of the highstand systems tract (Fig. 3.4). Highstand systems tracts are created due to decreasing rates of relative sea-level rise, i.e. during slow down of the eustatic rise and the initiation of a slow rate of sea-level fall

(Vail *et al.*, 1991). Generally this systems tract deposition is distinguished by progradational parasequence stacking pattern interpreted to be deposited during the eustatic highstand.

3.4.2.2-Sequence 2

This incomplete, but better-preserved, sequence is deposited above the Type 1 sequence boundary and comprises transgressive and highstand systems tracts (Facies 6-7; Fig. 3.3). The most preserved part of this sequence consists of two coarsening-upward parasequences bounded at the top by marine flooding surfaces and at its base by the sequence boundary. Above the sequence boundary, shale intercalated with subordinate fine-grained sandstone and siltstone represent the lower part of the lower parasequence, deposited in response to relative sea-level rise and increase in water depth. It may represent the lower part of a transgressive systems tract (Fig. 3.4). The lower Tahara sandstone was deposited above these sediments and is followed by bioturbated sandstone and shale of the lower part of the upper parasequence, which passes upwards into the upper Tahara sandstone. The lower and upper Tahara sandstones extend laterally southwestwards away from type well C1-49 and will be discussed separately.

Lower Tahara

The lower sandbody consists of horizontally laminated and structureless sandstone overlain by planar cross-bedded sandstone showing an overall slight coarsening-upward trend (Fig. 3.4). This sandbody has been interpreted as a shoreface deposit overlain by fluvio-deltaic deposits in the upper part (chapter 2). The latter has been recognized only in well C1-49 on the basis of sedimentary structures and mineralogical composition (see chapter 5). The upward-coarsening trend shows a gradation from shale to sandstone which is bounded at the top by a marine flooding surface defined by a transgressive marine shale.

Flooding of the preceding delta system and relative sea-level rise led to a low rate of sediment supply.

As discussed previously in chapter 2 (Sec. 2.2.6), the core available from well ATS2 shows well-preserved shoreface sands of the lower Tahara sandstone underlain by back-barrier deposits (heterolithic type 2). It appears that the shoreline migrated landwards and that the sequence represents shoreface transgression under conditions of relative sea-level rise, high subsidence or minimal sediment supply and reworking of the shoreface sands (Galloway 1986; Elliott 1986b; Reading *et al.*, 1996).

Evidence of fluvial processes is negligible in the other four wells probably due to distance from the source. On the other hand Miall (1997) argued that delta deposits are rarely formed during transgression because the fluvial sediment supply tends to be influenced by the rise in base level i.e shifted landward. In addition, the preservation of fluvial sediments depends on the rate of sea-level rise, marine processes and sediment supply from hinterland tectonics (Reading and Levell 1996).

Upper Tahara

The vertical stacking pattern of the upper Tahara sandstone closely resembles the lower part of the lower Tahara sandstone, in that it consists of horizontal laminated and structureless sandstone. This sandstone has been attributed to shoreline progradation. The upper Tahara sandstone with the underlying marine shale represents another coarsening-upward parasequence. This progradational parasequence is also bounded at the top by a marine flooding surface and may have formed part of a transgressive systems tract during continuous sea-level rise.

The middle part of the upper Tahara sandstone in well C1-49 contains an 80 cm thick muddy sandstone. In addition to the lithofacies description of these sediments in chapter 2, thin-section analysis shows the presence of carbonaceous material, disseminated ooids, some of which are composed of

feldspars, and high concentrations of glauconite and heavy minerals. These sediments represent both shallow-marine and fluvially-influenced depositional systems. The presence of glauconite indicates a shallow-marine environment and deposition under anaerobic or reducing conditions (Pettijohn 1957), and low sedimentation rates (Reineck and Singh 1973; Tucker 1991). Thus, the appreciable spiky pattern through the gamma ray log values in the middle of the upper sandstone (Fig. 3.5) results from this high concentration of heavy minerals and glauconite in this part of the sandbody, feldspars and detrital shale.

The transgressive systems tract is bounded at the top by a 2 m thick bioturbated sandstone with lag deposits. This bed was deposited following transgression which occurred sufficiently slowly to allow time for reworking. The base of the bed is related to the time of maximum transgressive and it probably represents a maximum flooding surface (Vail *et al.*, 1991), defining the contact between the transgressive systems tract and highstand systems tract above.

Ancient prograding shorelines forming coarsening-upward sequences deposited during transgressive periods have been mentioned by many authors (e.g., Oomkens 1970; Reinson 1984; Elliott 1986b and others).

There are three main factors that controlled the transgressive deposits attributed in this sequence:

- 1) relative rise in sea-level (Van Wagoner *et al.*, 1990);
- 2) the succession is bounded at the top by a maximum marine flooding surface; and
- 3) change in rate of subsidence and sediment supply.

The incompletely exposed marine shales and intercalated thin sandstone and siltstone laminae that overly the maximum flooding surface are interpreted to be related to progradation during deposition of the highstand deposits above (Fig. 3.4). It possibly records that part of the highstand systems tract (Van Wagoner *et al.*, 1990) that was deposited during a subsequent rise in sea-level (Dalrymple

1992). As sea-level continued to rise water depth increases result in a decrease in clastic sediment supply concomitant with an increase in marine shale facies.

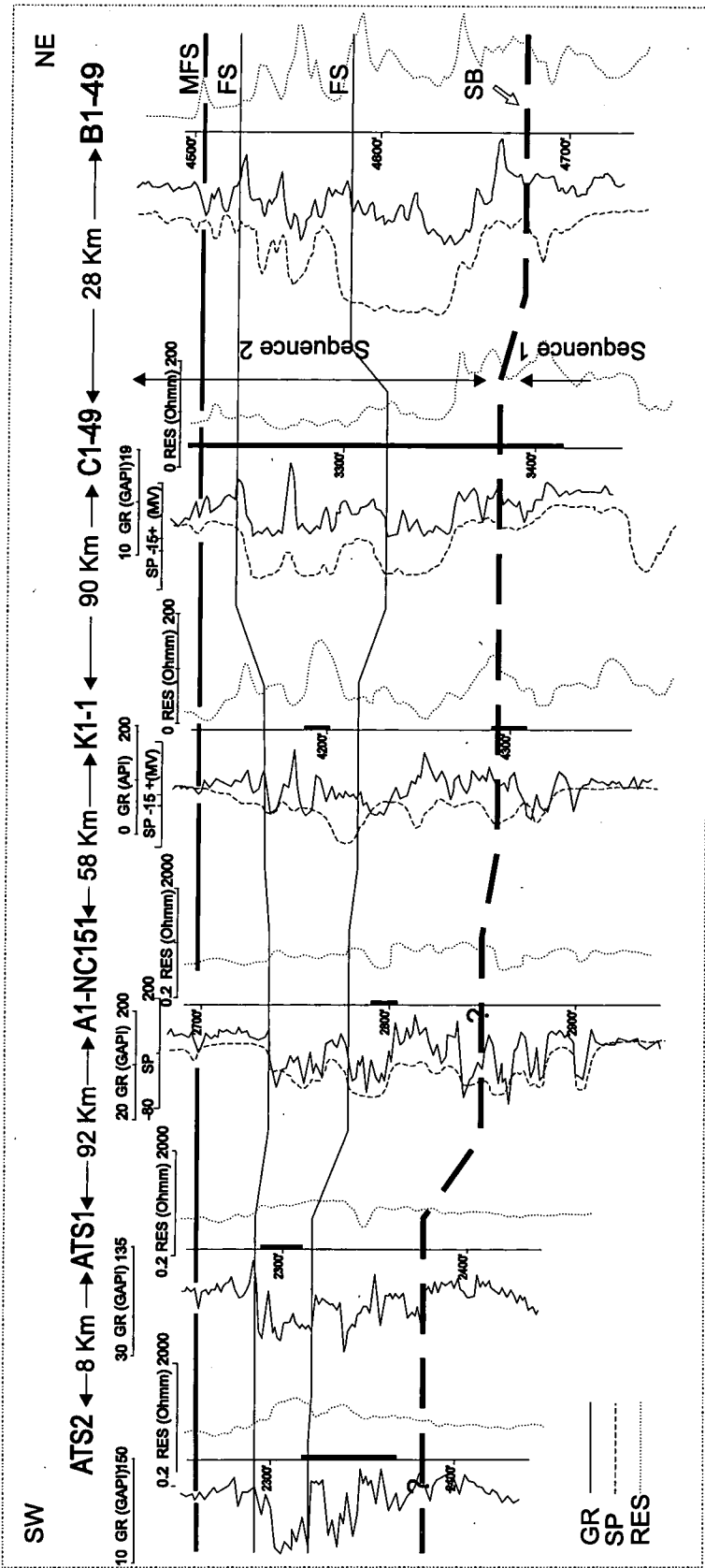


Fig. 3.6 Stratigraphic cross-section along southwest-northeast trend. It represents the core and well log through the Tahara Formation. MFS (maximum flooding surface) used as datum line and vertical black bars indicate the cored intervals. FS represents marine flooding surface deposited during continuous sea level rise. Dashed line represents the sequence boundary (SB) of a regressive surface of erosion during sea-level fall (lowstand). The succession thins laterally southwestwards. Note wireline log in well B1-49 is without scale (not in well file).

Chapter 4

Sequence Stratigraphy from Wireline Logs

4.1-Introduction

Sequence stratigraphic analysis of well log data is a new technique that can be used for facies and sedimentological interpretation. Wireline logs analysis is an important and essential part of analysing subsurface data and is used extensively in the petroleum industry. The aim of this chapter is to review the use of wireline logs in sequence stratigraphy and to define various characteristic log patterns, especially gamma ray patterns and integrate them with the core data (discussed in Chapter 2). Gamma ray wireline logs have been used to classify the wireline log trends of sandbodies (Selley 1976b; Galloway and Hobday 1983; Rider 1996) and to define electrofacies patterns (Rider 1996).

4.2-Geological Interpretation from Gamma Ray Log

The most useful wireline log curve in the Tahara succession, is the gamma ray log. This is because it is a common wireline log in these wells and has better resolution than most other logs. Figure 4.1 shows a suite of wireline logs from well C1-49 that have been used to select the different lithologies in the Tahara succession. For example, the gamma ray log clearly identifies upper and lower Tahara sandstone, and an unusual peak in the middle part of the upper Tahara sandstone (Fig. 4.1) attributed to the presence of a high concentration of glauconite and heavy minerals (placer deposits) (Rider 1996).

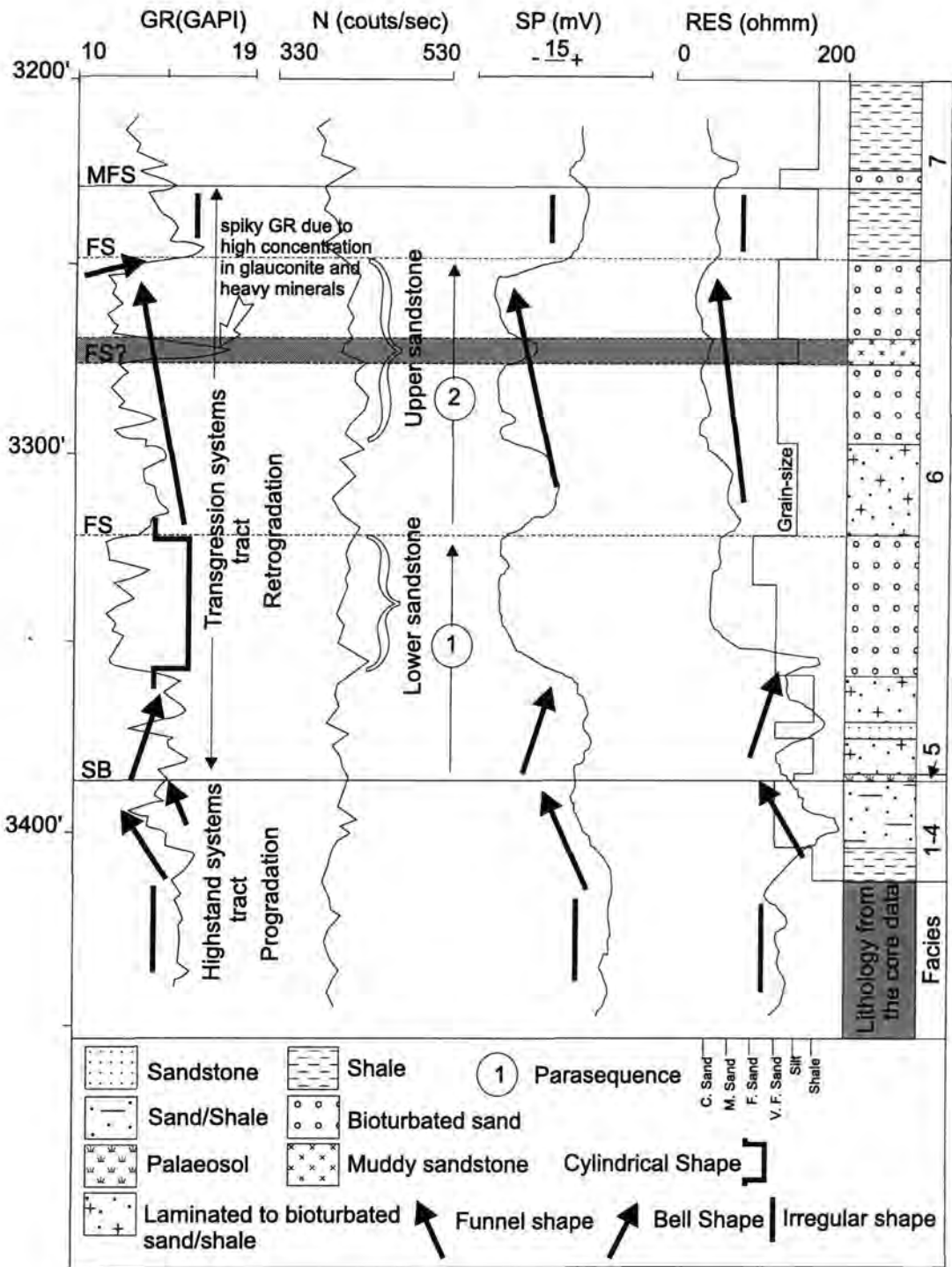


Fig. 4.1 Wireline logs from type well C1-49. Gamma ray log (GR), self potential (SP), neutron (N) and resistivity log (Res) related to core lithology, and showing the trends in systems tracts, parasequences and key of stratigraphic surfaces in incomplete sequence 1 and 2.

The gamma ray log records the presence of natural radioactivity (potassium (K), uranium (U) and thorium (Th)) which is highest in clay minerals (Cant 1984 b; Rider 1990; Miall 1996). The high gamma ray readings indicate shale content or may indicate radioactivity from feldspar in arkosic sandstones as well as heavy minerals in lag deposits. The unit for radioactivity logging is the API (American Petroleum Institute) which conventionally increases to the right.

4.2.1-Gamma-ray log (GR) trends

Trends on the gamma ray logs may equate with depositional trends. Gamma ray log shapes may be used to determine: (1) sandstone grain-size; (2) depositional facies and environments, and (3) the deposition between sands and shales in mixed siliciclastic sequences (Selley 1976b; Galloway *et al.*, 1983; Cant 1984 b; Rider 1990) (Fig. 4.3). Gamma ray shapes may represent clean sandstone, interbedded sandstone and shale, and abrupt and gradational contacts. The gamma log has limited use in carbonate facies analysis where it can indicate fluctuations in clay content (Selley 1985). Description of various gamma ray shapes;

a) Bell shape: indicated by an upward increase in gamma ray value and a gradual upward decrease in grain-size trend indicating increasing clay content (e.g. change from sandstone to shale) and abrupt base. Such trends may represent deposition in channel or transgressive marine facies (Cant 1984 b; Rider 1990). For example, the transgressive marine shale below the lower Tahara sandstone (Fig. 4.1 and 4.2).

b) Funnel shape: shows a gradual upward decrease in the gamma ray value, related to gradual increase in grain-size indicative of a decrease in clay content. It is characterised by an abrupt top and coarsening-upward grain-size trend probably produced by prograding systems, for example, deltaic progradation or shallow-marine progradation. This trend is seen clearly in parasequence 2 in Fig. 4.1.

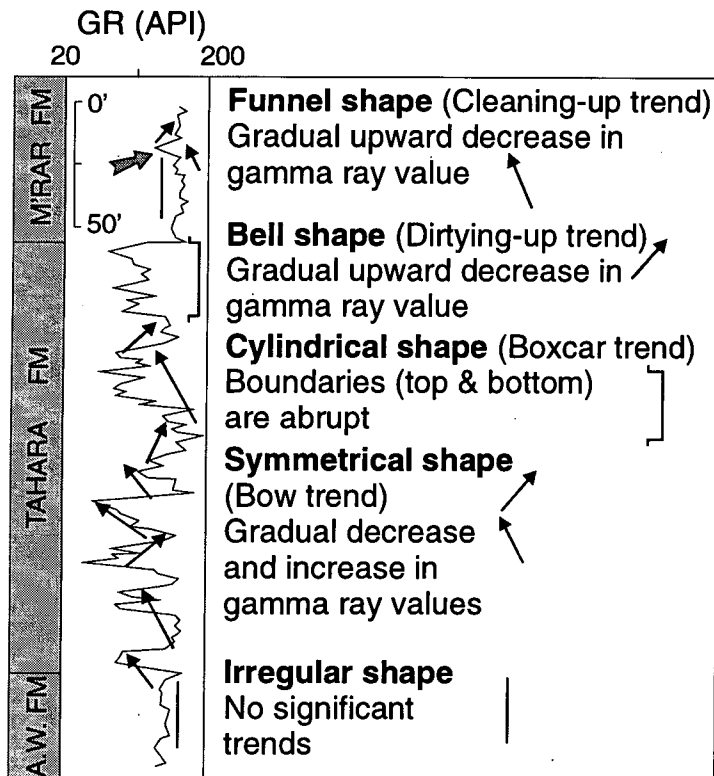


Fig. 4.2 Wireline log trends. Illustrated using the gamma-ray log from well A1-NC151. Maximum flooding surface (thick arrow). The top and bottom of Tahara Formation based on data from Sirte Oil. Co.

c) Boxcar shape (cylindrical trend): consists of low gamma ray value with constant reading, set within a higher gamma ray background value. The boundaries with the overlying and underlying shale are abrupt. This shape is recognized from the lower sandstone in well C1-49 (Fig 4.1) or upper sandstone in well ATS1 (Fig. 4.6).

d) Symmetrical shape: consists of coarsening, overlain by fining trend of similar thickness with no sharp break between the two. This trend is not common within wells of study area, but may be present in well A1-NC151 (Fig. 4.2).

e) Irregular shape (mixed clean and shaly): no systematic change observed—they lack the clean character of the boxcar shape. This trend may represent aggradation of a shale or silt succession (Emery and Myer 1996). Such a trend is

seen in the shale interval above the upper sandstone or lowermost part of the succession (Fig. 4.1)

Figs 4.3 and 4.4 show the general characteristic log curve shapes that are similar to the gamma ray shapes of this study, and which have been used to identify depositional environments and interpret the sequence stratigraphy. For example, the funnel and cylindrical shapes in both figures represent the lower and the upper Tahara sandstone, and bell shapes could represent marine transgressive shale passing upward into sandstone. Irregular shapes represent the marine shale facies (e.g. Facies 1 and/or Facies 7).

As a general concept the gamma ray readings are low in sands and high in shales. This concept indicates relationships between gamma ray value and grain-size, and between clay content and gamma ray value (Serra and Sulpice 1975; Selley 1976b; Galloway *et al.*, 1983; Rider 1990). The sedimentological interpretation of gamma ray log shapes depends on the variations of logs with grain size. Change in grain size will be followed by change in gamma ray value. High gamma ray values indicate shale (fine materials) and low gamma ray values indicate free clay formation (coarse grained materials). This relationship relates to the depositional energy of the environment. Thus, high gamma ray values represent low energy-settings whereas low gamma ray values represent high-energy settings. Sedimentological interpretation of this relationship leads to direct correlation between facies and log shapes. The funnel shape is usually related to an upward passage from shale-rich to shale free facies, i.e. a coarsening-upward trend.

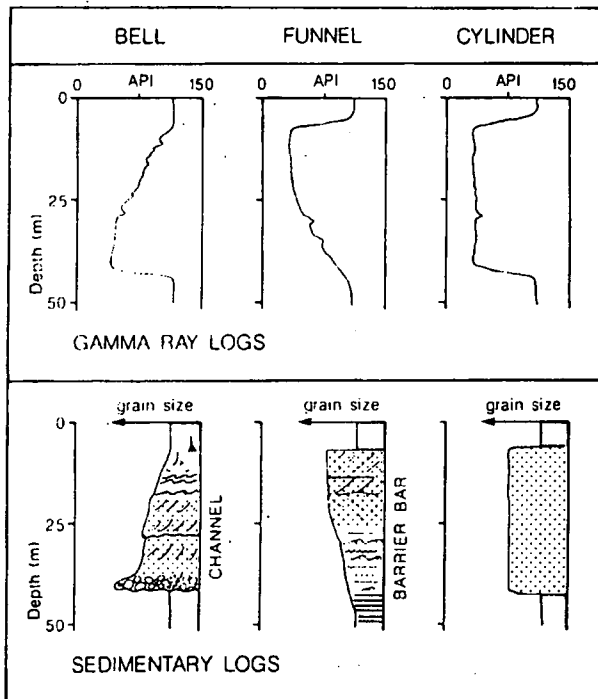


Fig. 4.3 Three principle gamma ray shapes and their corresponding sedimentary interpretation (After Rider 1990).

Cylindrical	Funnel Shaped	Bell Shaped	Symmetrical	Irregular
Clean, No Trend	Abrupt Top Coarsening Upward	Abrupt Base Fining Upward	Rounded Base and Top	Mixed Clean and Shaly, No Trend
aeolian, braided fluvial, carbonate shelf, reef, submarine canyon fill	crevasse splay, distributary mouth bar, clastic strand plain, barrier island, shallow marine sheet sandstone, carbonate shoaling-upward sequence, submarine fan lobe	fluvial point bar, tidal point bar, deep sea channel, some transgressive shelf sands	sandy offshore bar, some transgressive shelf sands, amalgamated CU and FU units	fluvial floodplain, carbonate slope, clastic slope, canyon fill

Fig. 4.4 Idealized log curve shapes from the gamma ray or (SP-Log). Depositional environment interpretation below each curve (After Cant 1984b).

The succession is interpreted to have been deposited along a prograding shoreline (shallowing-upward) as evidence by core. The bell shape, therefore, can be interpreted to indicate a fining-upward grain-size trend. This succession may reflect retreat of a shoreline, resulting in an upward deepening trend related to increasing water depth.

Boxcar shapes are typical of some types of fluvial channel sand, turbidite and aeolian sand (Cant 1984 b) (Fig. 4.4.). In addition, evaporites often have a boxcar response on the gamma ray log (Emery and Myer 1996) and they give very low gamma readings (as anhydrite and salt) or very high readings (potassium salt) (Reading 1986). A symmetrical shape is related to coarsening overlain by fining-upward trends, and results from variations in sedimentation rate in the basin, usually during the progradation and retrogradation of a mud-rich fan system (Emery and Myer 1996). Irregular shapes are unlikely in any shelf or paralic facies, where cyclic changes in water depth are likely to be recognised as cyclic log trends and identified as parasequences. By contrast, in deep-marine environments, the funnel and bell shapes are generally part of more symmetrical trends related to an increase and decrease in the sand/shale ratio of thinly bedded turbidites.

4.3-Sequence Stratigraphic Interpretation from Wireline Log Trends

Sequence stratigraphy is a concept that explains vertical and lateral variation of sedimentary intervals in terms of relative sea-level changes. Identification of sequences from subsurface data depends upon the use of electric logs and seismic data. Wireline log patterns may be used to interpret depositional environments, and determine vertical sequence and bedding architecture. A wireline log trend suitable for lithology and stratigraphic interpretation is shown in Figures 4.1 and 4.6. The interpretation of the depositional environment based on the study of core logs, has been discussed in chapter 2. Where these data are rare or absent, it is useful to analyse electric log patterns (e.g. gamma ray log) supplemented by available core data. For this reason Selley (1976b) pointed out that wireline log patterns never should be interpreted in isolation, and for better

resolution it is essential to use both core and log data. The interpretation of wireline log trends to identify falls and rises in relative sea-level is essential in order to show the sequence boundary, the maximum flooding surface and other minor marine flooding surface. Rider (1996) shows the schematic wireline log characteristics for the sequence stratigraphic interpretation of wireline logs (Fig. 4.5). This model indicates the key sequence stratigraphic surfaces (sequence boundary, maximum flooding surface and transgressive surface) that can be used to interpret these surfaces in Tahara succession as follow:

a) Sequence boundaries (SB) which result from a fall in relative sea-level may be difficult to recognize from the well log alone (Emery and Myer 1996). Rider (1996) claimed that there is no set of diagnostic responses, but evidence of a sequence boundary is its position in the sedimentary succession.

The sequence boundary may represent abrupt upward change from progradation to retrogradation in the succession. A sequence boundary may result from an abrupt change in log response in sandstone units or may be marked by change in shale type in the shale section (Rider 1996). This surface is recognized only from core control from wells C1-49 and K1-1. In wireline log patterns between wells it proved more difficult to recognise because core data is lacking and gamma ray signatures in this position are not clear in the other wells.

The degree of similarity of the wireline log curves between wells decreases with increased distance between wells. However, a sequence boundary away from well K1-1 is proposed on the limited available evidence from the wireline logs (Fig. 4.6).

b) A maximum flooding surface (MFS) can be identified from a gamma ray peak (high gamma ray values) on bell and funnel trends respectively (i.e. where these are fining-upward and coarsening-upward respectively, the maximum flooding surface may be a gamma maximum). It should not be assumed that every gamma ray peak is a maximum flooding surface (Emery and Myer 1996). However, in core and well log data, the maximum flooding surface may be easily recognized by its distinct, relatively high gamma ray log values (Partington *et al.*,

1993). Maximum flooding surface could be the surface above retrogradational and below progradational intervals.

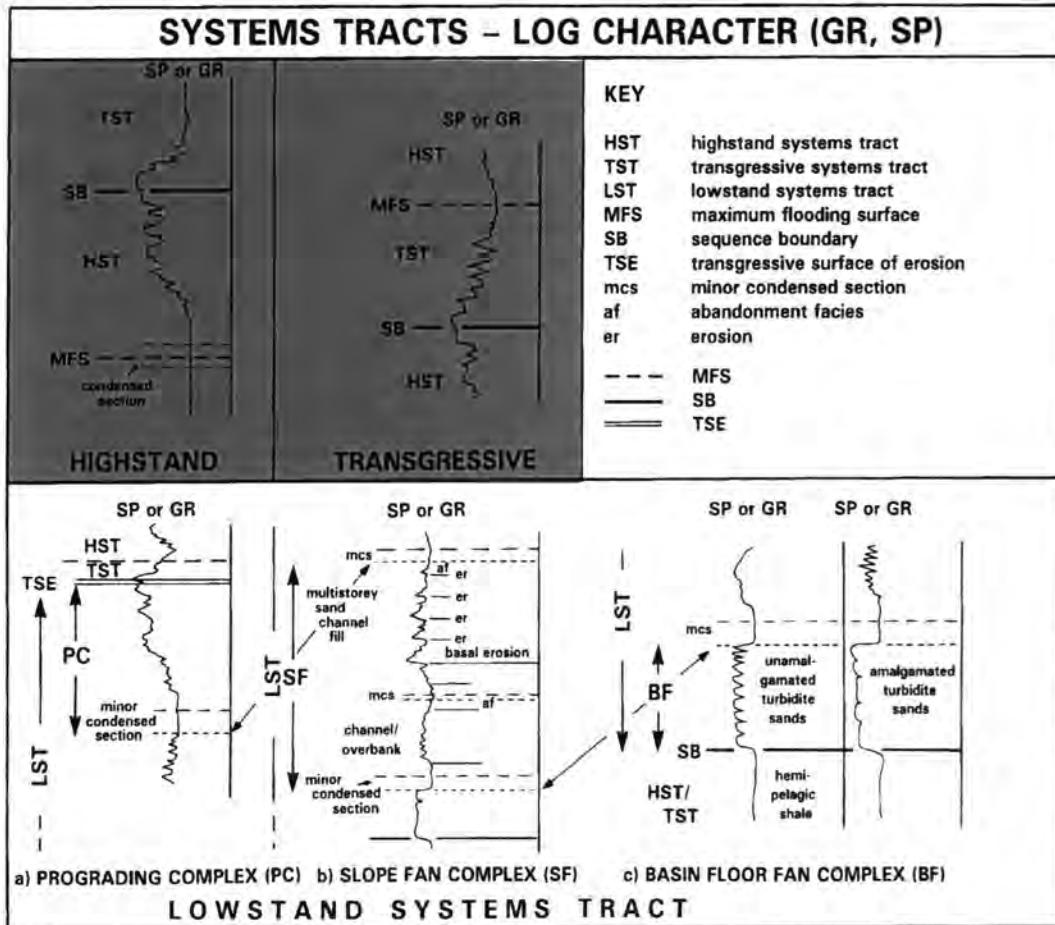


Fig. 4.5 Schematic wireline log patterns for sequence stratigraphy interpretation. Shaded area represents the systems tracts (TST and HST) with their key surfaces recognized within the study area (from Rider 1996).

In the study area the maximum flooding surface is marked in the core by a bioturbated sandstone bed (well C1-49) and overlying deeper water shale environment, and could be easily recognized in wells without core control. This surface lies at the point of maximum gamma ray response and can be traced laterally into basinward settings where shale is separated by thin bioturbated sandstone (Fig 4.1). It correlates very well between wells, because the gamma ray signature of the maximum flooding surface has a more distinctive peak and

forms a good marker horizon (used as datum line marker in cross-sections in this study).

c) Marine flooding surfaces (FS) as opposed to maximum flooding surface can be recognized from a sudden change in log value (abrupt increase in gamma ray reading). It indicates a change in lithology, such as shale resting sharply on sandstone. This surface typically terminates coarsening-upward trends. The example (Fig. 4.1) shows that the lower and/or upper Tahara sandstone was followed by transgressive marine shale that represents a parasequence, bounded at the top by a marine flooding surface. It can be easily correlated between wells. The facies successions are frequently bounded by this surface (Fig. 4.6).

4.4-Depositional System Tracts of the Tahara Succession from Wireline Logs

Recognition of the key sequence stratigraphic surfaces from the succession (Facies 1-7) described above allows the stratigraphy to be divided into parasequences which together form a systems tracts deposited during relative sea-level rise and fall. Transgressive and highstand systems tracts are recognized in this succession and have been discussed in the chapter on sequence stratigraphy. In this section an attempt will be made to identify these systems tracts from wireline log trends.

a) Progradation can be recognized from an upward decrease in gamma ray values resulting in an upward increase in grain-size (i.e. increase in sand/shale ratio). Progradation represents the funnel trends (Figs 4.1 and 4.6). The vertical pattern of upward coarsening and thickening reflects the progradational succession.

b) Retrogradation is indicated by fining-upward stacking patterns, which imply upward deepening (upward increase in gamma ray values). Retrogradation successions show vertical stacking patterns from sandstone to shale facies

4.4.1-Transgressive systems tract

From core examination, Facies 7 (chapter 2) shows two prominent sandstones which together with the underlying bioturbated sandstone and shale form two coarsening-upward parasequences. Two these parasequences are seen in the gamma ray log profile (Figs 4.1 and 4.6) emphasising the relationship between the core data and gamma ray log trends. Gamma ray log shapes in both sandstones are variable from funnel to roughly cylindrical shape (Cant 1984 b) as illustrated in Fig. 4.6. The log pattern from this Figure is not clearly defined in some cases. Cant (1983; 1984 b) shows an example from the Spirit River Formation, which has similar gamma log patterns to those in the lower sandstone in well ATS2, interpreted as irregular to cylindrical gamma ray log pattern. By contrast, "There is no simple pattern of mechanical log response that could be considered characteristic of subsurface transgressive shoreline deposits, because the variability of lithologies and contacts within a sequence is high" (Reinson 1984).

The lower Tahara sandstone shows a serrate cylindrical gamma ray shape in well C1-49 and ATS2, and a funnel gamma ray shape in wells K1-1, A1-NC151 and ATS1. The upper Tahara sandstone shows funnel gamma ray shape in well C1-49 and well K1-1 shows a complex gamma ray trend, whereas it shows a serrate cylindrical gamma ray log shape in well A1-NC151, ATS1 and ATS2 (Fig. 4.6). Both parasequences are bounded at their top by marine flooding surfaces, as indicated by a high gamma ray reading. Both parasequences represent a progradational pattern and these are reflected in the typical gamma ray log profiles. The serrate shape of gamma ray log patterns in parasequence sandstones is due to contrasting grain sizes within stratification and cross-bedding. Parasequences represent the shoreline progradation setting. The vertical pattern of upward coarsening and thickening reflects the progradational deposits. Parasequences are part of sequence 2, deposited in transgressive systems tract in response to sea-level rise. This systems tract, is bounded at the top by a maximum flooding surface, and the bottom by a lowstand sequence boundary (Figs 4.1 and 4.6).

4.4.2-Highstand systems tract

The lowermost part of the deposit below the sequence boundary consists of two small parasequences, separated by a minor marine flooding surface, both of which are recognized in core data. This package consists of facies 1-4 (chapter 2) has been described and interpreted as shelf-nearshore environments. The parasequences are not evident on the wireline logs, the only evidence is an irregular shape followed by a funnel shape which reflects a gradual upward decrease in gamma ray value (Fig. 4.4). The irregular shape corresponds to the finer material (shale with subordinate sandstone and siltstone lamina of Facies 1) and may represent a deeper water setting.

The schematic wireline log (GR or SP) characteristics of both transgressive and highstand systems tracts with their key sequence stratigraphic surfaces are shown in Fig. 4. 5.

4.5-Tahara Formation in Response to Sea-Level Changes

Gamma ray log correlation between wells in cross section (Fig. 4.6) shows an irregular trend followed by a funnel shape below the sequence boundary, especially in well C1-49. These shapes consist of shale with increase sand-upward. This is interpreted to represent the coarsening-upward progradation part of the upper part of sequence 1 in response to sea-level rise followed by a fall. The upper and lower Tahara sandstones mostly show the funnel or cylindrical shapes but may be serrated, and the nature of the contacts are gradational or abrupt according to the gamma ray signatures (Fig. 4.6). Each sandstone with underlying transgressive marine shale shows gamma ray trends indicative of deposition along a prograding shoreline possibly in response to part of a third order relative sea-level rise (Fig. 4.1). The relative sea-level curve shows that the sequence 1 was deposited in the regressive phase followed by the transgressive phase of the incomplete sequence 2 (Fig. 4.6).

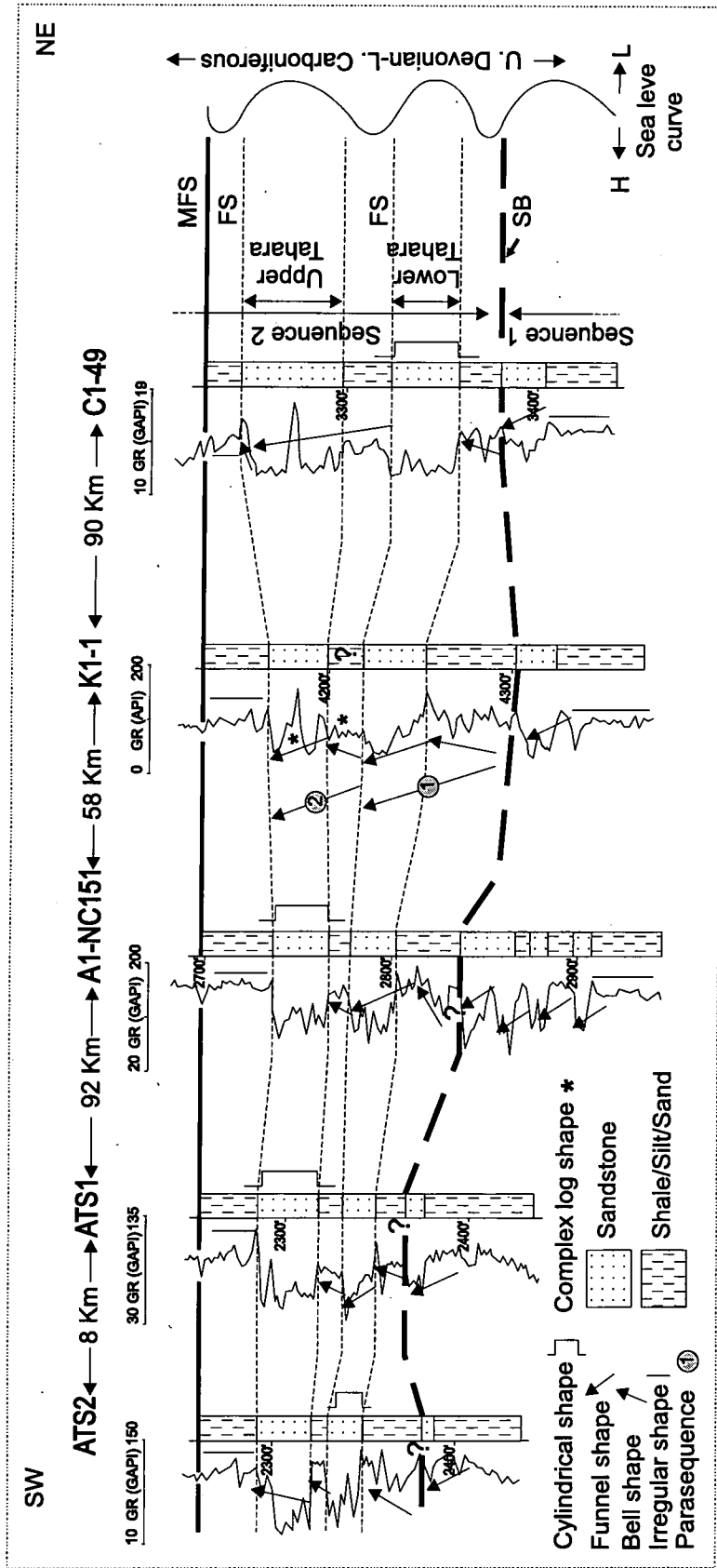


Fig. 4.6 SW-NE well log cross section showing gamma ray trends between wells from incomplete sequence 1 and 2, and sea-level curve based on the sequence stratigraphic interpretation. Lithologies recognized are based on core and log signatures.



Chapter 5

Sandstone Petrology

5.1-Introduction and Sampling Methodology

The purpose of the petrographic study is to examine the textural, mineralogical, diagenetic and porosity characteristics of the Tahara Formation. Mineral composition was determined by point counting 300 grains in each of 18 thin sections cut from samples taken from both the upper and the lower parts of the sandstone in well C1-49, and 11 thin sections cut from sandstone samples taken from wells K1-1, A1-NC151 and ATS2 (Fig. 1.2). The study is based mainly on data from well C1-49. In addition to the modal analysis, the diameters of 100 detrital quartz grains were measured in each thin section. The locations of these samples are shown in Fig. 5.1 and the results of the analysis in Tables 5.1 and 5.2.

5.2-Composition of Sandstones

5.2.1-Quartz

The sandstones in the Tahara Formation are composed mostly of quartz (38% to 95%). The grains are predominately monocrystalline with subordinate polycrystalline quartz grains. Most quartz grains are rounded to subrounded, but roundness is difficult to estimate because of the lack of well preserved grain boundaries, secondary overgrowths or replacement cement. In some cases where the boundaries between quartz grains are clear they are straight, sutured or embedded (many grain margins were corroded during diagenesis).

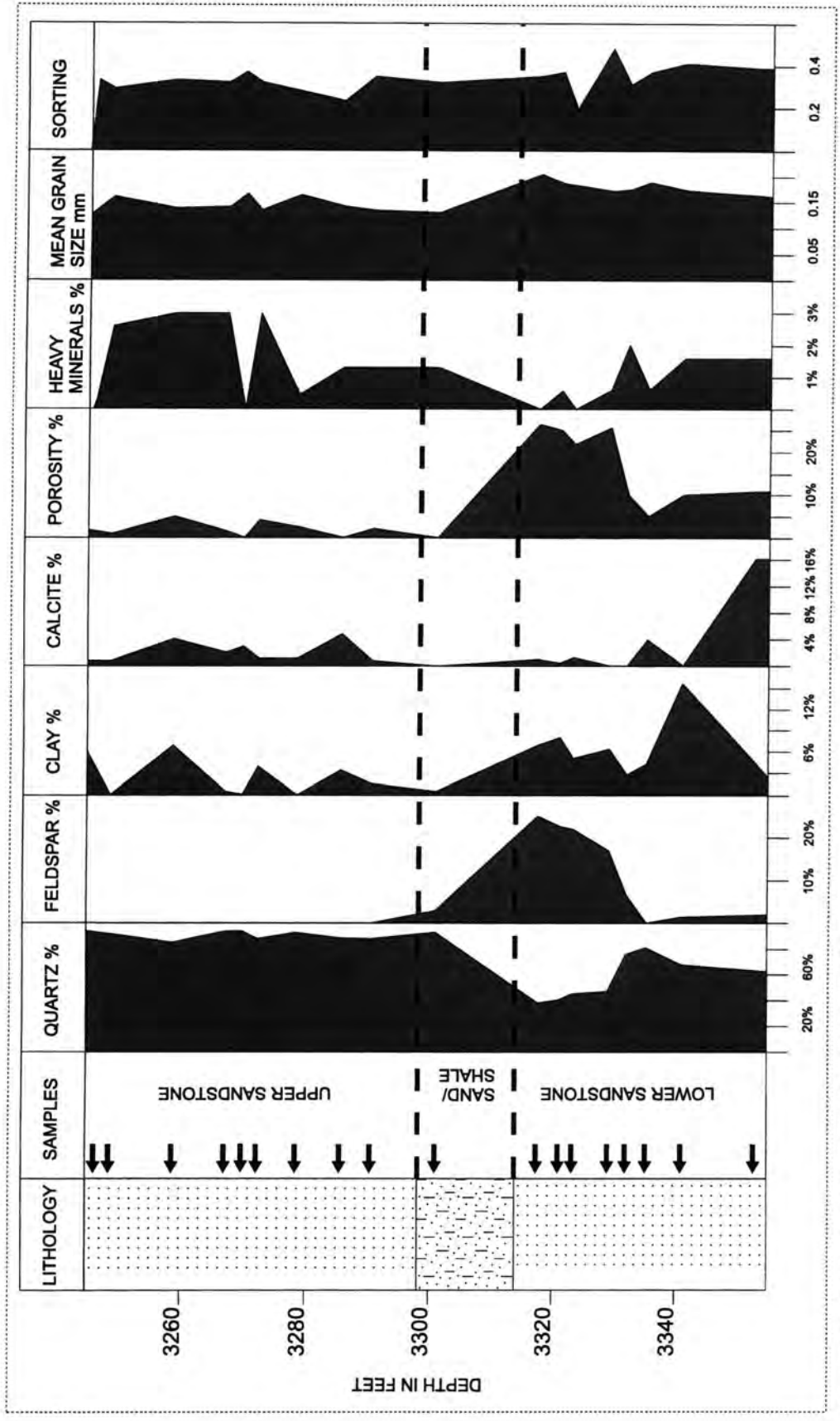


Fig. 5.1 Petrographic characteristics of the lower and upper sandstones from the Tahara Formation from well C-1-49 showing sample points (arrows), quartz, feldspar content, clay matrix, calcite cement, heavy minerals, porosity, mean grain size (mm) and sorting.

Secondary authigenic quartz overgrowths, defined by inclusions and dust rims, are common. Some quartz grains contain inclusions of heavy minerals.

5.2.2-Feldspar

Feldspar is the second most important mineral in the Tahara sandstones. The feldspar content varies from 0% up to 34% as illustrated in Tables 5.1 and 5.2, and Fig. 5.1. Feldspars in the lower sandstone are mainly plagioclase and potassium feldspar (microcline and untwinned orthoclase) most of which have been partially to completely dissolved during diagenesis; other crystals are relatively unaltered. The mean grain size of preserved feldspar crystals is 0.17 mm. These occur as angular to subangular detrital grains, but most of the margin crystal margins show evidence of corrosion.

The variety of feldspars abundant in a particular sandstone like the upper part of lower Tahara sandstone may depend on the tectonic setting and climate of the source area, and depositional site (Blatt 1982). The presence of microcline feldspar crystals implies a plutonic granitic igneous source (Pettijohn 1957).

5.2.3-Rock fragments

Rock fragments are an important constituent of the sandstones. The presence of rock fragments provides clue to source rock composition. Rock fragments are uncommon or present in small or trace amounts both in the upper and lower sandstone (up to 2%, Tables 5.1 and 5.2; Fig. 5.1). They consist of polycrystalline quartz rock fragments, rare chert, and a few shale fragments. Most of the polycrystalline quartz grains in thin section are subrounded to rounded in shape.

SLIDE NO.	1	2	3	4	5	6	7	8	9	10
QUARTZ	281	277	256	283	284	266	280	269	264	280
FELDSPAR	0	0	0	0	0	0	0	0	0	2
MICA	0	0	1	0	1	2	1	0	0	3
ROCK FRAGMENTS	1	1	0	1	1	1	0	4	0	6
PORE SPACE	3	2	12	3	0	10	6	0	25	0
CLAY	8	0	14	2	0	8	0	7	3	1
HEAVY MINERALS	2	9	1	1	0	9	2	4	4	4
OPAQUE MINERALS	2	8	3	2	5	1	3	1	2	4
CALCITE	2	2	13	6	9	3	8	15	2	0
GLAUCONITE	1	1	0	2	0	0	0	0	0	0
TOTAL	300	300	300	300	300	300	300	300	300	300

• Sample from sand and shale interval below sandbody.

Table 5.1 Modal composition of samples from the upper sandstone of the Tahara Formation.

SLIDE NO.	11	12	13	14	15	16	17	18
QUARTZ	144	122	136	141	227	242	203	189
FELDSPAR	75	68	66	51	20	1	5	6
MICA	0	2	2	0	0	0	2	0
ROCK FRAGMENTS	2	1	3	6	6	1	6	0
PORE SPACE	83	75	71	78	29	15	30	35
CLAY	21	24	15	19	8	27	47	13
HEAVY MINERALS	0	20	0	2	6	2	5	5
OPAQUE MINERALS	2	5	3	3	4	0	2	2
CALCITE	3	1	4	0	0	12	0	50
GLAUCONITE	0	0	0	0	0	0	0	0
TOTAL	300	300	300	300	300	300	300	300

Table 5.2 Modal composition of samples from the lower sandstone of the Tahara Formation.

5.2.4-Mica and clay minerals

Mica is a minor constituent of the Tahara sandstones. Muscovite is the most common mica seen in thin section. It occurs as flakes between 0.12 and 0.75 mm long with a some grains >1 cm long in the matrix. Detrital flakes of muscovite occur as shreds and tabular laths which may be bent through compaction and deformation around quartz grains. Finer detrital flakes tend to be abundant in shaly layers. Mica is winnowed out of high-energy environments and tends to be deposited in low energy environments. The predominance of muscovite is characteristic of most sandstones and reflects its greater resistance to chemical weathering than other mica types. Muscovite is produced by the break down and weathering of igneous and metamorphic rocks.

Clay minerals within the sandstone are represented by kaolinite (Fig. 5.1) which is present in amounts ranging from traces to 15.6%. Kaolinite, however, is a secondary mineral formed by weathering and/or diagenetic alteration of feldspar.

Other clay minerals present are glauconite which occurs as small granular, green ovoid grains. This occurs in amounts of less than 0.7% in the upper Tahara sandstone (Table 5.1) but is locally concentrated in larger amounts in the middle part of the upper sandstone particularly in the muddy sandstone bed. It is an important constituent mineral of marine sands and characteristic of relatively nearshore and shallow-water marine environments. The presence of glauconite in sandstone is a useful indicator of a marine origin. Glauconite forms at < 15° C, generally between 30 and 2,000 m (Porrenag 1967) under slow rates of sedimentation, and it may be reworked and transported (Pettijohn *et al.*, 1978; Blatt 1982; Tucker 1991).

5.2.5-Heavy minerals

Heavy minerals can provide evidence as to the composition of the source rocks, and they have proved useful in provenance studies (Tucker 1991). However, they are effected by weathering, transportation, deposition and diagenesis

(Morton 1985). Heavy minerals are present in small amounts of up to 3% in Tahara sandstones (Fig. 5.1) and are dominated by tourmaline, zircon and locally hornblende, which are resistant to mechanical and chemical weathering. Zircons are more abundant than other heavy minerals within the heavy mineral suite but the low overall amount of heavy minerals within the formation may imply a low content of heavy minerals in the source sediments.

5.2.6-Other minerals

Calcite crystals are present within Tahara sandstones as a cement and range from trace amounts to < 16.6%, in the form of coarse sparry calcite or micrite within the clay matrix (see diagenesis section for more details). Scattered opaque minerals (some organic material) are seen in most thin sections. Opaque minerals make up between 0.3% and 6.7% (Tables 5.1 and 5.2).

5.3-Diagenesis

Tahara sandstones show a variety of diagenetic phases. Mechanical compaction and chemical compaction include pressure dissolution and dissolution of minerals. The paragenetic sequence for the Tahara sandstones is a composite sequence, observed from thin sections, which is given schematically in Fig. 5.2. Authigenic phases preceding or post-dating the secondary porosity (for more detail of secondary porosity see page 115) yield clues to the chemical (composition of the fluid phase) and physical (temperature and pressure) conditions responsible for dissolution.

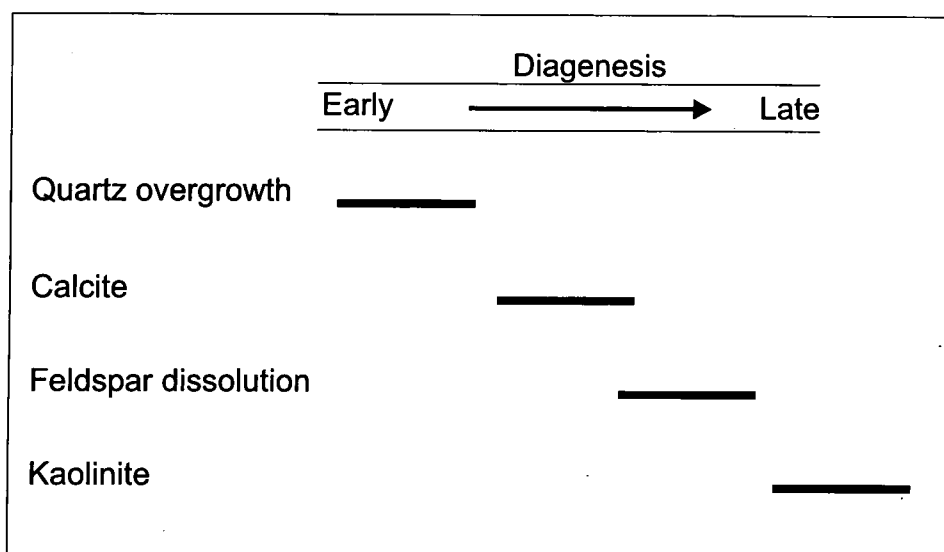


Fig. 5.2 Paragenetic sequence of diagenetic events in the Tahara sandstone.

5.3.1-Silica cementation

Silica cement is an early authigenic cement and common diagenetic phase in the Tahara sandstones. Authigenic silica cement is present in the form of overgrowths on detrital grains with well-developed crystal faces. Where clay rims are visible around detrital quartz grains they are well defined but in many cases the boundaries between detrital grains and overgrowth can not be clearly seen under the microscope (Fig. 5.3). The presence of clay rims may indicate shallow to intermediate depth burial between 1000 and 4000 feet (Galloway 1979). Authigenic quartz overgrowths occur on the majority of quartz grains in all samples. The original quartz grains are partially/or completely obscured by secondary overgrowths and the contact between grains is sutured or embedded suggesting that silica may have been precipitated from pressure solution processes and migration of fluid. Authigenic quartz may be introduced through meteoric water with a high silica content. Blatt (1979) pointed out that shallow-marine water contains an average of <1 ppm of silica and nonmarine (fluvial) water contains an average of 13 ppm silica. The equilibrium solubility of silica in ground-water at 25° C is 6 ppm. It increases to 21 ppm at 50° C and 140 ppm at 150° C (i.e., solubility of quartz increases with temperature) (Blatt 1979).

Solubility also increases with increase hydrostatic pressure and depth. The early diagenetic of silica has reduced the primary porosity. For example, the upper sandstone shows almost complete cementation by quartz and as a result a considerable loss of primary intergranular porosity.

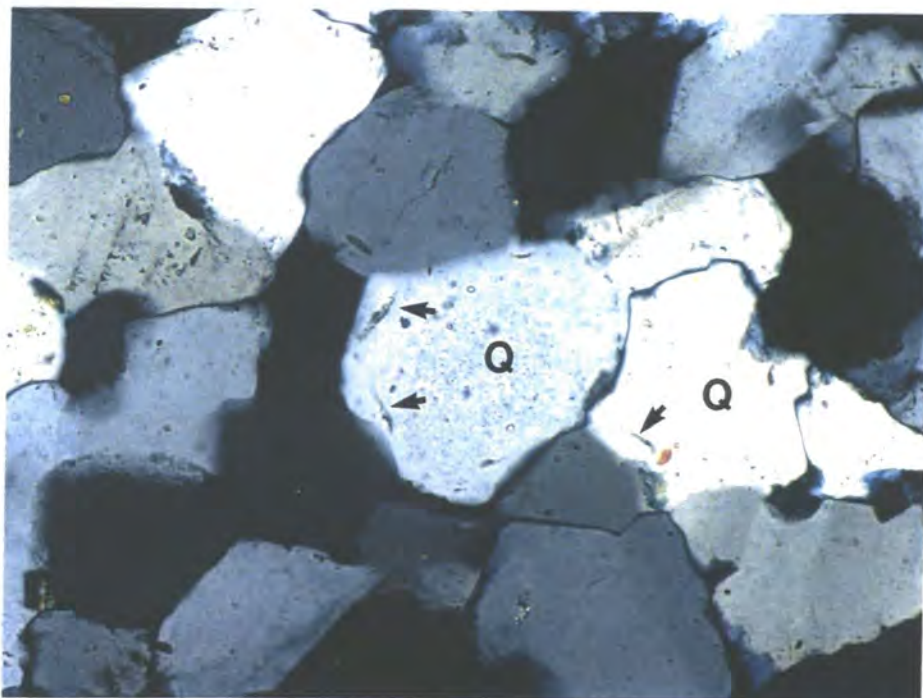


Fig. 5.3 Thin section of photomicrograph from the lower part of lower Tahara sandstone showing quartz overgrowth (Q), with well-developed crystal faces. Clay rims possibly present around detrital quartz grains (arrows). PPL (X20).

5.3.2-Carbonate cement

Carbonate cement is rare in the Tahara sandstones and it is primarily in the form of calcite. Calcite is a later precipitate, post-dating quartz overgrowths, which indicates the early timing of quartz diagenesis. Calcite occurs as randomly distributed pore-filling cement (Fig. 5.4), especially in the upper Tahara sandstone and the lower part of the lower Tahara sandstone but is less common in the upper part of the lower Tahara sandstone (Fig. 5.1; Tables 5.1 and 5.2). Calcite cement is present between quartz grains (<16.6%). The average grain size of calcite crystals exceeds 0.25 mm. The larger crystals (sparry calcite) of 1 cm or

more are present. Calcite crystals also occur as skeletal detritus in the upper Tahara sandstone. They occur as pore-filling cement between grains which form a poikilotopic texture. Carbonate cement probably drained from the pore water itself or from dissolution of carbonate skeletal grains in marine sandstone (Tucker 1991).

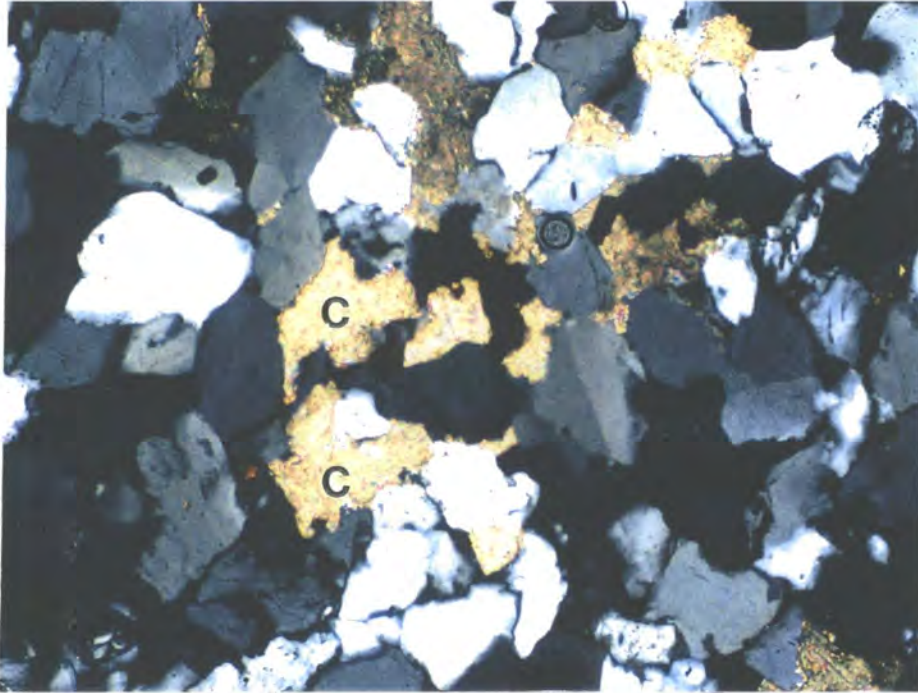


Fig. 5.4 Thin section of photomicrograph from the upper Tahara sandstone showing calcite cement (C). PPL (X10).

5.3.3-Feldspar dissolution

Dissolution of feldspars occurs in the lower sandstone, where they show evidence of partial and/or complete dissolution (see Fig. 5.12) and of secondary dissolution. Feldspars are more abundant in the upper part of lower Tahara sandstone.

5.3.4-Authigenic clay minerals

Kaolinite is the most common authigenic clay mineral developed within the Tahara sandstones. Kaolinite is a late stage authigenic mineral post-dating early quartz overgrowth. Kaolinite occurs as dispersed pore-filling cements between quartz grains or replacement of pre-existing detrital grains. It forms pore-occluding cement within the Tahara sandstones and where present contains microporosity (see Fig. 5.9). Kaolinite may precipitated from pore-fluid or alteration of detrital feldspars (Franks and Foster 1984) and by hydrothermal alteration or weathering (Selley 1976a). In the thin sections, kaolinite precipitation is partially controlled by the dissolution of feldspars, as evidenced by the presence of kaolinite within the dissolving feldspars (see Fig. 5.12). The origin and occurrence of clay minerals are poorly understood. However, kaolinite is the characteristic mineral of acid fresh water environments (Pettijohn 1957). Whereas Bjørlykke (1983) pointed out that fluvial sandstones and some shallow-marinesandstone may be flushed by meteoric water after deposition forming authigenic kaolinite.

5.4-Texture

Textural properties include shape, roundness, grain size and sorting. The grain size of clastic sediments is of considerable importance in that it may help to determine the depositional environment when combined with studies of sedimentary structures. The grain size of sediments also provides an indication of energy levels and physical processes operating at the depositional site. The detrital quartz grain size of the Tahara sandstones is generally fine to very fine-grained (mean size between 0.13 mm and 0.2 mm in diameter). The overall grain-size trends are slightly variable in both the upper and the lower sandstone (Fig. 5.1). However, the coarser grains (maximum mean grain size up to 0.2 mm in diameter) concentrate in the upper part of the lower sandstone. The quartz grains within the sandstone are rounded to subrounded and well sorted with a low sphericity.

The grain sizes in mm for all samples were plotted as cumulative frequency curves in order to calculate sorting (Figs 5.5-5.7). Cumulative frequency plots can be used to estimate percentages of suspension load, saltation load and traction load from samples (Visher 1969). Idealized cumulative frequency curves (Fig. 5.5) showing discrete segments may be equivalent to the traction load (coarse sand to granule), saltation load (coarse sand to fine sand) and suspension load (very fine sand to silt). This method can be used to assess the depositional environment together with other information, for example, sedimentary structures and facies sequences.

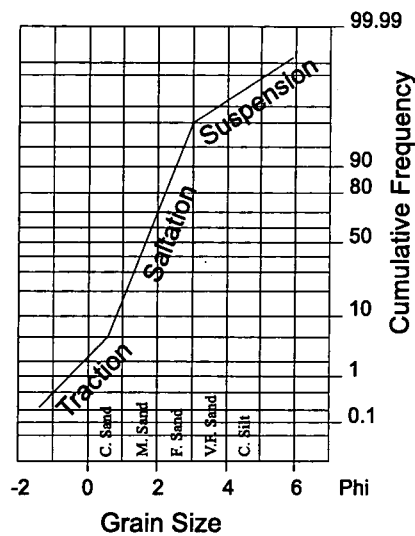


Fig. 5.5 Idealized cumulative frequency curve showing the three populations of suspension, saltation and traction (From Galloway 1976).

The cumulative frequency curve of both lower and upper Tahara sandstones (Figs 5.6 and 5.7) shows saltation population segment with no evidence of a traction segment when compared with the idealized curve of Visher (1969) (Fig. 5.5).

Figure 5.6 illustrates the grain-size distribution curves in 10 samples from the upper sandstone. These curves show prominent saltation population. The grain-size falls within the fine to very fine sand category (cf. Fig. 5.5). Characteristic of

these curves include: (i) very well sorted saltation population with a size range from approximately 1 to 3.5 phi; (ii) saltation population form high percentage (100%); and; (iii) two saltation population are present in some samples which are possibly related to swash and bachwash in shore zone.

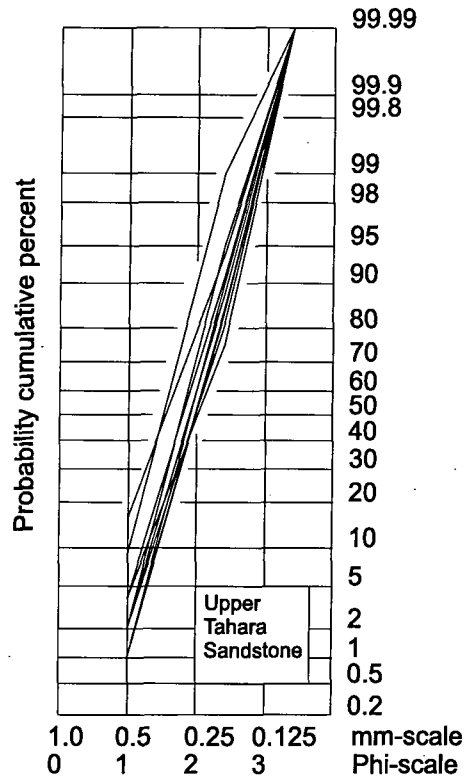


Fig. 5.6 Typical cummulative frequency grain size distribution curves for the upper sandstone of the Tahara Formation. All curves show similar shape and distribution of the grain sizes.

Figure 5.7 displays cumulative grain size frequency curves for 8 samples from the lower Tahara sandstone. The curves for the upper part of the lower sandstone show saltation population. The saltation load is well developed in this part of the sandstone occurred from 1 to 4.5 phi and absent of a traction load. However, possible the wave energy is not sufficient to remove the coarse-grained population and/or related to high load saltation material in transportation.

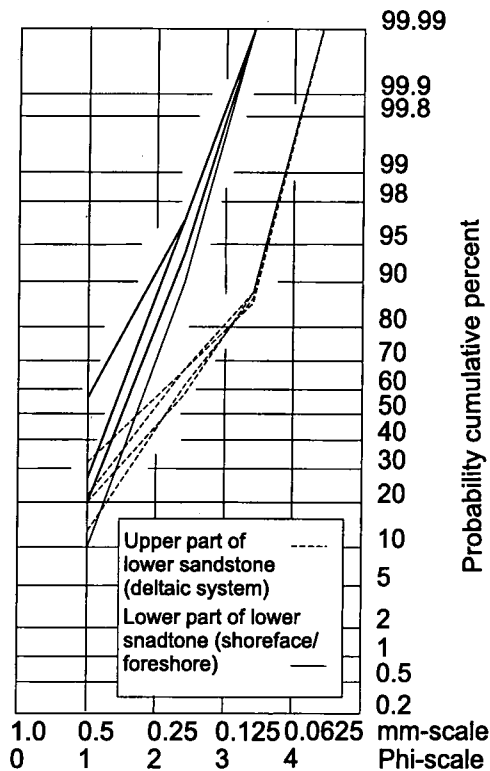


Fig. 5.7 Typical cumulative frequency grain size curves for the lower sandstone of the Tahara Formation.

Size distribution for upper part of lower Tahara sandstone show characteristics trends different from those in the upper sandstone and the lower part of the lower sandstone. The curves show a population with size range and sorting characteristic of saltation transported detritus and have dual saltation populations possible product of marine influences. Samples may contain a suspension population from 0 to less than 2 percentage. This may be a product currents winnowing out the suspension material or the proximity to source area.

It can be seen grain size distribution curves for the upper part of the lower sandstone show less degree of sorting falling within moderately well sorted category throughout the inter Tahara sandstones. Thus, coarser sands (maximum grain size in mm-scale in diameter) show less well sorted than finer sands in the Tahara sandstones. Samples from the lower part of the lower

sandstone (Fig. 5.7) show similar curves to the upper Tahara sandstone (Fig. 5.6).

5.5-Porosity

The study of porosity is important for reservoir rock assessment. Porosity in the Tahara sandstones mainly results from dissolution of the detrital material grains and authigenic phases. Porosity is the percentage of pore space to the total volume of the rock (Pettijohn 1957). Recognition of pore types in sandstone is also important in interpreting provenance. This study of the porosity of the Tahara sandstone may provide clues to reservoir conductivity and potential. During the mineralogical analysis of the upper and the lower Tahara sandstone a significant increase in the porosity of the lower sandstone was noted (Fig. 5.1), based on point counting 18 thin sections. Porosity values ranged from 0%-up to 27.6% no analysis of permeability of these samples has been attempted in this study and permeability data is not currently available. Three types of variable porosity can be recognized within the Tahara sandstone: primary, secondary and microporosity.

1-Primary intergranular pores. This is very rare and is only found as isolated pores.

2-Secondary porosity. This is the most common porosity, and results from the dissolution of unstable minerals. Dissolution porosity may originate by the removal of soluble detrital or authigenic grains during fluid movement. Well C1-49 has a predominance of secondary porosity, which is recognized in thin sections from the partial or complete dissolution of unstable minerals and corroded grains (Figs 5.1, 5.8 and 5.9).

In many sandstone reservoirs, secondary porosity is generated by the dissolution of early framework carbonate cements by solutions rich in carbonic acid released from the thermomaturation of source rocks (Fordham 1989). In the Tahara sandstone there is little development of early carbonate cements (Fig. 5.1). Thus

most of the secondary porosity developed in this sandstone is through the alteration of unstable detrital grains, particularly feldspars (Fig 5.6).

3-Microporosity occurs as pores within kaolinite clay minerals (fig. 5.9).

5.6-Classification

Tectonic setting of the provenance is the primary control on sandstone composition (Dickinson 1985). The sandstones of the Tahara Formation can be classified as quartz arenites and arkoses (Figs 5.10) in terms of their modal composition.

5.6.1-Quartz arenite

Quartz arenites are a common sedimentary rock in the geological record particularly in the Mesozoic and Palaeozoic. These are a common constituents of the Tahara sandstones, characterised by their high quartz contents of up to 95% (Table 5.1; Fig 5.11). They are dominated by monocrystalline quartz grains with polycrystalline quartz grains locally abundant. Quartz arenites are well cemented with quartz overgrowths, but calcite is also abundant. However, they have poor porosity. They show little or no feldspar grains and rock fragments.

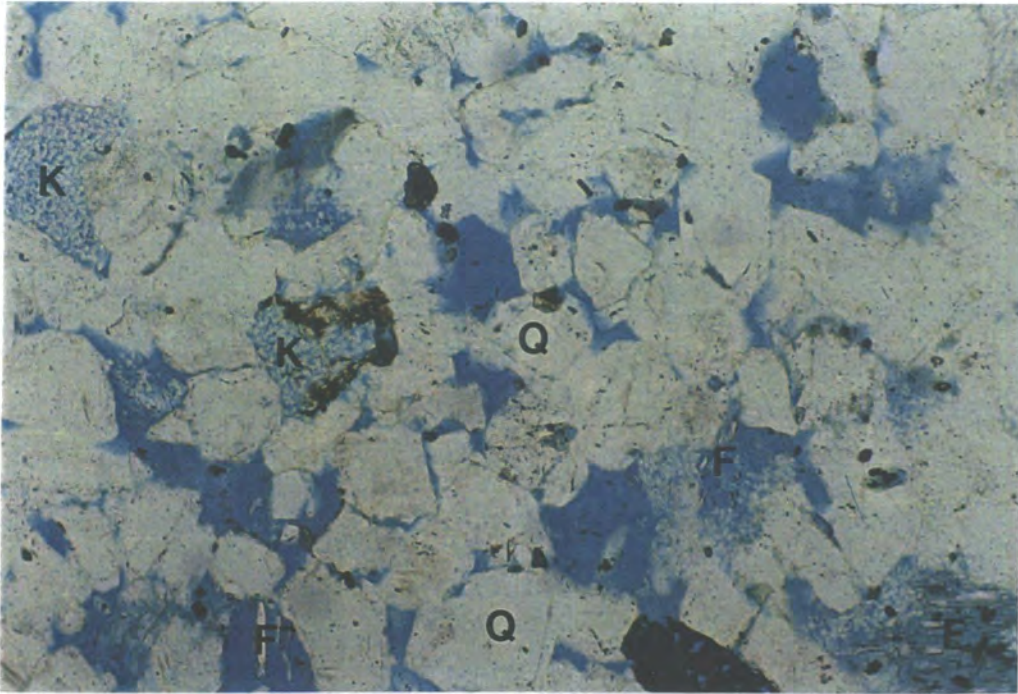


Fig. 5.8 Thin section of photomicrograph from the upper part of the lower Tahara sandstone showing quartz grains (Q) and dissolution of feldspars (F) resulting in secondary porosity (blue), and microporosity in kaolinite clay minerals (K). PPL (X10).

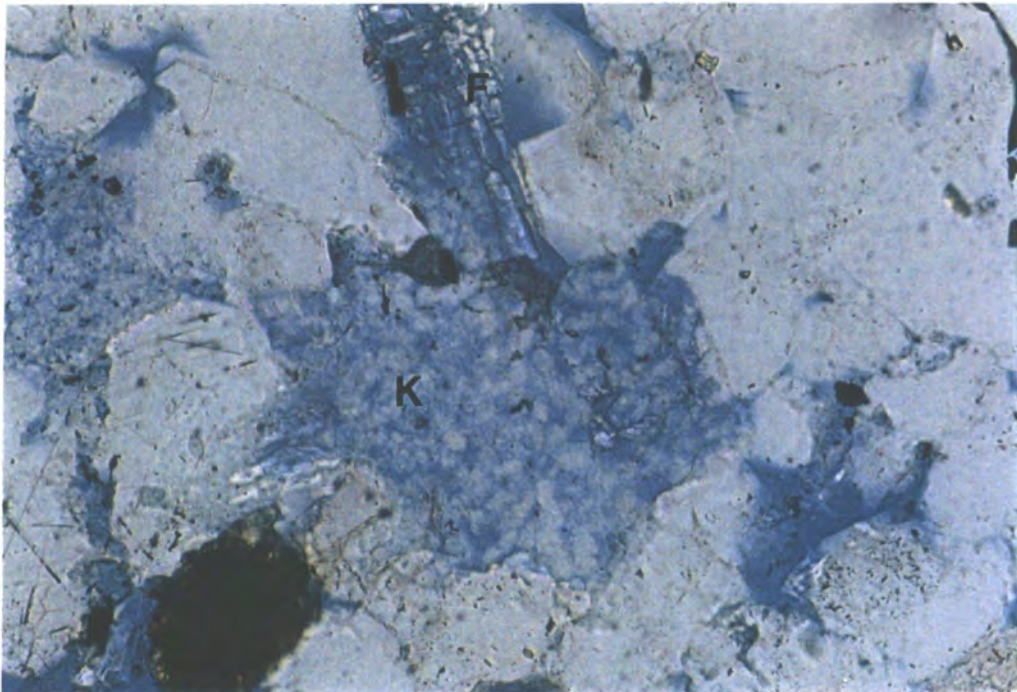


Fig. 5.9 Thin section of photomicrograph from the upper part of The lower Tahara sandstone showing secondary porosity (F) and microporosity (K). PPL (X20).

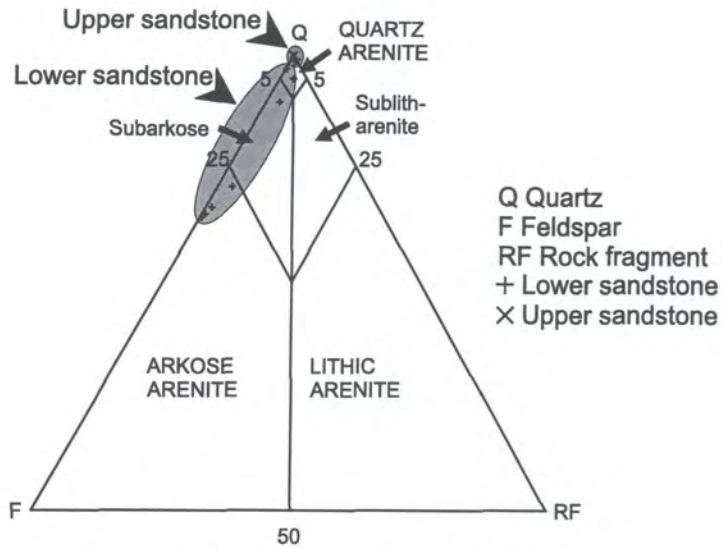


Fig.5.10 Ternary QFRF plot showing the composition of thin sections from well C1-49 (Classification modified from Pettijohn 1975). Note the lower part of the lower Tahara sandstone is concentrated in the quartz arenite area of the plot.

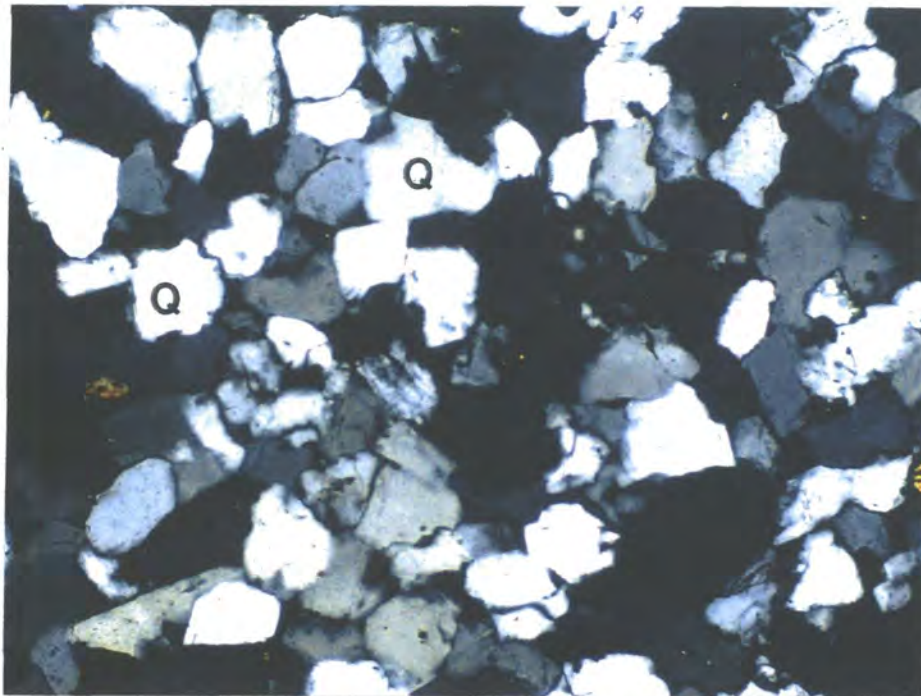


Fig. 5.11 Thin section of photomicrograph from the upper Tahara sandstone showing quartz arenite with high content of quartz grains (Q). PPL (X10).

5.6.2-Arkose

The composition of the lower Tahara sandstone can be divided into a lower part, which has similar characteristics to those of the upper Tahara sandstone, and an upper part which contains between 26% and 34% feldspar (Fig. 5.10).

These have a slightly coarser grain size than the quartz arenites (Figs 5.1 and 5.12) but with less quartz (65-71%). The grains are mainly subrounded and well sorted and mainly cemented by quartz, or rarely calcite. They contain a kaolinite clay matrix up to 8% and minor amounts of other minerals such as mica (<1%), heavy minerals (<7%) and opaque minerals including organic material (0.6-1.6%) (Table 5.2). Arkoses show higher porosity values within Tahara sandstones and have the best reservoir potential (Figs. 5.8 and 5.9).

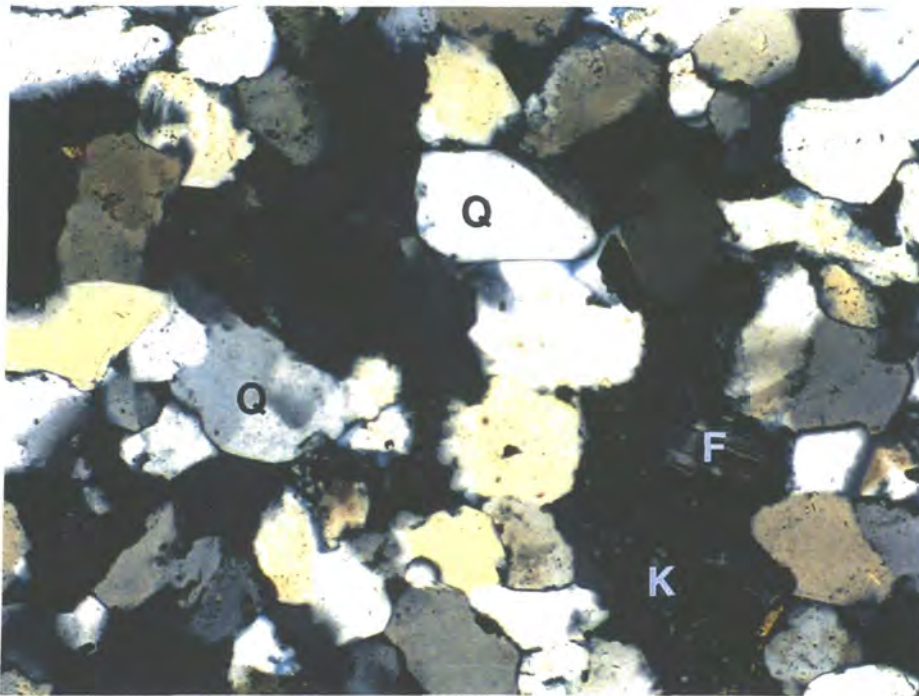


Fig. 5.12 Thin section of photomicrograph from the upper part of the lower Tahara sandstone showing arkosic composition with quartz grains (Q), feldspars (F) and kaolinite (K). PPL (X10).

5.7-Comparison Between Upper and Lower Tahara Sandstones

A petrographic study of the lower and upper sandstones of the Tahara Formation reveal variations in composition, texture and porosity. Although the differences are not great, they are significant in terms of their reservoir potential.

1-The first important difference is in the modal composition of the sandstones. The upper part of the lower Tahara sandstone differs significantly from the lower part of sandstone and the upper Tahara sandstone. It contains a much higher percentage of feldspars and is arkosic in composition, whereas the upper sandstone contains a very small amount of glauconite not observed in the upper part of the lower sandstone.

2-The upper part of the lower sandstone is significantly coarser grained than other sandstones within the Tahara Formation (maximum mean grain size up to 0.2 mm in diameter).

3-The upper part of the lower sandstone also has a much higher porosity (up to 27.6%) than that of the lower part of the lower sandstone and the upper sandstone. This higher porosity results from the secondary dissolution of feldspar and the development of secondary porosity and microporosity kaolinite clay minerals (Figs. 5.8 and 5.9). Porosity in the upper sandstone, for example is < 8.5% and it has poor reservoir potential.

5.8-Provenance

Sandstone composition can be a useful indicator of the composition, and tectonic setting of the source area (Swift *et al.*, 1991; Macdonald 1993). Quartz arenites may originate as first cycle deposits setting (Pettijohn *et al.*, 1978). They can also be a product of multiple recycling (Suttner *et al.*, 1981) of quartz grains from sedimentary source rocks or formed *in situ* through extensive chemical weathering. Quartz arenites are typically deposited in stable cratonic environments (Tucker 1991; Boggs 1995).

Arkoses of the upper part of the lower Tahara sandstone containing abundant microcline and orthoclase are originate from feldspar-rich rocks (granites or gneisses). They can also derive from a granitic source area or from *in situ* disintegration of these rocks, controlled by the rate of erosion and climatic setting (Pettijohn *et al.*, 1978; Tucker 1991). Arkoses can accumulate through tectonic uplift that bring granitic basement rocks up into the zone of erosion (Pettijohn *et al.*, 1978).

Ternary diagrams have been used to plot the sandstone composition data from both the upper and the lower Tahara sandstones (Figs 5.13 and 5.14). These indicate that they were derived from similar parent rocks (source rock) i.e., from the continental block provenance fields of Dickinson *et al.* (1983) as illustrated in Fig. 5.13. The upper sandstone and the lower part of the lower sandstone show a similar distribution pattern. They are quartz arenites with a sediment source within the cratonic source field (Dickinson *et al.*, 1983). The main sources of the craton-derived quartzose sands are low-relief granitic and gneissic exposures supplemented by recycling of associated sediments (Dickinson 1985). The arkoses of the upper part of the lower sandstone were derived from transitional continental-uplifted granitic basement blocks of high relief (Fig. 5.13). Both Tahara sandstones formed under humid climatic conditions from plutonic and metamorphic rocks (Fig. 5.14) (Suttner *et al.*, 1981).

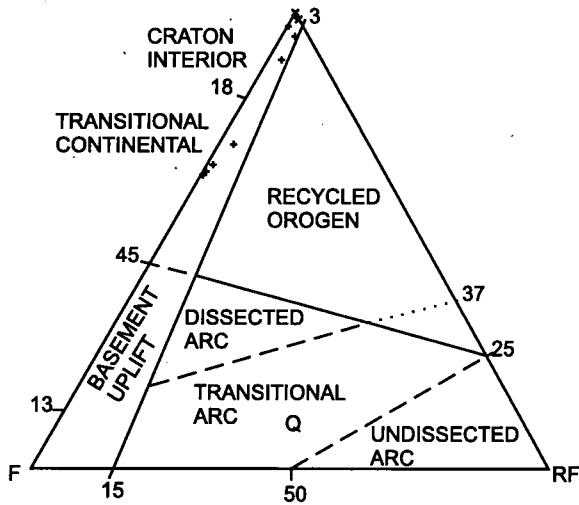


Fig. 5.13 Relation between framework composition of the lower and upper Tahara sandstones. The upper sand (quartz arenite) is derived from a cratonic area and the lower sand (arkose) derived from a transition-basement uplift (After Dickinson *et al.*, 1983). (See key in Fig. 5.10).

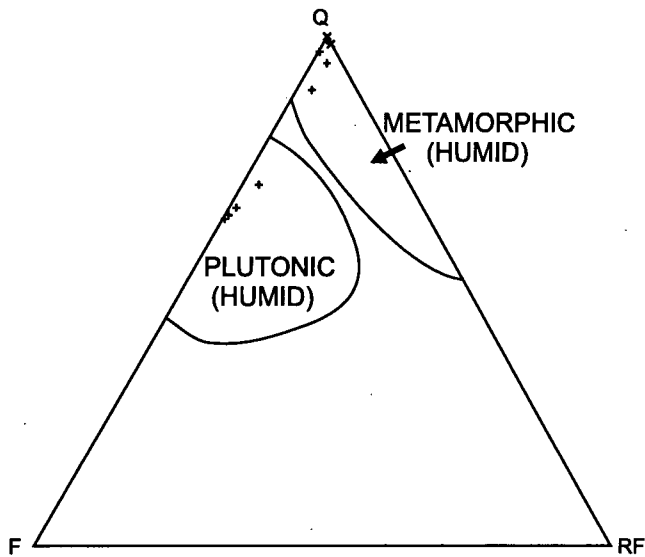


Fig. 5.14 Ternary QFRF plot showing the average composition of sandstone and source rock marked by humid climate (After Suttner *et al.*, 1981) (See key in Fig. 5.10).

Chapter 6

Conclusions

1-Regional Tectonic Setting and Palaeogeography of Libya in the Late Palaeozoic

In the Late Precambrian the cratons of Gondwana were welded together along extensive Gondwana mobile belts. Gondwana at this time was also surrounded along its southern and northern margins by peripheral subduction zones (Fig. 6.1) (de Wit *et al.*, 1992). Klitzsch (1981) points out that consolidation of North Africa (northern part of Gondwana) took place in Precambrian times, which was followed by periods of erosion. Passive margin conditions resulted along the southern and northern margin of Gondwana during Early Palaeozoic (Fig. 6.2) (de Wit *et al.*, 1992).

The Late Palaeozoic was a time of considerable tectonic activity. Throughout the Late Palaeozoic, Africa was part of a much larger continental domain which was probably not very different from Gondwana in the early Mesozoic (Shackleton 1981). During Palaeozoic to Early Mesozoic times Gondwana lithosphere was effected by distinct episodes of compression related to terrane accretion which occurred along the southern margin of Gondwana, whereas terrane extension and calving occurred along the northern margin of Gondwana (Fig. 6.3). The calving of terrane on the northern margin and large-scale break-up of Gondwana may be related to stresses transmitted across the Gondwana lithosphere during collision along the southern margin (Fig. 6.4). Tectonic disruption of the northern margin of Gondwana resulted in the formation of microplates which in turn were transferred across Tethys and accreted on to Eurasia (de Wit *et al.*, 1992).

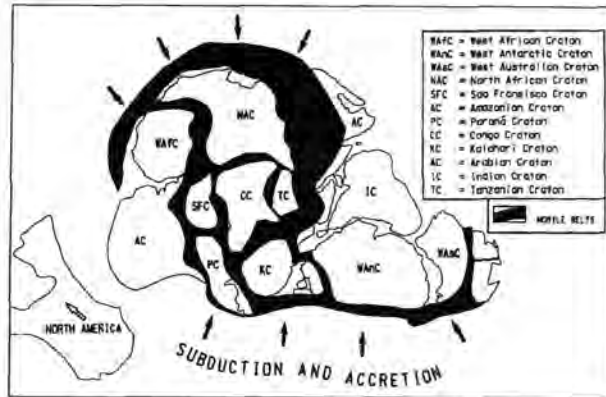


Fig. 6.1 Showing the cratons of Gondwana welded together along the Pan-Gondwana mobile belts in Late Precambrian (650+/-100 Ma) (de Wit et al., 1992).

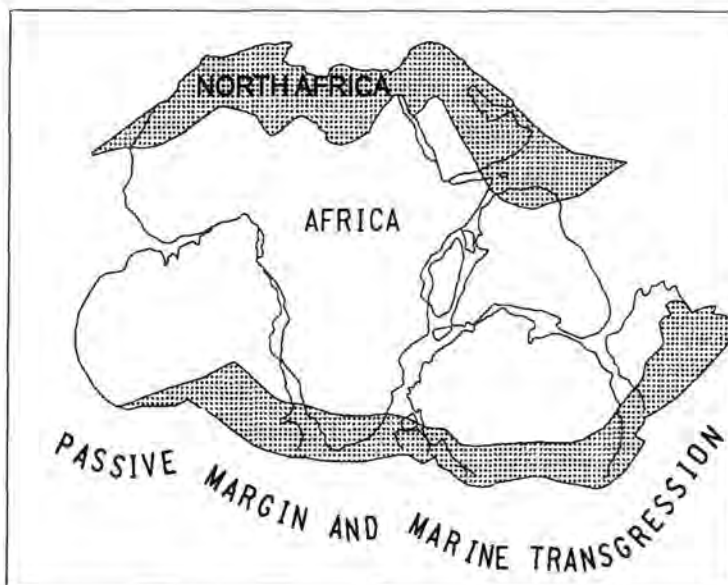


Fig. 6.2 Early Palaeozoic (500+/-100 Ma) palaeotectonic map showing southern and northern margins of Gondwana (de Wit et al., 1992).

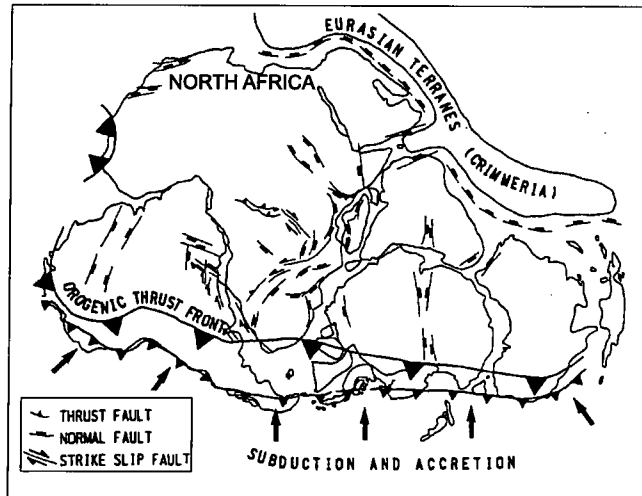


Fig. 6.3 Late Palaeozoic to Early Mesozoic (250 +/-50 Ma) palaeotectonic map showing tectonic regime along the southern margin of Gondwana (de Wit et al., 1992).

In Early Palaeozoic to Devonian times, North Africa was dominated by NW-SE striking structural axes forming uplifts and troughs oriented NW-SE. The strike axes of these structural elements was NNE-SSW in the southeastern part of North Africa and ENE-WSW to almost E-W in the northwestern part of North Africa (Klitzsch 1970). The northern margin of the African craton was transgressed from the west by marine incursions throughout the Palaeozoic period (Bellini and Massa 1980; Klitzsch 1981). This influenced the palaeogeographic evolution of the Palaeozoic basins of Libya. These marine transgressions from the west, in the Palaeozoic, were followed by Mesozoic and Tertiary transgressions from the north (present day Mediterranean Sea, Tethys seaway). The structural patterns of the Ghadames and Murzuq basins were formed in response to two distinct periods of tectonic movement (for more detail see chapter 1). These events were caused by Palaeozoic structural arches in southern Libya formed in response to the Caledonian orogeny (Fig. 1.3). However, the Gargaf uplift and/or Haruj uplift formed the structural and tectonic features that controlled the sedimentary fill of the Ghadames and Murzuq basins,

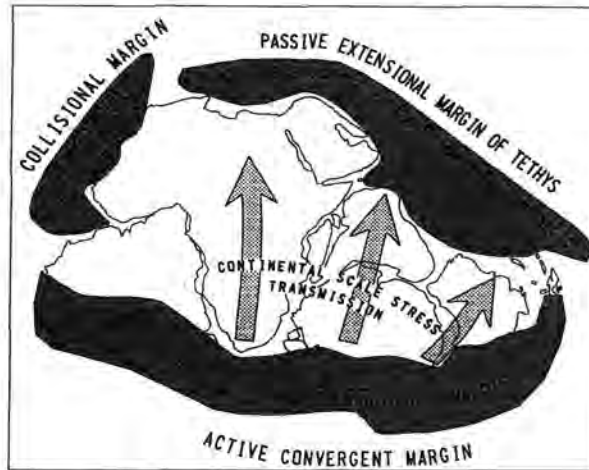


Fig. 6.4 Late Palaeozoic to Early Mesozoic (300+/-75 Ma) palaeotectonic map showing regional peripheral tectonic regimes of Gondwana. Stresses induced during terrane accretion along the southern margin of Gondwana were transmitted across the supercontinental lithosphere leading of disruption of its northern margin (de Wit *et al.*, 1992).

both of which contain evidence of uplift. For example, previous workers (Bellini and Massa 1980; Hammuda 1980) in the Ghadames basin show that the upper Palaeozoic sequence is thick in the centre and thins gradually towards the south of the basin away from the Gargaf arch suggesting that the Gargaf arch was a positive feature throughout the upper Palaeozoic.

A generalized palaeogeographic interpretation of the Tahara sandstones is shown below (Figs. 6. 5 and 6.6).

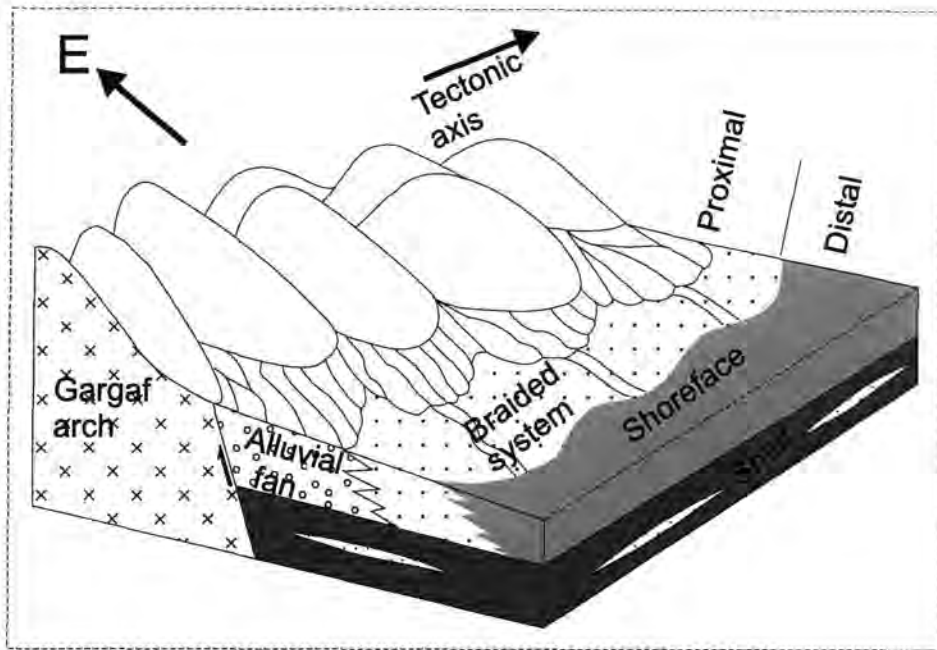


Fig. 6.5 Generalised model for the Tahara depositional system. The nature of the depositional system in the updip proximal area is inferred from evidence in the distal part of the depositional environment.

Sediments eroded from the rising mountain chain (e.g., Gargaf uplift) were deposited along the basin margin as alluvial fans, transverse to the tectonic axis (Fig. 6.5). Fans commonly develop at tectonically active margins (fault controlled scarps) in a variety of climatic settings. However, fans dominated by stream flow processes are typical of humid climates, whereas debris flows are more typical of arid climates, depending to some extent on bedrock geology in the source area (pers. communication, John McPherson, Mobil Oil Company, 1998). The presence of braided systems feeding the shoreline and the dominance of fines suggests that the climate was most probably humid. Alluvial fans, directly or indirectly related to fault lines, are the fills of basins flanking the uplifted source areas. Most modern fans extend not more than 5-20 km from mountain front into the adjacent lowland, and they are not normally more than three times the size of the drainage area feeding the fan (Bull 1972). The inferred fans adjacent to the Gargaf arch are of this order of magnitude. Work in Death Valley California also suggests that where the source area includes granitic rocks the slopes are

relatively low and the fans are dominated by stream flow processes. I infer a similar situation for the Gargaf arch alluvial fan systems which passed basinwards into braided rivers, as depicted in Fig. 6.5.

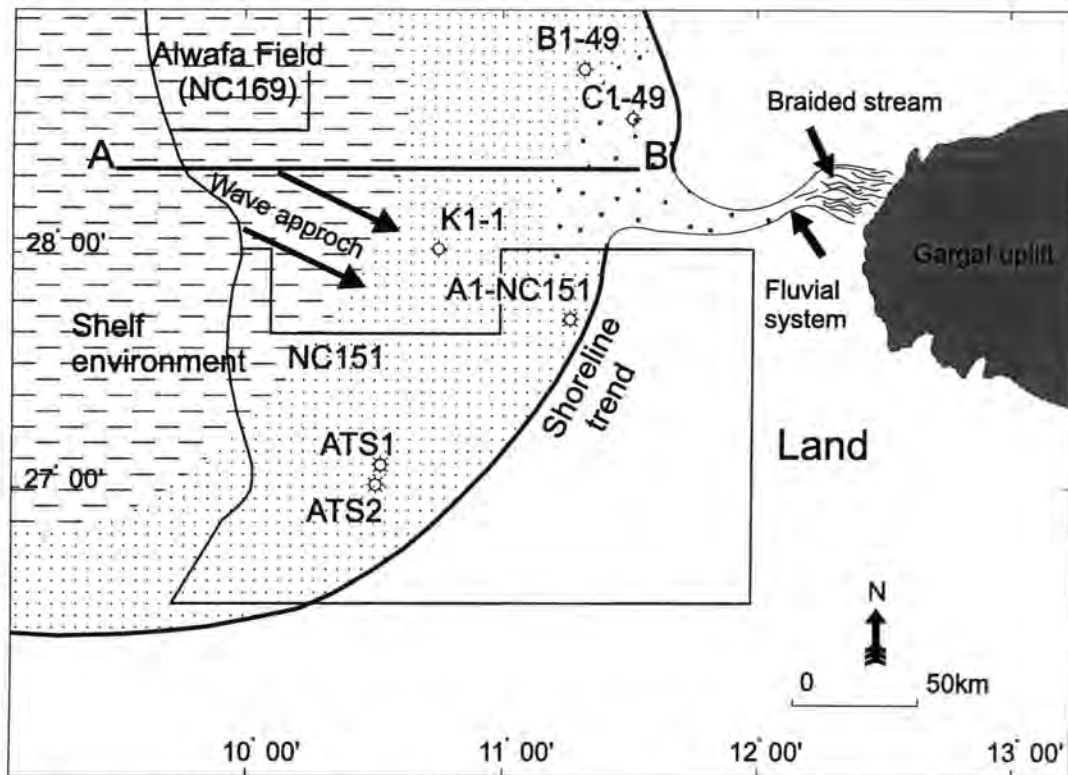





Fig. 6.6 Palaeogeographic interpretation of the Tahara Formation. Palaeoslope towards the west.

-  Delta sand (upper part of lower Tahara sandstone)
-  Shoreface sand (upper sandstone and lower part of lower Tahara sandstone)
-  Marine shale

2-Depositional Model

Palaeocurrent analysis is used to determine the flow direction of the currents responsible for sediment transport, and the local and regional palaeoslope. Unfortunately, detailed palaeocurrent data were not available for the study area. The only available palaeocurrent data are from a study of the transgressive sequences from Jabal Akakus and Jabal Tadrart (Silurian to Devonian) (Clark-

Lowes 1985; Clark-Lowes and Ward 1991), and the late Devonian in the Murzuq basin (Van Houten and Karasek 1981). Palaeocurrent data from Clark-Lowes (1985) for Jabal Akakus and Jabal Tadarat suggests that Palaeozoic structural arches in southern Libya (Gargaf arch and Tibisti/Haruj uplift) (Fig. 1.3) had no influence on palaeocurrent trends until the end of the early Devonian. Vos (1981 a) pointed out that the Gargaf arch was not a positive feature during the lower Palaeozoic. However, during the late Devonian tectonic uplift of these arches caused by the Palaeozoic Caledonian orogeny led to the deposition of fluvial-dominated and shallow-marine Devonian sediments. This indicates a change from continental to open-marine conditions as the influence of the uplifted structural arches waned through erosion/weathering. Palaeocurrent data obtained from previous studies shows that the palaeoslope was towards the west away from the Gargaf arch. However, the cross-section in Fig. 2.31 indicates that the Tahara sandstone comprises two thick sandstones separated by marine-shelf sediments. Each sandstone unit represents progradation of a marine shoreline over fine-grained marine-shelf deposits. The geometry of the sandstones and their sedimentary structures indicate that they were deposited mainly under high-energy conditions with the sandstones extending > 200 km to the west. Both Tahara sandstones are thickest in the northeast (well C1-49) and fine towards the southwest (well ATS2), where they pass into more shale-rich sandstone (e.g., well ATS1). This change, concomitant with the decrease in thickness of the sandstones, provides evidence of the palaeocurrent trend and their distal location relative to the source area. The relation between palaeocurrent patterns and depositional environments is illustrated in Fig. 6.7.

The differences in modal composition, texture and porosity of the two Tahara sandstones, especially the upper part of the lower sandstone is attributed to tectonic activity and uplift of the source area. These changes are reflected in changes in the coeval depositional environment and shoreline configuration, but there is no evidence to suggest a significant basinward shift at this time and the development of a lowstand sequence boundary below the upper part of the lower sandstone which was deposited as part of a more continuous depositional

process producing a gradual upward coarsening trend. This further implies that uplift may have been a gradual rather than an abrupt process dramatically affecting base level change.

The vertical stacking and repetition of similar facies patterns indicates a repetition of similar depositional processes. However, the succession was interrupted by episodic relative sea-level rises which produced repeated marine-shelf deposits. During tectonic activity the increased fluvial input, caused the depositional system to prograde seawards. This was followed by a gradual decrease in fluvial activity due to decreased tectonic activity and/or reduced source area relief through weathering and erosion. As a result marine transgression and a rise in relative sea-level occurred. The Tahara sandstones are mostly fine- to very fine-grained, well-sorted, mature sandstones. This suggests that: (1) the sands may have been reworked prior to deposition; (2) only fine grained sands were supplied by the source area; and (3) coarser sands were trapped in updip areas before arriving at the shoreline.

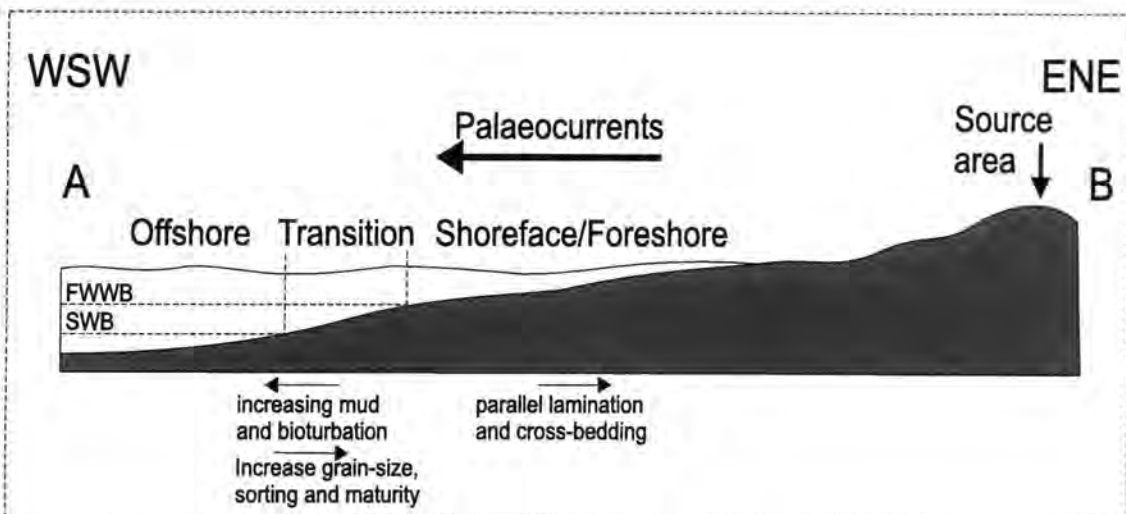


Fig. 6.7 Schematic cross-section along the line A-B in Fig. 6.6 showing facies, textures and sedimentary structures.

FWWB = Fair Weather Wave Base
 SWB = Storm Wave Base

Geological Evolution of the Tahara Formation

Simplified block diagrams illustrating the geological evolution of the Tahara Formation in the study area are shown in Fig. 6.8.

At stage one (Fig. 6.8a) sediment was deposited in a marine-shelf environment during periods of reduced detrital influx from the fluvial system with mud deposited mainly from suspension, intercalated with storm-dominated very fine sand and silt. The marine-shelf was subjected to sea-level rise, increase in water depth and accommodation space above the sequence boundary in the lower part of preserved sequence 2 (Fig. 3.4). These shelf suspension and coarser grained storm deposits are interpreted to form part of an early transgressive systems tract prior to deposition of the lower Tahara sandstone.

At stage two (Fig. 6.8b) source area uplift of the Gargaf arch and lowering of base level occurred, but because this was a gradual process it inhibited the development of a sequence boundary. This uplift influenced gradients and sediment supply as a fluvial system of possible braided character prograded basinward across the shoreline. This stage in the evolution of the depositional system is represented by the lower Tahara sandstone which consists of horizontally laminated and cross-bedded sandstone showing an overall slight coarsening-upward trend. It is interpreted as a shoreface deposit gradationally overlain by fluvio-deltaic influenced deposits as the depositional system gradually prograded basinwards across the shelf. The lower Tahara sandbody and underlying marine-shelf deposits, therefore, record shoreline progradation and increased fluvial sediment supply from a nearby uplifted source area to the east.

Stage three (Fig. 6.8c) represents a short-lived marine transgressive event which terminated lower Tahara sandstone progradation, as the depositional system temporarily retreated landwards. During transgression shales were deposited from suspension, under conditions of slow rates of deposition and increased accommodation space as relative sea-level rose, interrupted periodically by

storm deposition of horizontally laminated and cross-laminated sandstone. These sediments have characteristic features of marine-shelf environments.

Stage four (Fig. 6.8d) represents another phase of shoreline progradation during which the well sorted, fine to very fine-grained upper Tahara sandstone was deposited. This sandstone together with the underlying marine-shelf sediments shows a coarsening-upward trend consistent with shoreline progradation and the deposition of shelf to shoreface sediments. This records the final phase of shoreline progradation in this area and the development of another coarsening-upward package. It suggests that sediment may have been supplied to the shelf-shoreline system by a fluvio-deltaic system, although the location and influence of the source area is uncertain due to lack of data in the proximal areas. Progradation may be a response to variation in sediment supply (source) and/or shifts in sea-level. Intense winnowing and reworking (Coleman and Wright 1975) by marine processes led to the deposition of compositionally mature shoreface sandstone of the upper Tahara. These processes are attributed to diminished detrital influx allowing wave reworking of the sediments. Marine influences are also evidenced by the presence of vertical burrows and body fossils within the sandstone. They are indicative of a less active depositional system than deposition of the upper part of the lower Tahara sandstone, being overpowered by wave energy and shelf reworking processes. The shoreface-shelf environment was characterised by variable energy levels and intermittent deposition of higher and lower energy deposits.

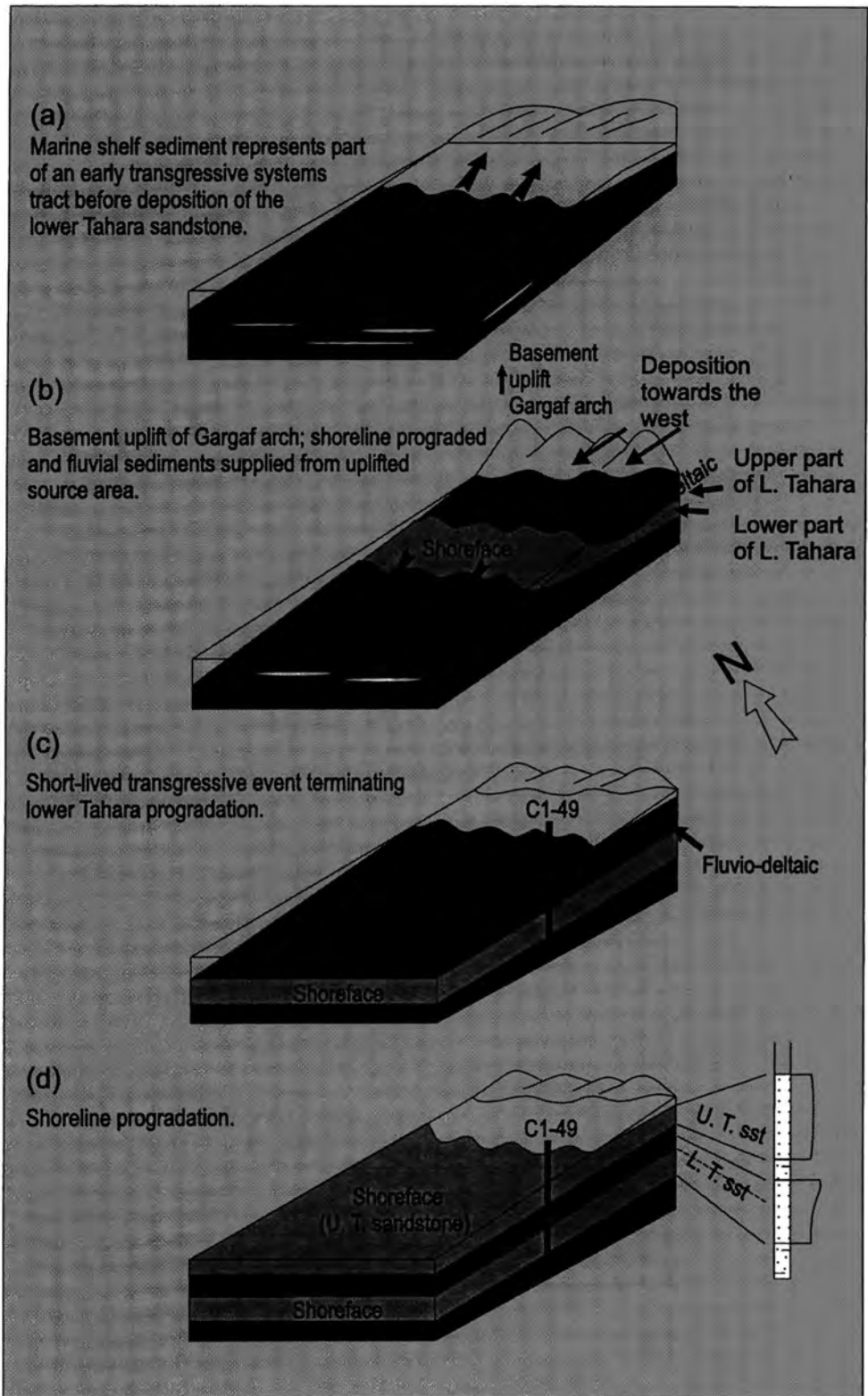


Fig. 6.8 Blocks diagram illustrating geological evolution of the Tahara Formation in the study area, during interpreted relative sea level changes. Not to scale.

3- Results of Study

Specific conclusions from this study of the Tahara sandstones are summarized below:

(a)-Sedimentological and textural analysis indicate that there are slight differences in the modal composition, texture and porosity between the lower and upper Tahara sandstones.

(b)-The sandstones are generally fine- to very fine, well-sorted and mature quartz arenites, except for the upper part of the lower sandstone which is coarser grained and arkosic.

(c)-Diagenetic cement is mainly in the form of quartz overgrowths, local calcite and clay matrix all of which have reduced the porosity, except in the coarser grained upper part of the lower Tahara sandstone.

(d)-The best porosity values are concentrated in the upper part of lower sandstone where values of up to 27.6% have been recorded, mostly in the form of secondary dissolution porosity and microporosity. The differences in mineral composition and porosity of the upper part of the lower sandstone are attributed to tectonism and uplift of an eroded source area to the east comprising a granitic and/or gneissic terrain. This is considered to have been the Gargaf arch. The upper part of the lower sandstone has been identified as a potential hydrocarbon reservoir and needs further investigation and modelling as described below to more fully assess its reservoir potential.

4-Recommendations

(a)-Sedimentological analysis of core from additional well(s) in order to supplement the results of this study. On the basis of this study it is recommended that additional wells should be drilled in updip proximal locations close to the Gargaf arch (Fig. 6.5) i.e., to the SE of C1-49 and ENE of ATS1/ATS2 (Fig. 6.9). This will provide additional details on the depositional environments and stratigraphic sequence of the Tahara Formation in more proximal locations where

similar and possibly better reservoir potential sand to that in C1-49 is likely to occur.

(b)-Determine the detailed permeability of the upper and the lower Tahara sandstones, especially the upper part of the lower Tahara sandstone in well C1-49.

(c)-Determine more precisely the palaeocurrent direction for the Tahara Formation, how this relates to earlier models, and how it fits the depositional models presented in this preliminary study.

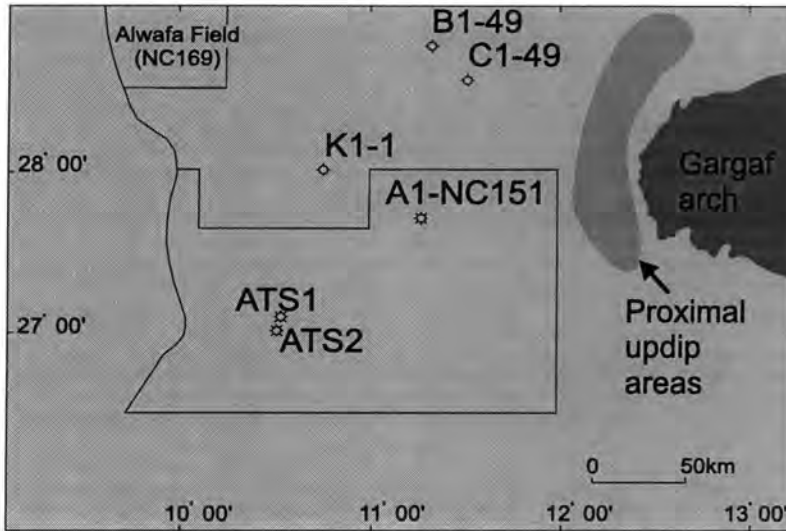


Fig. 6.9 Showing the proposed locations in possible updip areas proximal to the Gargaf arch, with reservoir potential in C1-49.

References

- Adams, A. E., MacKenzie, W. S. and Guilford, C. 1984.** Atlas of sedimentary rocks under the microscope. William Clowes (Beccles) Ltd. London. 104p.
- Adams, K., Glover, T., Fitches, B., Whittington, R. and Craig, J. 1997.** Controls on sequence development in lower Devonian sedimentary rocks of the intracratonic Murzuk basin, southwest Libya. BSRG, 36th annual meeting, University of Liverpool (20th-22nd Dec. 1997).
- Ahmadi, Z. M. 1997.** Sequence stratigraphy using wireline logs from the Upper Jurassic of England. DPhil. Thesis University of Durham, UK.
- Allen, J. R. L. 1960.** The Mam Tor sandstones: a "Turbidite " facies of the Namurian delta of Derbyshire, England. *Journal of Sedimentary Petrology*, 30, 193-208.
- Allen, J. R. L. 1963.** The classification of cross-stratified units with notes on their origin. *Sedimentology*, 2, 93-114.
- Allen, J. R. L. 1965.** Late Quaternary Niger delta, and adjacent areas: Sedimentary environments and lithofacies. *American Association of Petroleum Geologists Bulletin*, 49, 547-600.
- Allen, J. R. L. 1970.** Studies in fluvial sedimentation: a comparison of fining-upwards cyclothems, with special reference to coarse-member composition and interpretation. *Journal of Sedimentary Petrology*, 40, 298-323.
- Allen, A. P. and Allen, J. R. 1990.** Basin analysis. Blackwell Science, Oxford, 451p.
- Anderton, R. 1976.** Tidal-shelf sedimentation: an example from the Scottish Dalradian. *Sedimentology*, 23, 429-458.
- Armentrout, J. M., Malecel, S. J., Fearn, L. B., Shepard, C. E., Naylor, P. H., Miles, A. W., Desmarais, R. J. and Dunay, R. E. 1993.** Log-motif analysis of Paleogene depositional systems tracts, Central and Northern North Sea: defined by sequence stratigraphic analysis. *In: Parker J. R (ed) Petroleum geology of*

northwest Europe: proceedings of the 4th conference. Geological Society of London, 45-57.

Basu, A., Young, S. W., Suttner, L. J., James, W. C. and Mack, G. H. 1975. Re-evaluation of the use of undulatory extinction and polycrystallinity in detrital quartz for provenance interpretation. *Journal of Sedimentary Petrology*, 45, 873-882.

Basu, A. 1976. Petrology of Holocene fluvial sand derived from plutonic source rocks: implications to paleoclimatic interpretation. *Journal of Sedimentary Petrology*, 46, 694-709.

Baum, G. R. and Vail, P. R. 1988. Sequence stratigraphic concepts applied to Paleogene outcrops, Gulf and Atlantic Basins. *In: Wilgus C. K., Hastings B. S., Kendall C. G. St C., Posamentier H. W., Ross C. A. and Van Wagoner J. C (eds) Sea-Level Changes-An integrated approach.* Society of Economic Paleontologists and Mineralogists Special Publication, 42, 309-327.

Beaumont, E. A. 1984. Retrogradational shelf sedimentation: lower Cretaceous Viking formation, central Alberta. *In: Tillman R. W. and Siemers C. T (eds) Siliciclastic shelf sediments.* Society of Economic Paleontologists and Mineralogists Special Publication, 34, 163-177.

Bellini, E. and Massa, D. 1980. A stratigraphic contribution to the Palaeozoic of southern basins of Libya. *In: Salem M. J. and Busrewil M. T (eds) The Geology of Libya.* Academic press, London, I, 3-56.

Berg, R. R. 1975. Depositional environment of upper Cretaceous Sussex sandstone, House Creek Field, Wyoming. *American Association of Petroleum Geologists Bulletin*, 59, 2099-2110.

Bhattacharyya, D. P. 1989. Concentrated and lean ooids: examples from the Nubian formation at Aswan, Egypt, and significance of the oolite types in ironstone genesis. *In: Young T. p. and Tylor W. E. G (eds) Phanerozoic Ironstones.* Geological Society Special Publication, 46, 93-103.

Bhattacharyya, D. P. and Kakimoto, P. K. 1982. Origin of ferriferous ooids: An SEM study of ironstone ooids and bauxite pisoids. *Journal of Sedimentary Petrology*, 52, 849-857.

- Bhattacharya, J. P. 1993.** The expression and interpretation of marine flooding surfaces and erosional surfaces in core; examples from the upper Cretaceous Dunvegan Formation, Alberta foreland basin, Canada. *In: Posamentier H. W., Summerhayes C. P., Haq B. U. and Allen G. P (eds) Sequence stratigraphy and facies associations. International Association of Sedimentologists, 18, 125-160.*
- Blatt, H. H. 1979.** Diagenetic processes in sandstones. *In: Scholle P. A. and Schluger P. R (eds) Aspects of diagenesis. Society of Economic Paleontologists and Mineralogists Special Publication, 26, 141-157.*
- Blatt, H. H. 1982.** Sedimentary Petrology. W. H. Freeman and Company, San Francisco, 564p.
- Boggs, S Jr. 1995.** Principles of sedimentology and stratigraphy. 2nd edition, Prantice-Hall, Upper Sander River, New Jersey, 774p.
- Bosence, D. W. J. 1973.** Facies relationships in a tidally influenced environment: A study from the Eocene of the London Basin. *Geologie en Mijnbouw, 52 (2), 63-67.*
- Bourgeois, J. 1980.** A transgressive shelf sequence exhibiting hummocky stratification: The Cape Sebastian sandstone. (Upper Cretaceous), southwestern Oregon. *Journal of Sedimentary Petrology, 50, 681-702.*
- Boyd, R., Suter, J. and Penland, S. 1989.** Relation of sequence stratigraphy to modern sedimentary environments. *Geology, 17, 926-929.*
- Bjørlykke, K. 1983.** Diagenetic reactions in sandstones. *In: Parker A. and Sellwood B. W (eds) Sediment diagenesis. Publication Company, Dordrecht, Holland, 169-213.*
- Bracaccia, V., Carcano, C. and Drera, K. 1991.** Sedimentology of the Silurian-Devonian series in the southeastern part of the Ghadames basin. *In: Salem M. J. and Belaid M. N (eds) The Geology of Libya. Academic press, London, V, 1727-1744.*
- Brenchley, J. P., Newall, G. and Stanistreet, G. I. 1979.** A storm surge origin for sandstone beds in an epicontinental platform sequence, Ordovician, Norway. *Sedimentary Geology, 22, 185-217.*

- Brown, L. F. and Fisher, W. L. 1977.** Seismic-stratigraphic interpretation of depositional systems: examples from Brazil rift and pull-apart basins. *In: Payton C (ed) Seismic stratigraphy-applications to hydrocarbon exploration. American Association of Petroleum Geologists Memoir, 26, 213-248.*
- Bull, W. B. 1972.** Recognition of alluvial fan deposits in the stratigraphic record. *In: Rigby J. K. and Hamblin W. K (eds) Recognition of ancient sedimentary environments. Society of Economic Paleontologists and Mineralogists Special Publication, 16, 63-83.*
- Burollet, P. F. 1960.** Lexique stratigraphique international, 4, Libye, Congrès Geologique International Commission de Stratigraphie, Recherche, Scientifique, Paris, 62p.
- Campbell, C. V. 1971.** Depositional model-upper Cretaceous Gallup beach shoreline, Ship Rock area, northwestern New Mexico. *Journal of Sedimentary Petrology, 41, 395-409.*
- Cant, D. J. 1983.** Spirit River Formation-A stratigraphic-diagenetic Gas Trap in the deep basin of the Alberta. *American Association of Petroleum Geologists Bulletin, 67, 577-587.*
- Cant, D. J. 1984a.** Development of the shoreline-shelf sand bodies in a Cretaceous epeiric sea deposit. *Journal of Sedimentary Petrology, 45, 541-556.*
- Cant, D. J. 1984b.** Subsurface facies analysis. *In: Walker R. G (ed) Facies models. Geological Association of Canada, 297-310.*
- Castro, J. C. Dell Favera, J. C. and EL-Jadi, M. 1991.** Tempestite facies, Murzuq basin, Great Socialist People's Libya Arab Jamahiriya: Their recognition and stratigraphic implications. *In: Salem M. J. and Belaid M. N (eds) The Geology of Libya. Academic press, London, V, 1757-1765.*
- Cheng, K. Ly. 1982.** Sedimentology of nearshore marine bar sequences from a Palaeozoic depositional regressive shoreline deposit of the central coast of Ghana, West Africa. *Journal of Sedimentary Petrology, 52, 199-208.*
- Clark-Lowes, D. D. 1985.** Aspects of Palaeozoic cratonic sedimentation in southwest Libya and Saudi Arabia. Ph.D. Thesis University of London, UK.

Clark-Lowes, D. D. and Ward, J. 1991. Palaeoenvironment evidence from the Palaeozoic "Nubian Sandstone" of the Sahara. *In: Salem M. J., Sbeta A. M. and Bakbak M. R (eds) The Geology of Libya. Academic press, London, VI, 2099-2153.*

Clifton, H. E., Hunter, R. E. and Phillips, R. L. 1971. Depositional structures and processes in the non-barred high-energy nearshore. *Journal of Sedimentary Petrology, 41, 651-670.*

Clifton, H. E. 1969. Beach lamination-nature and origin. *Marine Geology, 7, 553-559.*

Clifton, H. E. 1982. Estuarine deposits. *In: Scholle P. A. and Spearing D (eds) Sandstone depositional environments. American Association of Petroleum Geologists Memoir, 31, 179-189.*

Coleman, J. M. and Gagliano, S. M. 1965. Sedimentary structures: Mississippi river deltaic plain. *In: Middleton G. V (ed) Primary sedimentary structures and their hydrodynamic interpretation. Society of Economic Paleontologists and Mineralogists Special Publication, 12, 133-148.*

Coleman, J. M. and Wright, L. D. 1975. Modern river deltas: variability of processes and sand bodies. *In: Broussard M. L (ed) Deltas, models for exploration. Houston Geological Socitey, Houston, 99-150.*

Coleman, J. M. 1976. Deltas: processes of deposition and models for exploration. Continuing Education Publication Company, USA, 102p.

Coleman, J. M. and Prior, D. B. 1982. Deltaic Environments of Deposition. *In: Scholle P. A. and Spearing D (eds) Sandstone depositional environments. American Association of Petroleum Geologists Memoir, 31, 139-178.*

Collinson, J. D. 1986. Alluvial sediments. *In: Sedimentary environments and facies (ed. Reading H. G), Blackwell Scientific Publications, 2nd edition, 20-62.*

Collinson, J. D. and Thompson, D. B. 1989. Sedimentary structures. Academic division of Unwin Hyman Ltd, 2nd edition, 207p.

Conant, L. C. and Goudarzi, G. H. 1967. Stratigraphic and tectonic framework of Libya. *American Association of Petroluem Geologists Bulletin, 51, 719-730.*

Cotter, E. 1975. Deltaic deposits in the upper Cretaceous Ferron sandstone, Utah. *In: Broussard M. L (ed) Deltas: models for exploration.* Houston Geological Society, Houston, 471-484.

Dalrymple, R. W. 1992. Tidal depositional systems. *In: Walker R. G. and James N. P (eds) Facies models.* Geological Association of Canada, 195-218.

Davis, H. R., Byers, C. W. and Pratt, L. M. 1989. Depositional mechanisms and organic matter in Mowry shale (Cretaceous), Wyoming. *American Association of Petroleum Geologists Bulletin*, 73, 1103-1116.

Davies, S. J. and Elliott, T. 1996. Spectral gamma-ray characterisation of high resolution sequence stratigraphy: examples from Upper Carboniferous fluvio-deltaic systems, County Clare, Ireland. *In: Howell J. A. and Aitken J. F (eds) High Resolution Sequence Stratigraphy: innovations and applications.* Geological Society Special Publication, 104, 25-35.

De Raaf, J. F. M., Reading, H. G. and Walker, R. G. 1965. Cyclic sedimentation in the lower Westphalian of north Devon, England. *Sedimentology*, 4, 1-52.

De Raaf, J. F. M., Boersma, J. R. and Van Gelder, A. 1977. Wave-generated structures and sequences from a shallow-marine succession, lower Carboniferous, County Cork, Ireland. *Sedimentology*, 24, 451-483.

De Wit, M. J. and Ransome I. G. D. 1992. Regional inversion tectonics along the southern margin of Gondwana. *In: De Wit M. J. and Ransome I. G. D (eds) Inversion tectonics of the Cap Fold Belt, Karoo and Cretaceous Basins of Southern Africa.* Balkema, Rotterdam, 15-26.

Dickinson, W. R., Beard, L. S., Brakenridge, G. R., Erjavec, J. L., Ferguson, R. C., Inman, K. F., Knep, R. A., Lindberg, F. A. and Ryberg, P. T. 1983. Provenance of North American Phanerozoic sandstone in relation to tectonic setting. *Geological Society of American Bulletin*, 94, 222-235.

Dickinson, W. R. 1985. Interpreting provenance relations from detrital modes of sandstone. *In: Zuffa G. G (ed) Provenance of Arenites.* NATO ASI Series C: Mathematical and Physical Sciences, 184, 333-362.

Donaldson, A. C., Martin, R. H. and Kanies, W. H. 1970. Holocene Guadeloupe delta of Texas gulf coast. *In: Morgan J. P (ed) Deltaic sedimentation modern and*

ancient. Society of Economic Paleontologists and Mineralogists Special Publication, 15, 107-137.

Dott, R. H. and Bourgeois, J. 1982. Hummocky stratification: significance of its variable bedding sequences *Geological Society of American Bulletin*, 93, 663-680.

Driese, S. G., Fischer, M. W., Easthouse, K. A., Marks, G. T., Gogola, A. R. and Schoner, A. E. 1991. Model for genesis of shoreface and sandstone shelf sequences, south Appalachians: palaeoenvironmental reconstruction of an Early Silurian shelf system. *In: Swift D. J. P., Oertel G. F., Tillman R. W. and Thorne J. A (eds) Shelf sand and sandstone bodies. International Association of Sedimentologists Special Publication, 14, 309-338.*

Duke, W. L. 1985. Hummocky cross-stratification, tropical hurricanes, and intense winter storms. *Sedimentology*, 32, 167-194.

Duke, W. L., Fawcett, P. J. and Brusse, W. C. 1991. Prograding shoreline deposits in the lower Medina Group, Ontario and New York: storm-and tide-influenced sedimentation in a shallow epicontinental sea, and the origin of enigmatic shore-normal channels encapsulated by open shallow-marine deposits. *In: Swift D. J. P., Oertel G. F., Tillman R. W. and Thorne J. A (eds) Shelf sand and sandstone bodies. International Association of Sedimentologists Special Publication, 14, 339-375.*

Duval, B. C. C. and Vail, P. 1992. Types and hierarchy of stratigraphic cycles. Abstract for conference on sequence stratigraphy of European Basin. CNRS-IFP, Dijon, France (18-20th May 1992), 44-45.

Ekdalee, A. A., Bromley, R. G. and Pemberton, S. G. 1984. Ichnology trace fossils in sedimentology and stratigraphy. Society of Economic Paleontologists and Mineralogists Short Course, 15, 317p.

Elliott, T. 1974. Interdistributary bay sequences and their genesis. *Sedimentology*, 21, 611-622.

Elliott, T. 1983. Facies, sequences and sand-bodies of the principal clastic depositional environments. *In: Parker A. and Sellwood B. W (eds) Sediment diagenesis. Publication Company, Dordrecht, Holland, 1-56.*

Elliott, T. 1986 a. Deltas *In: Reading H. G (ed) Sedimentary environments and facies.* Blackwell Scientific Publications, 2nd edition, 113-154.

Elliott, T. 1986 b. Siliciclastic shorelines *In: Reading H. G (ed) Sedimentary environments and facies.* Blackwell Scientific Publications, 2nd edition, 155-188.

Emery, D. and Myer, K. J. 1996. Sequence stratigraphy. Blackwell Science, Oxford, 297p.

Ethridge, F. G. 1977. Petrology, transport, and environment in isochronous upper Devonian sandstone and siltstone units, New York. *Journal of Sedimentary Petrology*, 47, 53-65.

Fail, T. R., 1973. Tectonic development of the Triassic Newark-Gettysburg Basin in Pennsylvanian. *Geological Society of America Bulletin*, 84, 725- 740.

Figueiredo, A. G., Sanders, J. E. and Swift, D. J. P. 1982. Storm-graded layers on inner continental shelves: examples from southern Brazil and the Atlantic coast of the central United States. *Sedimentary Geology*, 31, 171-190.

Fischer, A. G. 1961. Stratigraphic record of transgressing sea in light of sedimentation on Atlantic Coast of New Jersey. *American Association of Petroleum Geologists Bulletin*, 45, 1656-1666.

Fordham, C. E. 1989. The influence of sedimentary structures and facies on the fluid flow (permeability) in the Fell sandstone, Northumberland. MPhil. Thesis University of Newcastle, UK.

Franks, P. C. 1980. Models of marine transgression-Example from Lower Cretaceous fluvial and paralic deposits, north-central Kansas. *Geology*, 8, 56-61.

Franks, S. G. and Foster, R. W. 1984. Relationships among secondary porosity, pore-fluid chemistry and carbon dioxide, Texas Gulf Coast. *In: Mc Donald D. A. and Surdam R. G (eds) Clastic diagenesis.* *American Association of Petroleum Geologists Memoir*, 37, 63-79.

Frey, R. W. 1975. The study of trace fossils. A synthesis of principles, problems and procedures in ichnology. Springer-Verlag New York, 562p.

- Frey, R. W. and Pemberton, S. G. 1984.** Trace fossil facies models. *In: Walker R. G (ed) Facies models. Geoscience Canada, Reprint series, 1, 189-209.*
- Fruit, D. J. and Elmore, R. D. 1988.** Tidal and storm-dominated sand ridges on a muddy shelf: Cottage Grove sandstone (Upper Pennsylvanian), northeastern Oklahoma. *American Association of Petroleum Geologists Bulletin, 10, 1200-1211.*
- Galloway, W. E. 1976.** Sediments and stratigraphic framework of the Copper River Fan-Delta, Alaska. *American Association of Petroleum Geologists Bulletin, 46, 726-737.*
- Galloway, W. E. 1979.** Diagenetic control of reservoir quality in Arc-Derived Sandstone: Implications for petroleum exploration. *In: Scholle P. A. and Schluger P. R (eds) Aspects of diagenesis. Society of Economic Paleontologists and Mineralogists Special Publication, 26, 251-262.*
- Galloway, W. E. 1986.** Reservoir facies architecture of microtidal barrier system. *American Association of Petroleum Geologists Bulletin, 70, 787-808.*
- Galloway, W. E. 1989.** Genetic stratigraphic sequences in basin analysis I: Architecture and genesis of flooding-surface bounded depositional units. *American Association of Petroleum Geologists Memoir, 73, 125-142.*
- Galloway, W. E. and Hobday, D. K. 1983.** Terrigenous clastic depositional systems. Springer-Verlag, New York. 423p.
- Gautier, D. L. 1982.** Siderite concretions: indicators of early diagenesis in the Cammon Shale (Cretaceous). *Journal of Sedimentary Petrology, 52, 859-871.*
- Goudarzi, G. H. 1980.** Structure-Libya. *In: Salem M. J. and Busrewil M. T (eds) The Geology of Libya. Academic press, London, Ill, 879-892.*
- Greensmith, J. T., Hatch, F. H. and Rastall, R. H. 1971.** Petrology of the sedimentary rocks. Thomas Murby and Co. Revised 5th edition, 502 p.
- Greenwood, B. and Sherman, D. J. 1986.** Hummocky cross-stratification in the surf zone: flow parameters and bedding genesis. *Sedimentology, 33, 33-45.*

Hadley, D. F. and Elliott, T. 1993. The sequence-stratigraphic significance of erosive-based shoreface sequences in the Cretaceous Mesaverde Group of northwestern Colorado. *In: Posamentier H. W., Summerhayes C. P., Haq B. U. and Allen G. P (eds) Sequence stratigraphy and facies associations. International Association of Sedimentologists, 18, 521-535.*

Hallam, A. and Bradshaw, M. J. 1979. Bituminous shales and oolitic ironstones as indicators of transgressions and regressions. *Journal of the Geological Society of London, 136, 157-164.*

Hallam, A. 1988. A reevaluation of Jurassic eustasy in the light of new data and the revised Exxon curve. Society of Economic Paleontologists and Mineralogists Special Publication, 42, 261-273.

Hamblin, A. P. and Walker R. G. 1979. Storm-dominated shallow-marine deposits: the Fernie-Kootenay (Jurassic) transition, southern Rocky Mountains. *Canadian Journal of Earth Sciences, 16, 1673-1690.*

Hammuda, O. S. 1980. Geological factors controlling fluid and anomalous freshwater occurrences in the Tadrart sandstone, Al Hamadah al Hamra area, Ghadames basin. *In: Salem M. J. and Busrewil M. T (eds) The Geology of Libya. Academic press, London, II, 501-507.*

Haq, B. U., Hardenbol, J. and Vail, P. R. 1987. Chronology of fluctuating sea-levels since the Triassic. *Science, 235, 1156-1166.*

Haq, B. U. 1991. Sequence stratigraphy, sea-level change, and significance for the deep sea. *In: Macdonald D. I. M (ed) Sedimentation, Tectonics and Eustasy sea-level changes at active margins. International Association of Sedimentologists, 12, 3-39.*

Harms, J. C., South J. B. and Walker, R. G. 1975. Depositional environments as interpreted from primary sedimentary structures and stratification sequences. Society of Economic Paleontologists and Mineralogists, Tulsa, Oklahoma, Short Course 2, 161p

Hayes, J. R. 1962. Quartz and feldspar content in south Platte, Platte, and Missouri River Sands. *Journal of Sedimentary Petrology, 32, 793-800.*

- Hayes, M. O 1975.** Morphology of sand accumulation in estuaries: an introduction to the symposium. *In: Cronin L. E (ed) Estuarine research. Geology and engineering, Academic Press, New York, 2, 3-22.*
- Hayes, M. O. and Kana, T. W. 1976.** Terrigenous clastic depositional environments some modern examples. *American Association of Petroleum Geologists*, technical report no. 11-CRD, 185p.
- Hein, F. J., Robb, G. A., Wolberg, A. C. and Longstaffe, F. J. 1991.** Facies descriptions and associations in ancient reworked (? transgressive) shelf sandstones: Cambrian and Cretaceous examples. *Sedimentology*, 38, 405-431.
- Ho, C. and Coleman, J. M. 1969.** Consolidation and cementation of recent sediments in the Atchafalaya basin. *Geological Society of America Bulletin*, 80, 183-192.
- Hobday, D. K. and Horne, J. C. 1977.** Tidal influenced barrier island and estuarine sedimentation in the upper Carboniferous of southern west Virginia. *Sedimentary Geology*, 18, 97-122.
- Homewood, P. and Allen, P. 1981.** Wave-, tide-, and current-controlled sandbodies of Miocene Molasse, western Switzerland. *American Association of Petroleum Geologists Bulletin*, 65, 2534-2545.
- Howard, D. J. and Reineck, H. E., 1981.** Depositional facies of high-energy beach-to-offshore sequence: comparison with low-energy sequence. *American Association of Petroleum Geologists Bulletin*, 65, 807-830.
- Howard, J. D. and Nelson, C. H. 1982.** Sedimentary structures on a delta-influenced shallow shelf, Norton Sound, Alaska. *Geologie en Mijnbouw*, 61, 29-36.
- Howell, A., Flint, S. S. and Hunt, C. 1996.** Sedimentological aspects of the Humber group (upper Jurassic) of the south central Graben, UK, North Sea. *Sedimentology*, 43, 89-114
- Johnson, K. G. and Friedman, G. M 1969.** The Tully clastic correlatives (upper Devonian) of New York State: a model for recognition of alluvial, dune (?), tidal, nearshore (bar and lagoon), and offshore sedimentary environments in a tectonic delta complex. *Journal of Sedimentary Petrology*, 39, 451-485.

Johnson, H. D. 1975. Tidal- and wave-dominated inshore and shoreline sequences from the late Precambrian, Finnmark, north Norway. *Sedimentology*, 22, 45-74.

Johnson, H. D. and Levell, B. K. 1995. Sedimentology of a transgressive, estuarine sand complex: the Lower Cretaceous Woburn Sands (Lower Greensand), southern England. *In: Plint A. G (ed) Sedimentary Facies Analysis.* International Association of Sedimentologists, 22, 17-46.

Johnson, H. D. and Baldwin, C. T. 1996. Shallow clastic seas. *In: Reading H. G (ed) Sedimentary environments: processes, facies and stratigraphy.* Blackwell Scientific Publications, Oxford. 3rd edition, 232-280.

Keith, D. A. W. 1991. Truncated prograding strandplain or offshore sand body?-sedimentology and geometry of the Cardium (Turonian) sandstone and conglomerate at Willesden Green field, Alberta. *In: Swift D. J. P., Oertel G. F., Tillman R. W. and Thorne J. A (eds) Shelf sand and sandstone bodies: Geometry, facies and sequence stratigraphy.* International Association of Sedimentologists Special Publication, 14, 457-487.

Kelley, V. C. 1951. Oolitic iron deposits of New Mexico. *American Association of Petroleum Geologists Bulletin*, 35, 2199-2228.

Kimberly, M. M. 1979. Origin of oolitic iron formations. *Journal of Sedimentary Petrology*, 49, 111-132.

Kiteley, L. W. and Filed, M. E. 1984. Shallow-marinedepositional environments in the upper Cretaceous of northern Colorado. *In: Tillman R. W. and Siemers C. T (eds) Siliciclastic shelf sediments.* Society of Economic Paleontologists and Mineralogists Special Publication, 34, 179-204.

Klein, C. and Hurlbut, C. S. 1993. Manual of mineralogy. John Wiley and Sons, Inc. 2nd edition, 681p.

Klitzsch, E. 1970. Problems of continental Mesozoic strata of southwestern Libya. *In: Dessauvage T. F. and Whiteman A. J (eds) African Geology,* Department of Geology, University of Ibadan, Nigeria, 483-493.

Klitzsch, E. 1981. Lower Palaeozoic rocks of Libya, Egypt and Sudan. *In:* Holland C. H (ed) Lower Palaeozoic of Middle East, Eastern and Southern Africa and Antarctica, III, 131-163.

Kumar, N. and Sanders, J. E. 1974. Inlet sequence: a vertical succession of sedimentary structures and textures created by the lateral migration of tidal inlets. *Sedimentology*, 21, 491-532.

Kumar, N. and Sanders, J. E. 1976. Characteristic of shoreface storm deposits: modern and ancient examples. *Journal of Sedimentary Petrology*, 46, 145-162.

Leckie, D. A. and Walker, R. G. 1982. Storm and tide-dominated shoreline in Cretaceous Moosebar-Lower Gates interval-outcrop equivalents of deep basin gas trap in western Canada. *American Association of Petroleum Geologists Bulletin*, 66, 138-157.

Loutit, T. S. Hardenbol, J., Vail, P. R. and Baum, G. R. 1988. Condensed sections; the key to age determination and correlation of continental margin sequences. *In:* Wilgus C. K., Hastings B. S., Kendall C. G. St C., Posamentier H. W., Ross C. A. and Van Wagoner J. C (eds) Sea-Level Changes-An integrated approach. Society of Economic Paleontologists and Mineralogists Special Publication, 42, 183-213.

Lowe, D. R. 1976. Subaqueous liquefaction and fluidized sediment flows and their deposits. *Sedimentology*, 23, 285-308.

Macdonald, D. I. M. 1993. Controls on sedimentation at convergent plate margins. In Frostick L. E. and Steel R. J (eds) Tectonic controls and signatures in sedimentary successions. *International Association of Sedimentologists*, 20, 225-257.

Madon, M. B. H J. 1991. Depositional setting and origin of berthierine oolitic ironstones in the lower Miocene Terengganu shale, Tenggol arch, offshore Peninsular Malaysia. *Journal of Sedimentary Petrology*, 62, 899-916.

Mashinsky, H. F., Dishroon, C. P. and Palen, F. S. 1987. Hydrocarbon potential of Atshan area (W. Libya), (unpublished).

Massa, D. and Collomb, G. R. 1960. Observations nouvelles sur la region d' Aouinet Ouenine et du Djebel Fezzan (Libya). 21st International Gelo Congre's. International, Section 12, 65-73.

Massa, D. and Moreau-Benoit, A. 1976. Essi de synthese stratigraphique et palynologique du systeme Devonien en Libye Occidental. *Revue de L'institut du Francis Petrole*, 31 (2), 287-333.

Masters, C. D. 1967. Use of sedimentary structures in determination of depositional environments, Mesaverde formation, Williams Fork Mountains, Colorado. *American Association of Petroluem Geologists Bulletin*, 51, 2033-2043.

McCubbin, G. D. 1982. Barrier-Island and Strand-Plain Facies. *In: Scholle P. A. and Spearing D (eds) Sandstone depositional environments. American Association of Petroleum Geologists Memoir*, 31, 247-279.

McGregor, A. A. and Biggs, C. A. 1968. Bell Creek field, Montana: a rich stratigraphic trap. *American Association of Petroluem Geologists Bulletin*, 52, 1869-1887.

Miall, A. D. 1984. Deltas. *In: Walker R. G (ed) Facies models. Geological Association of Canada*, 119-142.

Miall, A. D. 1992. Alluvial deposits. *In: Walker R. G (ed) Facies models. 2nd edition, Geological Association of Canada*, 105-118.

Miall, A. D. 1996. The geology of fluvial deposits. Springer, 582p.

Miall, A. D. 1997. The geology of stratigraphic sequences. Springer, 433p.

Mitchum, R. M. Jr 1977. Seismic stratigraphy and global changes of sea-level, Part 1: glossary of terms used in seismic stratigraphy. *In: Payton C. E (ed) Seismic stratigraphy-applications to hydrocarbon exploration. American Association of Petroleum Geologists Memoir*, 26, 205-212.

Mitchum, R. M. Jr., Vail, P. R. and Thompson, S. 1977. Seismic stratigraphy and global changes of sea-level, Part 2: the depositional sequence as a basic unit for stratigraphic analysis. *In: Payton C. E (ed) Seismic stratigraphy-*

applications to hydrocarbon exploration. *American Association of Petroleum Geologists Memoir*, 26, 53-62.

Mitchum, R. M. Jr. and Van Wagoner, J. C. 1991. High-frequency sequences and their stacking patterns: sequence-stratigraphic evidence of high-frequency eustatic cycles. *Sedimentary Geology*, 70, 131-160.

Morton, A. C. 1985. Heavy minerals in provenance studies. *In: Zuffa G. G (ed) Provenance of Arenites. NATO ASI Series C: Mathematical and Physical Sciences*, 184, 247-277.

Nahon, D., Carozzi, A. V. and Parron, C. 1980. Lateritic weathering as a mechanism for the generation of ferruginous ooids. *Journal of Sedimentary Petrology*, 50, 1287-1298.

Nichol, S. L., Zaitlin, B. A. and Thompson, B. G. 1997. The upper Hawkesbury River, New South Wales, Australia: a Holocene example of an estuarine bayhead delta. *Sedimentology*, 44, 263-286.

Nummedal, D., Riley, G. W. and Templet, P. L. 1993. High-resolution sequence architecture: a chronostratigraphic model based on equilibrium profile studies. *In: Posamentier H. W., Summerhayes C. P., Haq B. U. and Allen G. P (eds) Sequence stratigraphy and facies associations. International Association of Sedimentologists*, 18, 55-68.

O'Mara, P. T. and Turner, B. R. 1997. Westphalian B marine bands and their subsurface recognition using gamma-ray spectrometry. *Yorkshire Geological Society*, 15, 307-316

Oomkens, E. 1970. Depositional sequences and sand distribution in the postglacial Rhone delta complex. *In: Morgan J. P (ed) Deltaic sedimentation modern and ancient. Society of Economic Paleontologists and Mineralogists Special Publication*, 15, 198- 212.

Oomkens, E. 1974. Lithofacies relations in the late Quaternary Niger delta complex. *Sedimentology*, 21, 195-222.

Orton, J. G. and Reading, G. H. 1993. Variability of deltaic processes in terms of sediment supply, with particular emphasis on grain size. *Sedimentology*, 40, 475-512.

- Partington, M. A., Mitchener, B. C., Milton, N. J. and Fraser, A. J. 1993.** Genetic sequence stratigraphy for the North Sea Late Jurassic and Early Cretaceous: distribution and prediction of Kimmeridgian-Late Ryazanian in the North Sea and adjacent areas. *In: Petroleum Geology of Northwest Europe: proceedings of the 4th conference. Geological Society, London, 347-370.*
- Payton, C. E. 1977.** Seismic stratigraphy-applications to hydrocarbon exploration. *American Association of Petroleum Geologists Memoir, 26, 516.*
- Pemberton, S. G., MacEachent, J. A. and Frey, R. W. 1992.** Trace fossil facies models: environmental and allosignificance. *In: Walker R. G. and James N. P (eds) Facies models. Geological Association of Canada, 47-72.*
- Penland, S., Body, R. and Suter, J. R. 1988.** Transgressive depositional system of the Mississippi delta plain: A model for barrier shoreline and shelf sand development. *Journal of Sedimentary Petrology, 58, 932-949.*
- Pettijohn, F. J. 1957.** Sedimentary rocks. New York, Harper and Brother, 2nd, edition, 718p.
- Pettijohn, F. J., Potter, R. E. and Siever, R. 1978.** Sand and sandstone. New York, Spring-Verlag. 2nd edition, 553p.
- Pierobon, E. S. T. 1991.** Contribution to the stratigraphy of the Murzuq basin, SW Libya. *In: Salem M. J. and Belaid M. N (eds) The Geology of Libya. Academic press, London, V,1767-1783.*
- Pitman, W. C. 1978.** Relationship between eustasy and stratigraphic sequences of passive margins. *American Association of Petroleum Geologists Bulletin, 89, 1389-1403.*
- Plint, A. G., Eyles, N., Eyles, C. H. and Walker, R. G. 1992.** Control of sea-level change. *In: Walker R. G. and James N. P (eds) Facies models. Geological Association of Canada, 15-25.*
- Porrenga, D. H. 1967.** Glauconite and chamosite as depth indicators in the marine environment, *Marine Geology, 5, 495-501.*
- Posamentier, H. W. and Vail, P. R. 1988.** Eustatic controls on clastic deposition II-sequence and systems tract models. *In: Wilgus C. K., Hastings B. S., Kendall*

C. G. St C., Posamentier H. W., Ross C. A. and Van Wagoner J. C (eds) Sea-Level Changes-An integrated approach. Society of Economic Paleontologists and Mineralogists Special Publication, 42, 125-154.

Posamentier, H. W., Jervey, M. T. and Vail, P. R. 1988. Eustatic controls on clastic depositional-conceptual framework. *In*: Wilgus C. K., Hastings B. S., Kendall C. G. St C., Posamentier H. W., Ross C. A. and Van Wagoner J. C (eds) Sea-Level Changes-An integrated approach. Society of Economic Paleontologists and Mineralogists Special Publication, 42, 109-124.

Posamentier, H. W. and James, D. P. 1993. An overview of sequence-stratigraphic concepts: uses and abuses. *In*: Posamentier H. W., Summerhayes C. P., Haq B. U. and Allen G. P (eds) Sequence stratigraphy and facies associations. International Association of Sedimentologists Special Publication 18, 3-18.

Prave, A. R., Duke, W. L. and Slattery, W. 1996. A depositional model for storm- and tide-influenced prograding siliciclastic shoreline from the Middle Devonian of the central Appalachian foreland basin, USA. *Sedimentology*, 43, 611-629.

Rahmani, R. A. 1988. Estuarine tidal channel and nearshore sedimentation of a late Cretaceous epicontinental sea, Drumheller, Alberta, Canada. *In*: De Boer P. L. Van Gelder A. and Nio S. D (eds) Tidal-influenced sedimentary environments and facies. Reidal, Dordrecht, 433-47.

Rahmani, R. A. 1994. Facies, depositional environments and reservoir properties of Tahara and F3 sand in core from A6-NC169, Al-Wafa Field (unpublished).

Ramos, A. and Galloway, W. E. 1990. Facies and sand-body geometry of the Queen City (Eocene) tide-dominated delta-margin embayment, NW Gulf of Mexico basin. *Sedimentology*, 37, 1079-1098.

Rampino, M. R. and Sanders, J. E. 1982. Holocene transgression in south-central long island, New York-Reply. *Journal of Sedimentary Petrology*, 52, 1020-1025.

Reading, H. G. 1986. Facies. *In:* Reading H. G (ed) Sedimentary environments and facies. Blackwell Scientific Publications, 2nd edition, Oxford, 4-19.

Reading, H. G. and Levell, B. K. 1996. Controls on the sedimentary rock record. *In:* Reading H. G (ed) sedimentary environments: processes, facies and stratigraphy. Blackwell Scientific Publications, Oxford. 3rd edition, 5-36.

Reading, H. G. and Collinson, J. D. 1996. Clastic coasts. *In:* Reading H. G (ed) Sedimentary environments: processes, facies and stratigraphy. Blackwell Scientific Publications, Oxford. 3rd edition, 154-231.

Reineck, E. H. and Wunderlich, F. 1968. Classification and origin of flaser and lenticular bedding. *Sedimentology*, 11, 99-104.

Reineck, H. E. and Singh, I. B. 1972. Genesis of laminated sand and graded rhythmites in storm-sand layers of shelf mud. *Sedimentology*, 18, 123-128.

Reineck, H. E. and Singh, I. B. 1973. Depositional sedimentary environments. Springer-Verlag, Berlin, 439 p.

Reinson, G. E. 1984. Barrier island and associated strand plain systems. *In:* Walker R. G (ed) Facies models. Geological Association of Canada, 119-140.

Reinson, G. E., Clark, J. E. and Foscolos, A. E. 1988. Reservoir geology of Crystal Viking Field, lower Cretaceous estuarine tidal channel-bay complex, south-central Alberta. *American Association of Petroleum Geologists Bulletin*, 72, 1270-1294.

Reinson, G. E. 1992. Transgressive barrier island and estuarine systems. *In:* Walker R. G. and James N. P (eds) Facies models. Geological Association of Canada, 179-194.

Reynolds, A. D. 1994. Sequence stratigraphy from core and wireline log data: the Viking Formation, Albian, south central Alberta, Canada. *Marine and Petroleum Geology*, 11, 258-282.

Rice, D. D. 1984. Widespread, shallow marine, storm-generated sandstone units in the Upper Cretaceous Mosby Sandstone, Central Montana. *In:* Tillman R. W. and Siemers C. T (eds) Siliciclastic shelf sediments. Society of Economic Paleontologists and Mineralogists Special Publication, 143-161.

Rider, M. H. 1990. Gamma-ray log shape used as a facies indicator: critical analysis of an oversimplified methodology. *In: Hurst A., Lovell M. A. and Morton A. C (eds) Geological Applications of Wireline Logs. Geological Society Special Publication, 48, 27-37.*

Rider, M. H. 1996. The geological interpretation of well logs. 2nd edition, Whittles Publishing, 175p.

Rine, M. J. and Ginsburg, N. R. 1985. Depositional facies of a mud shoreface in Surinam, south America-a mud analogue to sandy shallow-marine deposits. *Journal of Sedimentary Petrology, 55, 633-652.*

Sanders, E. J. 1965. Primary sedimentary structures from turbidity currents and related resedimentation mechanisms. *In: Middleton V. G (ed) Primary sedimentary structures and their hydrodynamic interpretation. Society of Economic Paleontologists and Mineralogists Special Publication, 12, 192- 219.*

Scholle, P. A. 1979. A colour illustrated guide to constituents, textures, cements, and porosities of sandstones and associated rocks. *American Association of Petroleum Geologists Memoir, 28, 201p.*

Seilacher, A. 1967. Bathymetry of trace fossils. *Marine Geology, 5, 413-428.*

Selley, R. C. 1976 a. An introduction to sedimentology. 2nd edition. Academic press Inc. (London) Ltd, 408 p.

Selley, R. C. 1976 b. Subsurface environmental analysis of North Sea sediments. *American Association of Petroleum Geologists Bulletin, 60, 184-195.*

Selley, R. C. 1985. Ancient sedimentary environments. 3rd edition. Chapman and Hall, London, 317p.

Serra, O. and Sulpice, L. 1975. Sedimentological analysis of sand-shale series from well logs. The Society of Professional Well Log Analysts, 16th Annual Logging Symposium, paper W, 1-23.

Shanmugam, G. 1985. Types of porosity in sandstones and their significance in interpreting provenance. *In: Zuffa G. G (ed) Provenance of Arenites. NATO ASI Series C: Mathematical and Physical Sciences, 184, 115-137.*

- Sloss, L. L. 1963.** Sequences in the cratonic interior of North America. *Geological Society of American Bulletin*, 74, 93-114.
- Sverdrup, E. and Prestholm, E. 1990.** Synsedimentary deformation structures and their implications for stylolitization during deeper burial. *Sedimentary Geology*, 68, 201-210.
- Suttner, L. J., Basu, A. and Mack, G. H. 1981.** Climate and the origin of quartz arenites. *Journal of Sedimentary Petrology*, 51, 1235-1246.
- Swift, D. J. P. 1969.** Inner shelf sedimentation: processes and products. *In:* Stanley D. J (ed) The new concepts of continental margin sedimentation: application to the geological record. American Geological Institute, Washington, DS-4-1-DS-4-46.
- Swift, D. J. P., Phillips, S. and Thorne, J. A. 1991.** Sedimentation on continental margins IV: lithofacies and depositional systems *In:* Swift D. J. P., Oertel G. F., Tillman R. W. and Thorne J. A (eds) Shelf sand and sandstone bodies: Geometry, facies and sequence stratigraphy. International Association of Sedimentologists Special Publication, 14, 89-152.
- Talbot, M. R. 1974.** Ironstones in the upper Oxfordian of south England. *Sedimentology*, 21, 433-450.
- Talbot, M. R. and Allen P. A 1996.** Lakes *In:* Reading H. G (ed) Sedimentary environments: processes, facies and stratigraphy. Blackwell Scientific Publications, Oxford. 3rd edition, 83-124.
- Tankard, J. A. and Barwis, J. H. 1982.** Wave-dominated deltaic sedimentation in the Devonian Bokkeveld basin of South Africa. *Journal of Sedimentary Petrology*, 52, 959-974.
- Tanner, W. F. 1959.** Near-shore studies in sedimentology and morphology along the Florida Panhandle Coast. *Journal of Sedimentary Petrology*, 29, 564-574.
- Tawadros, E. 1994.** Petrographic of the F3 sand and Tahara Formation cores in the well A6-NC169 (Al Wafa Field, unpublished).

Taylor, K. G. and Curtis, C. D. 1995. Stability and facies association of early diagenetic mineral assemblages: an example from a Jurassic ironstone-mudstone succession, UK. *Journal of Sedimentary Research*, 65, 358-368.

Terwindt, J. H. J. 1973. Sand movement in the in-and offshore tidal area of the SW. part of the Netherlands. *Geologie en Mijnbouw*, 52, 69-77.

Teyssen, T. A. L. 1984. Sedimentology of the Minette oolitic ironstones of Luxembourg and Lorraine: a Jurassic subtidal sandwave complex. *Sedimentology*, 31, 195-211.

Thompson, W. O. 1937. Original structures of beaches, bars, and dunes. *American Association of Petroleum Geologists Bulletin*, 48, 723-751.

Tucker, M. E. 1991. Sedimentary petrology: a introduction to the origin of sedimentary rocks. 2nd edition, Blackwell Scientific, Oxford 260p.

Turner, B. R. 1980. Palaeozoic sedimentology of the southeastern part of Al Kufrah basin, Libya: a model for oil exploration. *In: Salem M. J. and Busrewil M. T (eds) The Geology of Libya. Academic press, London, II, 351-374.*

Turner, B. R. and Benton, M. J. 1983. Palaeozoic trace fossils from the Kufra basin, Libya. *Journal of Paleontology*, 57, 447-460.

Turner, B. R. 1991. Palaeozoic deltaic sedimentation in the southeastern part of Al Kufrah basin, Libya. *In: Salem M. J. and Belaid M. N (eds) The Geology of Libya. Academic press, London, V, 1713-1726.*

Turner, P. 1980. Continental red beds. Elsevier, Amsterdam, 562p.

Vail, P. R., Mitchum, R. M. Jr. and Thompson, S. III. 1977. Seismic stratigraphy and global changes of sea-level, part 3: relative changes in sea-level from coastal onlap. *In: Payton C. E (ed) Seismic stratigraphy-applications to hydrocarbon exploration. American Association of Petroleum Geologists Memoir*, 26, 63-97.

Vail, P. R. and Wornardt, W. W. 1990. Well log-seismic sequence stratigraphy: an integrated tool for the 90'S. GCSSEPM Foundation Eleventh Annual Research Conference, 379-388.

Vail, P. R., Audemard, F., Bowman, S. A., Eisner, P. N. and Perezcruz, C. 1991. The stratigraphic signatures of tectonics, eustasy and sedimentology-an overview. *In: Einsele G., Ricken W. and Seilacher A (eds) Cycles and events in stratigraphy.* Berlin, Springer-Verlag, 617-659.

Van Beek, J. L. and Koster, E. A. 1972. Fluvial and estuarine sediments exposed along the Oude Maas (the Netherlands). *Sedimentology*, 19, 237-256.

Van den Berg, J. H. 1982. Migration of large-scale bedforms and preservation of cross-bedded sets in highly accretional parts of tidal channel in the Oosterchelde, SW Netherlands. *Geologie en Mijnbouw*, 61, 253-263.

Van Houten, F. B. and Karasek, R. M. 1981. Sedimentology framework of late Devonian oolitic iron formation, Shatti Valley, west central Libya. *Journal of Sedimentary Petrology*, 51, 415 -427.

Van Houten, F. B. and Arthur, M. A. 1989. Temporal patterns Phanerozoic oolitic ironstones and oceanic anoxia. *In: Young T. p. and Tylor W. E. G (eds) Phanerozoic ironstones.* Geological Society Special Publication, 46, 33-49.

Van Straaten, L. M. J. U. 1959. Minor structures of some recent littoral and neritic sediments. *Geologie en Mijnbouw*, 21, 197-216.

Van Wagoner, J. C., Posamentier, H. W., Mitchum, R. M., Vail, P. R., Sarg J. F., Loutit, T. S. and Hardenbol, J. 1988. An overview of the fundamentals of sequence stratigraphy and key definitions. *In: Wilgus C. K., Hastings B. S., Kendall C. G. St C., Posamentier H. W., Ross C. A. and Van Wagoner J. C (eds) Sea-Level Changes-An integrated approach.* Society of Economic Paleontologists and Mineralogists Special Publication, 42, 39-45.

Van Wagoner, J. C., Mitchum, R. M., Campion, K. M. and Rahmanian, V. D., 1990. Siliciclastic sequence stratigraphy in well logs, cores and outcrop: concepts for high resolution correlation of time and facies. *American Association of Petroleum Geologists, Methods in Exploration Series, No. 7*, 55p.

Visher, G. S. 1969. Grain size distributions and depositional processes. *Journal of Sedimentary Petrology*, 39, 1074-1106.

Vos, R. G. and Eriksson, K. A. 1977. An emphyment model for tidal and wave swash deposits occurring within a fluviially dominated middle Proterozoic sequence in South Africa. *Sedimentary Geology*, 18, 161-173.

Vos, R. G. 1977. Sedimentology of an upper Palaeozoic river, wave and tide influenced delta system in Morocco. *Journal of Sedimentary Petrology*, 47, 1242-1260.

Vos, R. G. 1981 a. Sedimentology of an Ordovician fan complex, western Libya. *Sedimentary Geology*, 29, 153-170.

Vos, R. G. 1981 b. Deltaic sedimentation in the Devonian of western Libya. *Sedimentary Geology*, 29, 67-88.

Walker, R G. 1966. Shale Grit and Grindslow shales: transition from turbidite to shallow-water sediments in the upper Carboniferous of northern England. *Journal of Sedimentary Petrology*, 36, 90-114.

Walker, R. G. 1990. Facies modelling and sequence stratigraphy. *Journal of Sedimentary Petrology*, 60, 777-786

Walker, R. G. and Plint, A. G. 1992. Wave- and storm-dominated shallow-marinesystems. *In: Walker R. G. and James N. P (eds) Facies models.* Geological Association of Canada, 219-238.

Walker, R. G. 1992. Facies, facies models and modern stratigraphic concepts. *In: Walker R. G. and James N. P (eds) Facies models.* Geological Association of Canada, 1-14.

Walls, R. A. 1975. Late Devonian-early Mississippian subaqueous deltaic facies in a portion of the southeastern Appalachian basin. *In: Broussard M. L (ed) Deltas models for exploration.* Houston Geological Society, Houston, 359-367.

Watts, A. B. 1982. Tectonic subsidence, flexure and global changes of sea-level. *Nature*, 297, 5866, 469-474.

Weimer, R. J., Howard, J. D. and Lindsay, D. R. 1982. Tidal flats and associated tidal channels. *In: Scholle P. A. and Spearing D (eds) Depositional environments.* *American Association of Petroleum Geologists Memoir*, 31, 191-245.

Weyant, M. and Massa, D. 1991. Contribution of conodonts to the Devonian Biostratigraphy of Western Libya. *In: Salem M. J. Hammuda O. S. and Eliagoubi B. A (eds) The Geology of Libya. Academic press, London, IV, 1297-1322.*

Whitbread, T. and Kelling, G. 1982. M'rar formation of western Libya-evolution of an early Carboniferous delta system. *American Association of Petroleum Geologists Bulletin*, 66, 1091-1107.

Wilgus C. K., Hastings B. S., Kendall C. G. St C., Posamentier H. W., Ross C. A. and Van Wagoner J. C. 1988. Sea-Level Changes-An integrated approach. Society of Economic Paleontologists and Mineralogists Special Publication, 42,407.

Williams, P. F. 1968. The sedimentation of Westphalian (Ammanian) measures in the little Haven-Amroth Coalfield, Pembrokeshire. *Journal of Sedimentary Petrology*, 38, 332-362.

Williams, G. D. 1993. Tectonics and seismic sequence stratigraphy: an introduction. *In: Williams G. D. and Dobb A (eds) Tectonic and Seismic Stratigraphy. Geological Society Special Publication*, 71, 1-13.

Wilson, R. C. L. 1991. Sequence Stratigraphy: an introduction. *Geoscientist*, 1, 13-23.

Wunderlinch, F. 1970. Genesis and environment of the "Nellenkopfschichten" (lower Emsian, Rheinian Devon) at Locus Typicus in comparison with modern coastal environment of the German bay. *Journal of Sedimentary Petrology*, 40, 102-130.

Young, R. G. 1955. Sedimentary facies and intertonguing in the upper Cretaceous of the book cliffs, Utah, Colorado. *Geological Society of America Bulletin*, 66, 177-202.

